This is to certify that the

dissertation entitled

A Chemical Analysis of the Role of Molecular and Conformational Structure in the Adaptation of Microorganisms to Extreme Environments

presented by

Jeongrim Lee

has been accepted towards fulfillment
of the requirements for

Ph.D. degree in Chemistry

Major professor

Date 5/5/97

A CHEMICAL ANALYSIS OF THE ROLE OF MOLECULAR AND CONFORMATIONAL STRUCTURE IN THE ADAPTATION OF MICROORGANISMS TO EXTREME ENVIRONMENTS

By

Jeongrim Lee

A DISSERTATION

Submitted to
Michigan State University
in partial fulfillment of the requirements
for the degree of

DOCTOR OF PHILOSOPHY

Department of Chemistry

1997

ABSTRACT

A CHEMICAL ANALYSIS OF THE ROLE OF MOLECULAR AND CONFORMATIONAL STRUCTURE IN THE ADAPTATION OF MICROORGANISMS TO EXTREME ENVIRONMENTS

By

Jeongrim Lee

To understand how the membrane can function in the adaptation of microorganisms to extreme environments, the membrane has to be characterized at several levels including structure of the individual membrane lipids, their conformations, order and dynamics. *Sarcina ventriculi*'s adaptability to extreme environments was used to relate the structures of the bacterial membrane to various modes of adaptation.

Sarcina ventriculi grown at pH 3 was found to be capable of a variety of unusual and dramatic adaptative processes including tail-to-tail and head-to-head coupling of membrane lipids. The tail-to-tail coupling is the chemical linking of hydrocarbon chains from opposite ends of the membrane bilayer to form transmembrane bifunctional fatty acid species that span the bilayer. This is a swift, effective, universal and dynamically regulated adaptative response without requiring new protein or lipid synthesis.

Another adaptation mode was the formation of the novel glycolipids, β-1-*O*-alkyl & acyl-sophorosides as major glycolipids. These glycolipids might have some function in regulating the membrane stability at low pH.

A trisaccharide containing a β-1,3 and a β-1,4-linkage and a hexasaccharide that is a β-1,4-linked dimer of the trisaccharide unit were also observed. This is the first report

of β-glucan biosynthesis in a Gram-positive organism. Their occurrences support an even more general link between β-glucan synthesis and the adaptability of bacteria.

To determine whether the peptidoglycan has any unusual structural feature, the peptidoglycan structure was characterized. The basic peptidoglycan subunit consisted of *N*-GlcNAc-β-1,4-*N*-MurNAc-Ala-*i*Gln-A_2pm(-Gly)-Ala. The structure of dimeric muropeptide was GlcNAc-MurNAc-Ala-*i*Gln-A_2pm(-Gly)-Ala→GlcNAc-MurNAc-Ala-*i*Gln-A_2pm(-Gly)-Ala-Ala, cross-linked by a glycine residue. The inter-peptide bridge of dimeric structure was short and the degree of cross-linking was high. This is necessary for stability at low pH.

The conformation of MGDG in solution was determined by NOESY experiments and molecular mechanics calculation. The rotamer populations for the glycerol moiety were obtained from vicinal spin-spin coupling constants. This information will allow us to characterize the packing and stability of bilayer containing these molecules.

The conformational and packing behavior of β-1-*O*-hexadecylsophoroside was studied by a powerful combination of various techniques. The long range goal of this approach is to gain enough information of the packing order and stabilities of the individual lipid components to allow us to predict how they can combine to form new species. This will explain the large degree of diversity of lipid structures.

ACKNOWLEDGMENTS

This has been quite a long journey to reach this moment. During this journey I have met so many nice people who gave me the encouragement and energy that I needed to achieve my goals.

First and foremost, I would like to express my sincerest thanks to my advisor, Dr. Rawle I. Hollingsworth, for his continuous advice, encouragement and support. I was very lucky to meet Rawle and to learn science with his guidance. He has taught me about how skepticism is important in science in order to reach new views beyond the present level and how to base hypothesis and thoughts on fundamental principles.

I also owe my gratitude to the members of my committee members: Dr. William H. Reusch, Dr. Gary Blanchard, Dr. Douglas Gage, and Dr. Kris A. Berglund for their invaluable advice and suggestions during my dissertation.

I also would like to thank the Hollingsworth group members in this small kingdom, past and present. I have greatly enjoyed our discussions not only about chemistry but also our multicultural backgrounds. This was very important in refreshing my mind and ideas for my success.

I would like to thank members of the Mass Spectrometry Facility, especially Dr. Zhi-Heng Huang for sharing his experiences and knowledge. I would like to thank to Dr. Long Le and Dr. Kermit Johnson at the NMR Facility for all of their assistance.

I would like to show my gratitude to my parents for their unconditional love and support. My father made me realize how much learning is an important part of our life. My thanks to my brothers and their familys, especially to my eldest brother who encouraged and supported me. I also cannot thank my-parents-in-law enough for their support.

Lastly and deeply, I wish to thank my husband, Jungtaek and my daughter, Jean for their unconditional love, patience, understanding, and encouragement at all times. This place and time will be remembered preciously and beautifully in my life because of them. They are the reason for me to have been able to finish this work.

TABLE OF CONTENTS

LIST OF TABLES

LIST OF FIGURES

LIST OF ABBREVIATIONS

Ala	alanine
A_2pm	diaminopimelic acid
DAG	diacylglycerol
DGalDG	digalactosyl diacylglycrol
DGDG	diglucosyl diacylglycerol
DSC	differential scanning calorimetry
DQF-COSY	double quantum filtered-correlated spectroscopy
EI	electron ionization
ESI	electrospray ionization
FAB-CAD-MS/MS	fast atom bombardment-collision activated dissociation-tandem mass spectrometry
FAB/MS	fast atom bombardment / mass spectrometry
FAME	fatty acid methyl ester
FD	field desorption
*i*Gln	*iso*-glutamine
GC/MS	gas chromatography / mass spectrometry
GlcNAc	N-acetyl glucosamine

Gly	Glycine
HMQC	heteronuclear multiquantum coherence
HOHAHA	homonuclear Hartmann-Hahn spectroscopy
HPLC	high performance liquid chromatography
lyso-PC	lysophosphatydylcholine
MALDI	matrix assisted laser desorption ionization
MDO	membrane-derived oligosaccharide
MGDG	monoglucosyl diacylglycerol
MGalDG	monogalactosyl diacylglycerol
MD	molecular dynamics
MM	molecular mechanics
NMR	nuclear magnetic resonance
NOE	nuclear Overhauser effect
NOESY	nuclear Overhauser and exchange spectroscopy
PC	phosphatidylcholine
PE	phosphatidylethanolamine
PG	phosphatidylglycerol
S. ventriculi	*Sarcina ventriculi*
TFA	trifluoroacetic acid
TLC	thin layer chromatography
TOCSY	total correlation spectroscopy
UDP-Gal	uridine diphosphate-galactose

CHAPTER I

INTRODUCTION

The structures of the membrane lipids in bacteria reflect much about their function and about the habitat of the organism. How bacteria survive under extreme environmental conditions has not been well explained at a molecular level. To accomplish this, studies which relate the structures of the bacterial membrane to various modes of adaptation need to be carried out on organisms that are adaptable to a broad range of conditions. We focus here on *Sarcina ventriculi* which has a broad range of adaptability to conditions such as low pH, high temperature or high concentrations of organic solvents [1]. Attempts to explain its extremophilicity have been based on the suggestion that the molecular mechanisms that confer extremophilicity influence structure and stability of the membrane [2-4]. We are therefore interested in the detailed chemical analysis of the individual membrane lipids and other cell wall components of *Sarcina ventriculi* grown under an extreme environmental condition in this case at pH 3. From such a study we will gain insight into the adaptative mechanisms and can propose a model at the molecular level to explain how the microorganisms are able to adjust to such a broad continuum of external environmental conditions. There are several factors that determine how the membrane can function in the adaptation of microorganisms to extreme environmental conditions. These include the actual structures of the individual membrane lipids, their conformations, how they are packed in a supramolecular sense and how mobile they are. Adaptation is therefore a complex process and the role of the membrane has to be characterized at several levels including structure, conformation, order and dynamics.

This review is divided into four sections. First, a general overview of membrane adaptation of microorganisms to environmental stress will be discussed. The second part will focus on describing bulk membrane properties such as fluidity and stability from the

point of view of adaptation. Subsequently, the conformation and packing properties of membrane lipids will be reviewed. Finally, a brief description of lipid analysis will follow.

Heterogeneity and Adaptability of Membrane Lipids

The prokaryotic cell is the most simple of cells because it has no intracellular membranes. The boundary of the cytoplasm is defined by the plasma membrane. The plasma membrane is a cell membrane containing mostly proteins and lipids in sheets only a few molecules thick. The plasma membrane provides areas with defined microenvironments and allows for controlled transport of solutes. Even the most primitive of life forms require at least one membrane to enclose the constitutive functions. The boundary role represents only the most basic of needs and functions for a cell membrane, in particular the plasma membrane. The membrane of bacterial cells is a complex macromolecular structure with many thousands of molecules normally held together by noncovalent forces. The current view of membrane structure is similar in many aspects to the general outline of membrane structure developed more than two decades by Singer and Nicolson [5]. In this model, membranes are said to be composed of proteins incorporated either wholly or partly in a fluid-like, bilayer sea of lipids. In addition to the plasma membrane, cells usually also have a cell wall. Peptidoglycan is a uniquely bacterial macromolecule that forms the rigid cell wall of both Gram-negative and Gram-positive bacteria. Gram-positive bacteria have a single bilayer membrane and Gram-negative bacteria have two (Figure 1.1). Although considerable variations in the actual composition and specific structural features of the cell wall occur when bacteria are

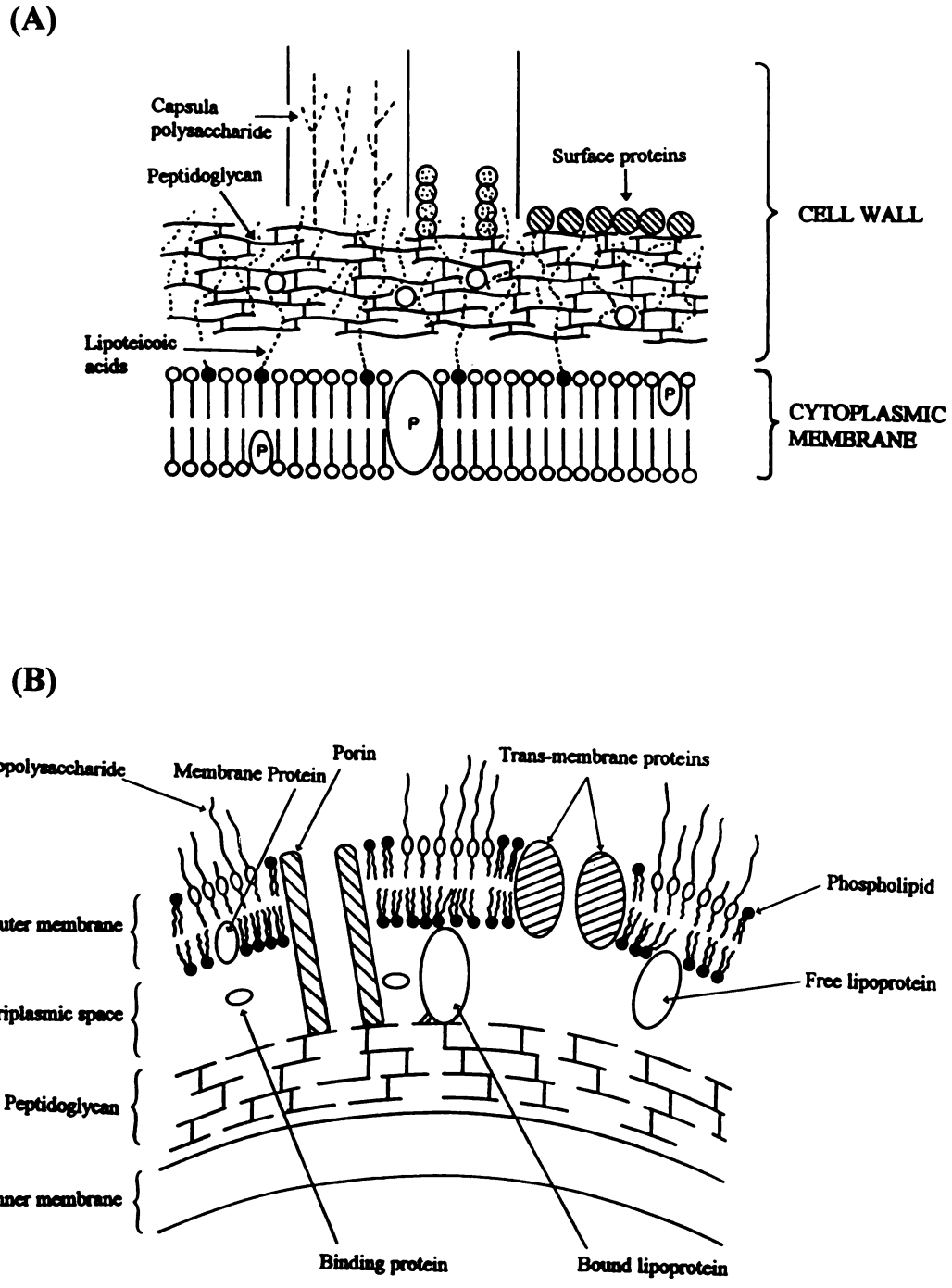

Figure 1.1: Representation of the cell envelopes of Gram-positive bacteria (A) and Gram-negative bacteria (B). (adapted from ref. 6)

grown under different conditions, the basic organization of the peptidoglycan is generally well conserved from bacterium to bacterium. It consists of a glycan backbone of alternating units of *N*-acetylglucosamine (GlcNAc) and *N*-acetylmuramic acid (MurNAc) of the linkage type [GlcNAcβ1→4-MurNAc] with a short peptide chain (typically 3-5 amino acids long) linked to the lactyl moiety of muramic acid. Muramic acid is the 3-lactyl ether of glucosamine. There is crosslinking between the oligopeptides of adjacent glycan strands leading to the formation of a complex three-dimensional macromolecule surrounding the cell [7].

The most striking feature of membrane lipids is their enormous diversity. The major membrane lipids are demonstrated in Figure 1.2. In eucaryotic membranes the glycerol-based phospholipids are predominant, including phosphatidylcholin(PC), phosphatidylethanolamine (PE), phosphatidylserine (PS), phosphatidylinositol (PI), and cardiolipin. Spingosine-based lipids, including sphingomyelin and the glycosphingolipids, also constitute a major fraction. The glycolipids, which can also include carbohydrate-containing glycerol-based lipids, play major roles as cell-surface-associated antigens and recognition factors in eucaryotes. Cholesterol is also a major component of eucaryotic membranes, particularly in mammalian plasma membranes. Among the prokaryotes, the major lipids of Gram-negative bacteria are PE, phosphatidylglycerol (PG), and cardiolipin. Membranes of Gram-positive bacteria also contain PE, PG, and cardiolipin along with mono- and diglycosyldiacylglycerols. In addition to phospholipids and glycolipids, many Gram-positive bacteria contain another class of lipids, which have been designated phosphoglycolipids. In plant membranes on

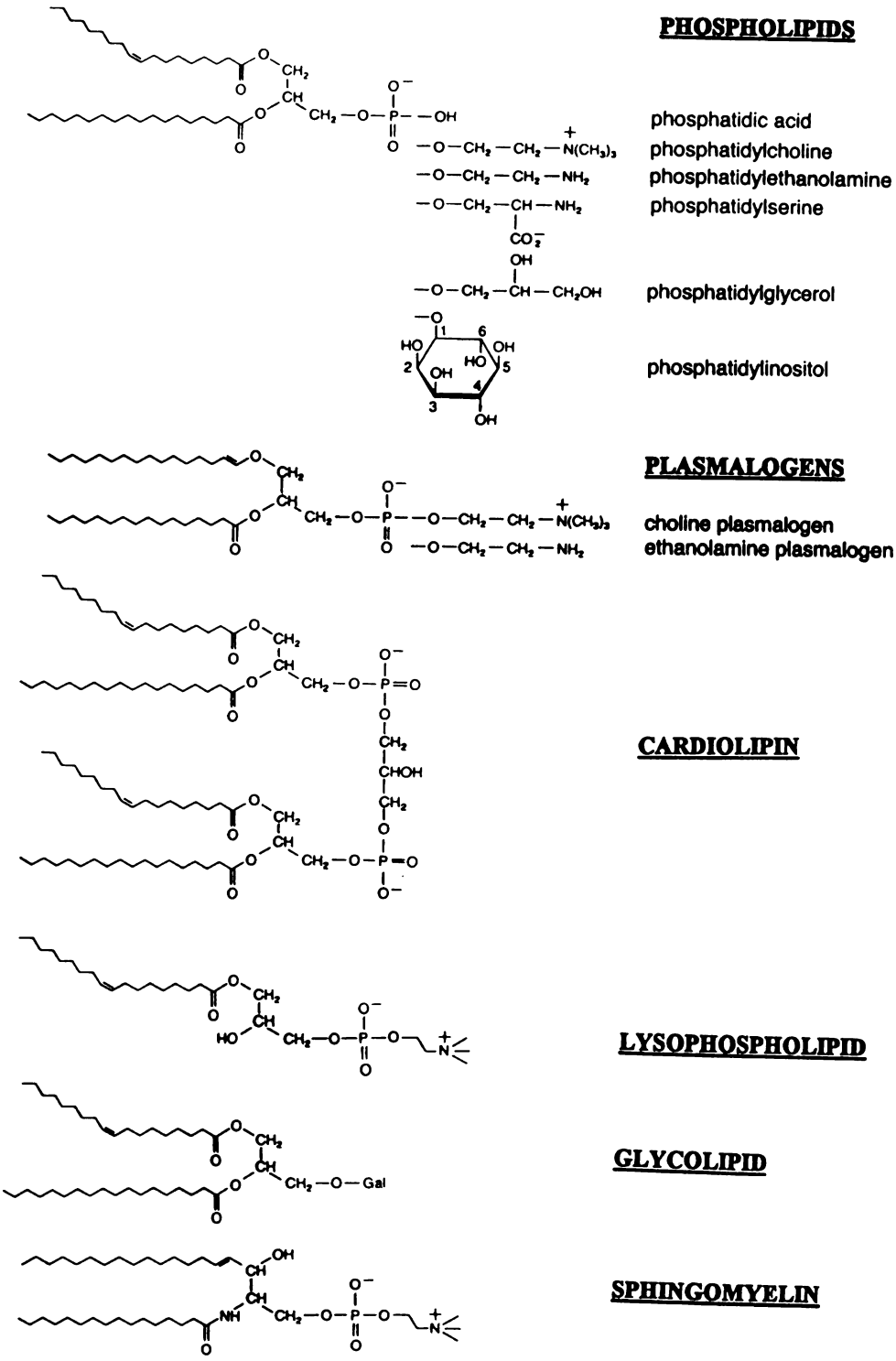

Figure 1.2: Structures of some class of membrane lipids. (adapted from ref. 42)

other hand, lipids such as monogalactosyl and digalactosyldiacylglycerols can form the majority components of membranes such as the chloroplast membrane. These observations give some impression of the lipid diversity in membranes, but it must be emphasized that this diversity is much more complex. Minority species such as sulfolipids, phospholipids with phosphorylated head groups, and lysolipids (lacking one of the two fatty acyl chains on glycerol) are also formed. In addition to this, each lipid species may exhibit a characteristic fatty acid composition. In general, there is a tremendous degree of variability of fatty acyl and alkyl species. It is known that the number of different molecular species of phospholipids in a membrane can easily exceed 100 and might be orders of magnitude more. This listing of lipid species given above does not cover the entire spectrum of lipid classes. There are some very unusual lipid species especially in the membranes of those organisms living in extreme environments.

The reasons for the great variety of lipids found in biological membranes and the factors regulating changes in lipid composition in response to external variables are not well understood [8]. The motional state or dynamics of membrane lipids is critical for their function. Biomembranes exist at a phase transition between a fluid or mobile phase and a solid or gel phase. Modifications of lipid structure occur in state if external events or conditions that could change it are applied.

Prokaryotic microorganisms such as bacteria can differ from eukaryotic cells in part because they can adapt to growth under extreme growth conditions of temperature (>100°C), salinity (saturated NaCl), pH (<2.0, >10), and substrate stress (limited chemical free energy or on toxicants) [9]. Temperature determines both the rates of

molecular motion of membrane components and the phase state (fluid or liquid) and order of membranes. It has been suggested that rather small change in external pH and ionic strength can induce alterations in transition temperature of fluid vs. gel phases lipid bilayers. The degree of dissociation of lipid head groups can strongly influence the main transition temperature and thus the fluidity of phospholipid bilayer systems and induce a phase change from a lamellar or sheet to a hexagonal or packed tube-type structure. The dynamic state of lipids in biological membranes is a central feature of current models of membrane structure and function. Bacteria have relatively simple envelopes containing one or two membranes, the composition of which can be manipulated genetically or by altering the growth conditions. Some bacteria which inhabit variable environments or which have adapted to extreme environments have an ability to change their membrane constituents swiftly and effectively so that lipids of appropriate physical properties which give membrane dynamics that are matched to the prevailing environmental conditions are produced. Growth temperature is the environmental factor which has been most extensively studied for its effect on membrane structure and dynamics. These studies have focused mainly on lipid unsaturation and were prompted by the knowledge that lipids undergo a phase transition from crystalline to liquid-crystalline over the temperature range in which microorganisms are able to grow. The most common response to increased temperature is a reduction of unsaturated fatty acids and a corresponding increase in the proportion of unsaturated fatty acids with decreased temperature. In addition to modulation of acyl chain unsaturation, there is an increase in fatty acid chain length at higher temperature and a corresponding decrease at lower temperature. Microorganisms that inhabit extreme thermal or pH environments frequently

possess significant amounts of branched chain fatty acids [10]. It has been demonstrated that the motional rate of membrane lipids in the bilayer remains constant as a consequence of the change of fatty acid composition and unsaturation with growth temperature. This has been viewed as a homeostatic mechanism (homeoviscous mechanism), and has been demonstrated for *Escherichia coli* [11], *Acholeplasma laidlawii* [12], and *Bacillus stearothermophilus* [13]. Similar responses have been demonstrated during adaptation of microorganisms to the presence of organic solvents such as alcohols, in their culture media. Bacteria have other, more dramatic mechanisms for adapting to more extreme environmental perturbations. These include synthesis of polynuclear aliphatic compounds called hopanes and the synthesis of monocyclic hydrocarbons [14,15].

The extreme versatility of lipids in adapting membrane structure and properties to a specific environment is best illustrated by the survival of archaebacteria. All classes of archaebacteria (the halophiles, methanogens and thermoacidophiles) possess unique tetraether to diether lipids linked via ether linkages (Figure 1.3), obtained by condensation of glycerol or more complex polyols with two isoprenoid alcohols at 20, 25 or 40 carbon atoms [16]. The presence of ether linkages instead of ester groups provides the greater resistance of these bonds to chemical and enzymatic attack. In the lipids containing C40 alkyl chains, head groups on either side of the bilayer are joined by the 40 carbon transmembrane chain. By covalently linking the two sides of the membrane, these tetraethers stabilize it at high temperatures. The auxotroph *Butyrivibrio* S2 has a novel mechanism enabling it to maintain membrane packing and fluidity at a fairly constant level. In addition to being unable to manipulate the chain length and degree of

unsaturation of membrane fatty acids in the manner of most microorganisms, it synthesizes a novel very long dicarboxylic acid with methyl branching. In addition, the esterfication of hydroxyl groups of glycolipids with butyric acid is thought to contribute to maintaining the required membrane fluidity [17]. Novel four-chain ether phospholipids in *Clostrium butyricum* grown on petroselinic acid in the absence of biotin have been characterized (Figure 1.3) [18].

Changes occurred in the lipid composition and structure in *Sarcina ventriculi* in response to alternations of pH. At neutral pH, the predominant membrane fatty acids ranged in chain length from C_{14} to C_{18}. However, during growth at pH 3.0, a family of unique very long chain α,ω-dicarboxylic fatty acids containing 32 to 36 carbon atoms were synthesized. The long chain dicarboxylic fatty acids account for more than 50% of total membrane fatty acids [2,3].

Bulk Membrane Properties Required for Adaptation

Two kinds of restrictions seem to determine the membrane lipid composition in microorganisms. Firstly, a large proportion of the lipids is not allowed to enter the gel phase as this would inactivate the membrane-bound enzyme and transport activities. Secondly, non-lamellar lipid phases are not allowed to form permanently since this would break down the barrier properties of the membrane. Thus, the biological membrane is dynamically controlled to maintain both membrane fluidity and bilayer stability.

It has been shown for some bacterial membranes that at least 10-50% of the lipids must be in a liquid crystalline state in order to the organisms to grow and divide. It

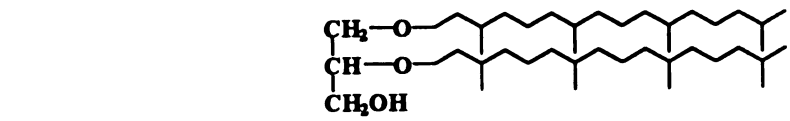

(A1)

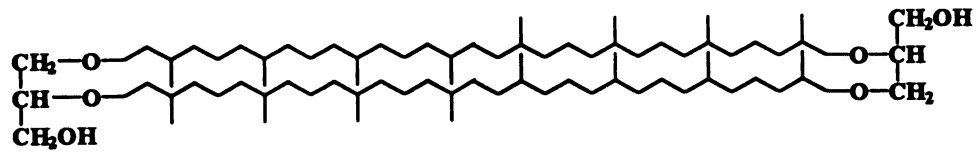

(A2)

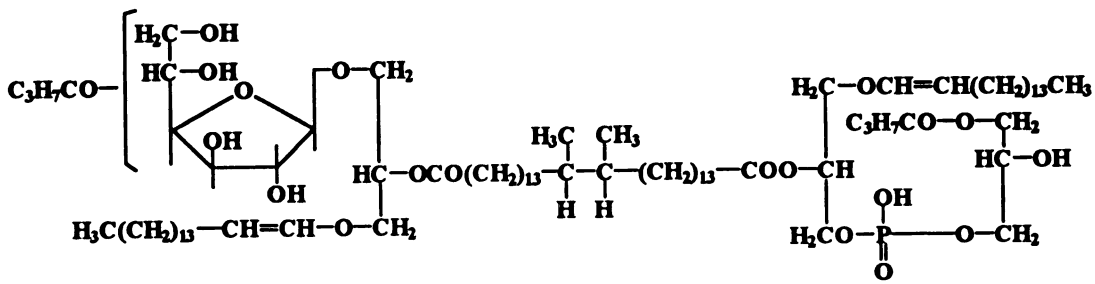

(B)

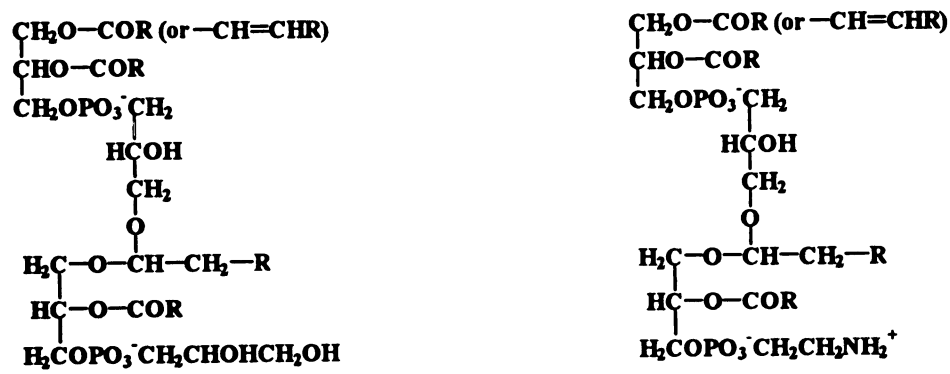

(C1) (C2)

Figure 1.3: Structures of novel lipids from bacteria. diether lipid (A1) and tetraether lipid (A2) from archaebacteria; a diabolic acid-containing phospholipid (B) from *Butyrivibrio* S2; phosphatidylglycerol (C1) and phosphatidylethanolamine (C2) acetals of plasmalogens from clostridia.

appears that membrane fluidity, which is the inverse of viscosity, regulates the activities of integral membrane enzymes [19]. To accomplish this, the composition of the membrane must be readily varied. Thus lipid diversity can be linked to adaptation since it is the result of the dynamic regulation of membrane fluidity by modifying lipid head groups or by controlling the distribution of fatty acids length, branching and unsaturation. This phenomenon, referred to as homeoviscous adaptation, was first described for *Escherichia coli* cells. The fluidity of membrane lipids from *Escherichia coli* cells grown at 43°C is lower than that of lipids from 15°C-cells when compared at a common temperature, whereas fluidities were nearly equivalent when compared at the respective growth temperatures [20]. This is a very important finding since it demonstrates a connection between a bulk property of a membrane, temperature and function. It seems clear that with a biological system at constant temperature, the degree of biomembrane fluidity is a direct reflection of the transition temperature of the lipids. This transition temperature varies with temperature in a dynamic fashion allowing the membrane to be at this critical state over an appreciable temperature range. This in turn can regulate the insertion, aggregation and diffusional movements of the protein and lipid components as well as the permeability characteristics of the membrane. It is thought by some that gel-state lipids do not appear to be present in most biological membranes (particularly those of eukaryotic cells) since the unsaturated nature of most naturally occurring lipids results in hydrocarbon transitions which occur well below physiological temperatures. Such analyses refer only to the alkyl chains which may occur in the gel state. At physiological temperatures most membrane lipids are thought to be fluid and completion of the

membrane melt below the growth temperature is common in Gram-positive bacteria. *Yersinia enterocolitica* grown at 37°C has its membrane fully melted by 8°C [21].

It has been emphasized, however, that control of membrane fluidity is not the only purpose for the occurrence of such a large variety of lipids in biological membranes [22,23]. All biological membranes contain a certain balance of bilayer-preferring and nonbilayer-preferring lipids and regulate this ratio by modification of the lipid composition in order to ensure an optimal degree of lipid stability and functionality. Furthermore, it has been suggested that local regions of lipids forming transitory nonlamellar phases may be advantageous to some membrane-mediated phenomena such as membrane fusion and transbilayer transport processes requiring local departures from bilayer organization.

Lipids in water spontaneously aggregate to produce a variety of supramolecular structures whose conformations depend on temperature, concentration, the presence of various ions, as well as the nature of the lipid molecule itself. The ability of lipids to form different supramolecular structures on hydration is commonly referred to as lipid polymorphism. These polymorphic structures include bilayer(lamellar), hexagonal and cubic phases (Figure 1.4). Examples of the non-bilayer forming lipids include unsaturated species of PE, plasmenylethanolamine, and monoglucosyldiacylglycerols (MGDG). Environmental factors such as temperature, divalent cations, ionic strength, and pH can strongly influence the polymorphic structural preferences of lipid systems. In the case of pure lipid systems, for example, reduction of the pH results in H_{II} phase structure for (unsaturated) PS and phosphatidic acid systems [8]. However, it is not clear why

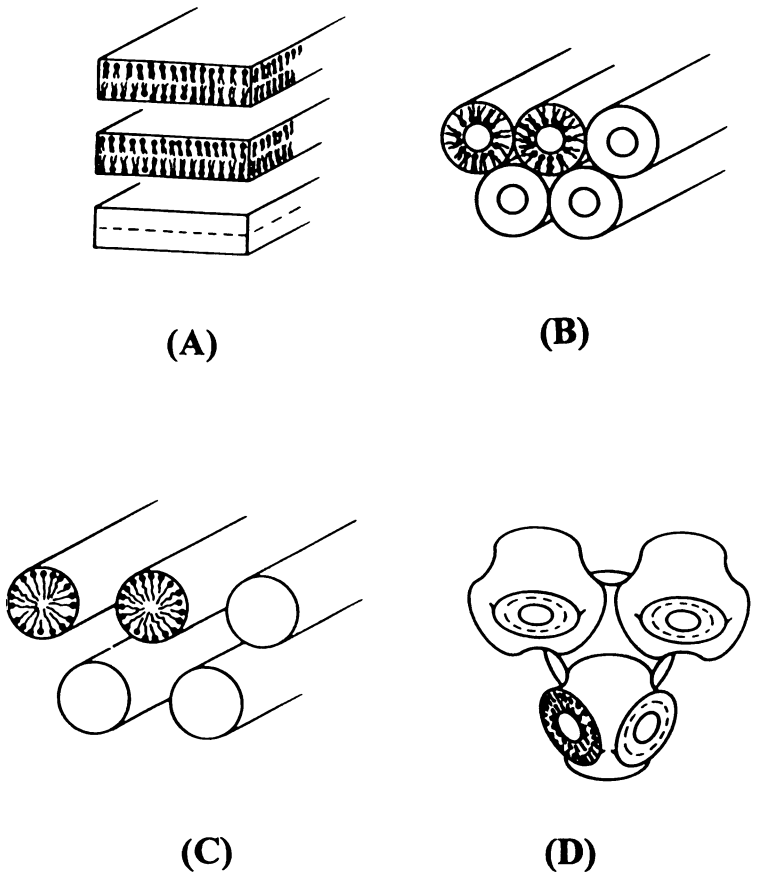

Figure 1.4: Lipid polymorphism in the liquid crystalline state. (A) lamellar phase (L_α); (B) hexagonal inverted phase (H_{II}); (C) hexagonal phase (H_I); (D) cubic phase. (adapted from ref. 25)

biomembranes should contain such a large proportion of non-bilayer lipids. For example, the membrane of *Escherichia coli* having a bilayer structure contains 70 per cent of PE, which has a strong tendency to aggregate in non-bilayer structure. In *E. coli* mutants lacking PE, membrane integration and functioning of important transport proteins were severely impaired and protein translocation was much reduced. It has been recently suggested that non-bilayer lipids in a biomembrane exert high internal lateral packing forces on membrane proteins and keep them in a functional state [24].

The various roles of non-bilayer lipids in membranes suggest the bilayer/nonbilayer lipid ratio needs to be closely regulated *in vivo*. The balance between bilayer-forming and non-bilayer forming lipids is actively regulated in cells growing under different environmental conditions. Two groups of bacteria that are either natural fatty acid auxotrophs or utilize exogenous fatty acids when endogenous synthesis is inhibited, *Acholeplasma laidlawii* and the butyric acid-producing clostridia, are capable of adjusting their lipid class compositions according to the degree of unsaturation of their aliphatic chains. As the content of *cis*-unsaturated fatty acids or temperature is increased, lipids that form an unstable lamellar phase at physiological temperatures are replaced with lipids that have larger effective polar head groups, and can therefore form more stable bilayers [26]. Studies of the packing and functioning of the membrane lipids of the bacterium *Acholeplasma laidlawii* led to a major hypothesis on the regulation of the lipid composition in the membrane, based on the equilibrium between lamellar and nonlamellar phases. The polar lipid composition in membranes of *Acholeplasma laidlawii* is extensively regulated as a response to environmental changes. The ratio between two major polar lipids, MGDG and diglucosyldiglyceride (DGDG) is altered

depending on temperature, configuration of incorporated fatty acids, and membrane cholesterol content. It was difficult to interpret this result based on models stressing the regulation of membrane fluidity since effect of lipid head group variation on total lipid phase transitions is small. MGDG prefers the hexagonal or cubic phase at physiological temperatures, whereas DGDG by itself forms a stable lamellar phase and can stabilize the lamellar phase of MGDG. As temperature, chain unsaturation, or cholesterol content is increased, the bilayer structure will be destabilized, and this tendency is counteracted by the conversion of MGDG to DGDG [27-29]. *Clostridium butyricum* cells are capable of regulating the stability of bilayer arrangement of the cell membrane by altering the ratio of the glycerol acetal of plasmenylethanolamine to the total PE in response to changes in lipid unsaturation [30,31]. The presence of H_{II} phase preferring PE in bilayer membranes increases the order in the hydrocarbon. This suggests that another major reason for lipid diversity in membranes. Their polymorphic capabilities may be directly related to establishing and regulating the order profile in the hydrocarbon chains [32].

Conformation and Packing of Membrane Lipids

The most of studies for the conformation of phospholipids have used the atom numbering and the notation of torsion angles introduced by Sundaralingam. In this convention the glycerol carbon atom to which the polar head group is attached is always designated C(1). This is inconsistent with the stereospecific numbering (*sn*) widely used to describe the stereochemistry of glycerolipids. In the *sn* convention the glycerol numbering of glycerolipids with the natural configuration is reversed in which the polar group is attached to carbon atom C(3) (Figure 1.5).

More specific structural information on the atomic level is necessary in order to obtain a detailed understanding of lipid-lipid and lipid-protein interactions and variations in structure and composition of lipids observed in different types of membranes. The molecules form disordered liquid-crystalline arrays and consequently classical techniques for determining molecular structure yield only a limited amount of information. For instance, X-ray and neutron diffraction experiments provide data on distance within the bilayer plane and on bilayer thickness and hydrocarbon chain separation, but, because of the presence of disorder, they cannot yield interatomic distances and angles such as are available from single-crystal experiments [33].

It is known from many fields that structural features in crystals often reflect conditions in less ordered system. In the gel state the molecules have such a close proximity that local order resembling that in solid state most likely exists. Even if the conformation of a molecule is dependent on its environment, intramolecular forces give rise to preferred conformations. The primary technique for deriving the three-dimensional structure in the solid state is X-ray crystallography. Provided that suitable single-crystals are available, it allows the determination of the positions of atoms in space with high precision yielding bond lengths, angles and torsion angles. Furthermore, details of the molecular packing arrangement and internuclear distances are obtained. It appears that the lipid structures in these crystals are similar to those adapted in the fully hydrated form. It was in 1974 that the first crystal structure of a phospholipid, PE, was reported [35]. The only crystal structure of a glycolipid that has been determined is so far for a cerobroside [36]. High-resolution structures from X-ray crystallography have been

(A)

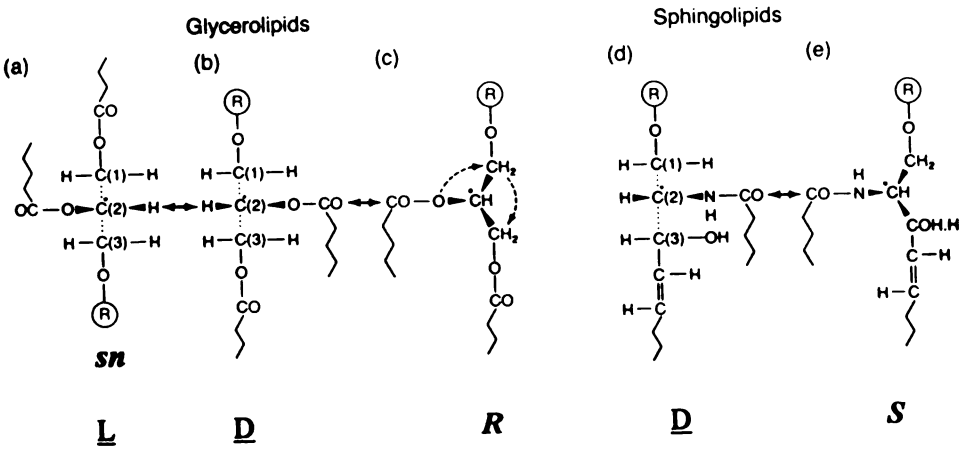

(B)

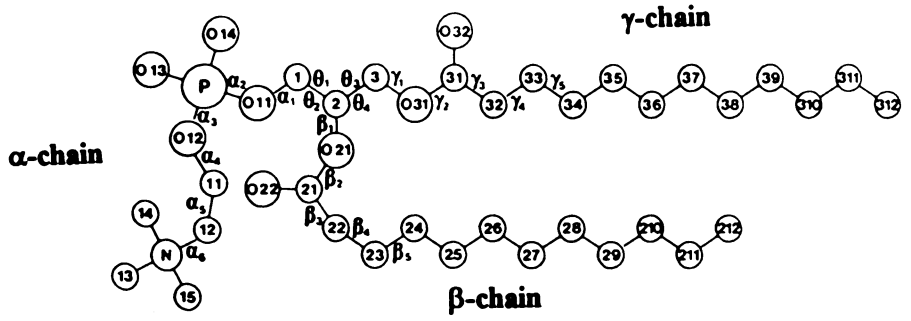

Figure 1.5: Stereochemical conventions and conformational notations for lipid molecules. (A) Stereochemistry of carbon atom C*(2) of glycerolipids and spingolipids. The *R/S*, D/L and *sn* nomenclature are illustrated for the C(2) positions; (B) Atom numbering and notation for torsion angles according to Sundaralingam illustrated for phosphatidylcholine. (adapted from ref. 34)

reported for several other membrane lipids: lyso-PC [37], dipalmitoyl-PA [38], dimyristoyl-PC [39], and dimyristoyl-PG [40]. The molecular structures of some of phspholipids obtained from single crystal analyses are shown in Figure 1.6. Several studies have also been carried out on the conformation of phospholipids in multibilayer preparations using deuterium NMR spectroscopy [41]. In general, the two principal features of the structures are the "bent-down" configuration of the headgroup and the nonequibalance of the two acyl chains. The orientation of head group is nearly parallel to the bilayer plane. This is true for PE, PC, and PG. The parallel orientation of the zwitter ionic head group of PC and PE is the most stable arrangement. Although there is a preferred conformation in the α-chain (head group), the orientation of the head group with respect to the diacylglycerol moiety varies widely. The acyl chain orientation is parallel to the surface normal in the liquid crystalline state and is either parallel or tilted to the normal in the gel state. In either case, X-ray crystallography as well as NMR spectroscopy studies indicate that the initial part of *sn*-2-fatty acid chain extends perpendicularly from the glycerol backbone but bends off at the second carbon atom to become parallel to the *sn*-1 chain. Therefore the β-chain does not extend as far into the bilayer as the γ-chain. The same type of chain stacking is found in the PE crystal [34]. This diglyceride conformation must therefore be considered to be a general, preferred feature in membrane phospholipid conformation. The axial displacement of the two fatty acid chains by 3.7 Å (3 methylen groups) is compensated in natural phospholipids by different chain lengths of the two fatty acids. This reduces the interdigitation of the ends of the hydrocarbon chains at the bilayer center. Deuterium NMR spectroscopy has been

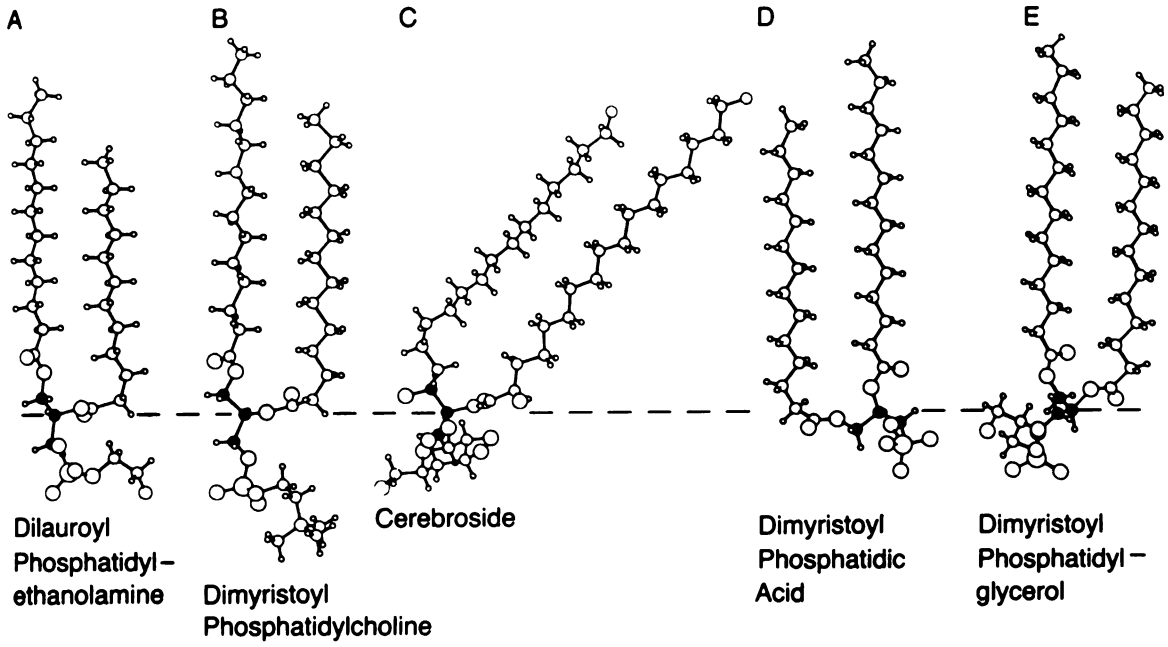

Figure 1.6: Structures of membrane lipids as determined by X-ray crystallography. The three glycerol and spingosine carbon backbone atoms have been colored black. (adapted from ref. 42)

used to probe the head group orientation and the motional characteristics of 1,2-di-*O*-tetradecyl-3-*O*-β-glucopyranosylglycerol. It has been shown that the head group is extended away from the bilayer surface and the glycerol backbone is found to have motional properties similar to those found for phospholipids, but to be more ordered than the carbohydrate moiety [43].

The most important feature of membrane-forming lipids is the balance of hydrophilic and hydrophobic forces between the polar head-group and non-polar acyl parts of the molecule. These forces in turn are governed by the size and charge of the head-group, the length of the hydrocarbon chain and the presence or absence of double bonds or methyl branches. The lipid continuum is created by lipid-lipid interactions by electrostatic bonding between charges or dipoles of the head-groups, hydrogen bonding between head-groups and van der Waals forces between the hydrocarbon chains of acyl (or alkyl) residues. The fundamental principle governing the molecular packing is maximization of these interaction energies between the various regions of the lipid molecule. Most glycerophospholipids pack tail-to-tail forming a typical bilayer structure. The hydrocarbon chains are essentially close-packed, with average intra- and intermolecular chain spacing of 4.6 Å. Nature has many ways of accommodating the mismatching in the bilayer form. For instance, excess area occupied by the head groups may be accommodated by chain tilting. Alternatively, stacking of the head groups may also reduce their total cross-section area. The angle of tilt of the hydrocarbon chain axis with respect to the bilayer normal (ϕ) is given by $\phi = \cos^{-1} n\Sigma/S$ (S = molecular area at the layer interface ; Σ = cross-sectional area of the hydrocarbon chains perpendicular to the

chain axis ; n = number of the hydrocarbon chains) [44]. In case of the crystal structure of PE, nΣ equals precisely the molecular area S, hence no chain tilt is observed. PC and cerebrosides are packed with chain tilting resulting from having a bulky headgroups (S > 2Σ). The molecular arrangement of PC is shown in Figure 1.7. In contrast, an extreme chain tilt of 57.5° is present in the crystal structure of 3-palmitoyl-PE where nΣ/S = 0.537. If the mismatching becomes too great to be accommodated by chain tilting, chain interdigitation may occur. At S ≥ 2nΣ, interdigitation occurs for lysophosphatidylcholine analogs [45].

The lipids can self-assemble into aggregates other than bilayers as discussed earlier. The theory to explain polymorphism involves an interplay of thermodynamics, interaction forces, and molecular geometry. The particular form which predominates depends on intrinsic factors such as the nature of the lipid head group, the length and degree of unsaturation of the lipid hydrocarbon chains or extrinsic factors such as temperature, pressure, ionic strength, hydration, divalent cations and pH [46]. The physical basis of lipid polymorphism has been explained by simplistic hypothesis that molecular geometry is a primary factor in determining the phase preference of lipids [8,47]. Lipid geometries are quantitatively described by a dimensionless packing parameter, $p = v/(a_o l_c)$, where v is the hydrophobic volume of the acyl domain which depends on their thermal motion, l_c is the length of the acyl chains, and a_o is the optimal surface area at the aqueous interface. The possible values of the packing parameter and the predicted aggregates are shown in Figure 1.8. Detergent-type lipids for which $p \leq$ 0.33 have an inverted cone shape which packs most efficiently in the form of spherical

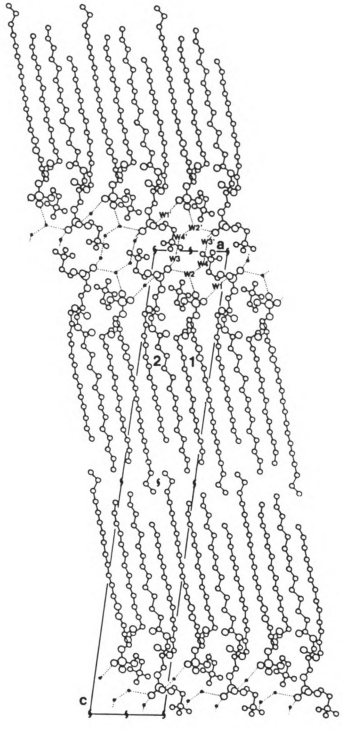

Figure 1.7: Molecular packing in the single-crystal structure of 2,3-dimyrisoyl-D-glycero-1-phosphatidylcholine dihydrate projected onto the a-c plane. (adapted from ref. 34)

LIPID	PHASE	MOLECULAR SHAPE	CRITICAL PACKING PARAMETER (v/l S.)
Lysophospholipids Detergents	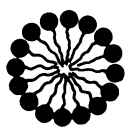 Micellar	 Inverted Cone	<⅓ (Sphere) ⅓ to ½ (Globular Shapes; Rods)
Phosphatidylcholine Sphingomyelin Phosphatidylserine Phosphatidylinositol Phosphatidylglycerol Phosphatidic Acid Cardiolipin Digalactosyldiglyceride	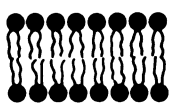 Bilayer	 Cylindrical	½ to 1
Phosphatidylethanolamine (Unsaturated) Cardiolipin - Ca^{2+} Phosphatidic Acid - Ca^{2+} (pH < 6.0) Phosphatidic Acid (pH < 3.0) Phosphatidylserine (pH < 4.0) Monogalactosyldiglyceride	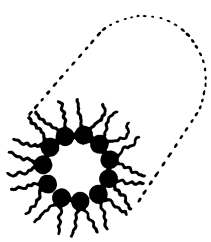 Hexagonal (H_{II})	 Cone	>1

Figure 1.8: Polymorphic phases, molecular shapes and critical packing parameter for some membrane lipids. (adapted from ref. 42)

micelles. Lipids for which $0.5 \leq p \leq 1.0$ posses a cylindrical geometry which packs most efficiently in the form of a bilayer. Most phospholipids are likely to form bilayers. Finally, in lipids for which $p \geq 1.0$, the hydrophobic volume is larger than the head group area, resulting in a conical geometry that packs most efficiently in the form of a hexagonal phase (H_{II}). Diacyl phospholipids possessing a small head group such as PE exemplify this class of lipids that favor nonbilayer structures. The molecular geometry is a dynamic attribute of lipid structure subject to perturbation by environmental factors. These perturbations can be sufficiently large to alter the most efficient packing arrangement.

Structural Analysis of Lipids

The analysis of membrane lipids is very tedious and time-consuming but challenging since membranes contain thousands of molecular species. It requires a combination of several analytical techniques including extraction, separation, derivatization and characterization. The solvent system most commonly used to extract membrane lipids is based on the procedure described by Bligh and Dyer [48], using chloroform and methanol. Various chromatography techniques including TLC, HPLC, and column chromatography using supports such as silicic acid, DEAE cellulose and aluminum oxide are typically employed for purification. The recent development of HPLC procedures for the separation and quantitative isolation of phospholipids has allowed detailed characterization of lipids in many biological samples [49-51]. However, HPLC of natural lipids has been hampered by the absence of easily detectable functional

groups on most lipids using the more common types of detectors. Most frequently, the phospholipids have been detected using ultraviolet absorption between 200-210 nm [52], fluorescence [53], flame ionization [54], and mass detection [55]. The excellent review presented by Shukla summarizes recent developments and applications on lipid analysis by HPLC [56].

Mass spectrometry methods have proven useful for the study of intact lipids. Phospholipids have traditionally been characterized by enzymatic degradation with specific phospholipases and subsequent chromatographic and mass spectral analyses of the reaction products after chemical derivatization. The structural analysis of intact lipids by mass spectrometry like other biological molecules has been restricted by the involatility and thermal instability. Mass spectrometry with a variety of soft ionization techniques such as field desorption (FD), plasma desorption (PD), fast atom bombardment (FAB), matrix assisted laser desorption ionization (MALDI), and electrospray ionization (ESI) has been used for the direct analysis of lipids. The various ionization techniques for the structural characterization of phospholipids have also reviewed [57-59]. Field desorption mass spectrometry has been used for the analyses of intact phospholipids [60], but its usefulness is somewhat reduced by the fact that numerous supramolecular ions are observed. FAB mass spectrometry has made a significant impact on the analysis of intact lipids. It provides abundant pseudomolecular ions as well as characteristic fragmentation ions in most cases [61-63]. FAB tandem mass spectrometry (FAB/MS/MS) is very powerful for the analysis of complex lipids even in mixtures because it adds a mass spectrometric separation step prior to final analysis [64,65]. FAB/MS/MS provides molecular and characteristic fragment ions to allow the

determination of the head group and acyl groups of the individual molecular species. In addition, the relative abundance of specific fragment ions in the product ion spectrum can, in most cases, be used to assign the position of the acyl groups on the glycerol backbone [66]. FAB/MS/MS of the carboxylate anions has been used to determine the positions of double bonds and branch points in the acyl groups by analysis of charge-site-remote fragmentation patterns [67]. FAB/MS and FAB/MS/MS has been also applied to the identification and classification of microorganisms, and also for the study of microbial physiology [68-70]. ESI/MS has recently been used for the analysis of phospholipids with several advantages over FAB/MS, including lower background signals, greater sensitivity, and compatibility with liquid chromatographs [71-73]. ESI/MS allows the simultaneous quantification of lipids having different surface activities because ESI is relatively insensitive to modest differences in surface activities of phospholipid classes [74]. Recently, Harvey and Marto have examined MALDI as a technique for the structural characterization of phospholipids [75,76].

Modern nuclear magnetic resonance (NMR) spectroscopy offers a convenient method to solve complex chemical structural problems. NMR spectroscopy serves as a simple, nonselective and nondestructive technique for the lipid analysis even without any need for prior separation. The powerful techniques of two-dimensional and multinuclear (1H, 13C, 31P) NMR spectroscopy open the new dimension for structural and conformational analysis of lipids. Phosphorous-31 NMR spectroscopy has been shown to provide an accurate qualitative and quantitative analysis of phospholipids [77]. It has been also attempted to identify lipid classes present in the membrane and to determine the relative concentrations using a data base of standard lipid characteristic resonances

derived from single membrane lipids and known mixture of them [78]. Rapid separation of total lipids into different classes using ion-exchange columns and NMR spectroscopy allows to assign glycerides, cholesterol, spingolipids and ether lipids as well as of diacylcholine and ethanolamine lipids [79]. As the cell membranes are one of the targets of drug treatment of cancer cells, their membrane composition and variations need to be analyzed. ^{31}P and ^{1}H spectroscopy was used to follow qualitative and quantitative modifications induced in the plasma membrane by malignant tumors [80]. Gradient selected 2D-NMR inverse heteronuclear chemical shift correlations have been used for signal assignment in proton, carbon and phosphorous spectra for neutral lipids and phospholipids [81].

REFERENCES

1. E. Canale-Parola, *Bacteriol. Rev.*, 1970, **34**, 82-97.
2. S. Jung, S.E. Lowe, R.I. Hollingsworth, and J. G. Zeikus, *J. Biol. Chem.*, 1993, **268**, 2828-2835.
3. S. Jung and R.I. Hollingsworth, *J. Lipid Res.*, 1994, **35**, 1932-1945.
4. L.R. Bérubé and R.I. Hollingsworth, *Biochemistry*, 1995, **34**, 12005-12011.
5. S.J. Singer and G.L. Nicolson, *Science*, 1972, **175**, 720-731.
6. C. Ratledge and S.G. Wilkinson, 1988, *Microbial Lipids* Vol. 1, pp 1-22, Academic Press, New York.
7. K.H. Schleifer and O. Kandler, *Bacteriol. Rev.*, 1972, **36**, 407-477.
8. P.R. Cullis and B. de Kruijff, *Biochim. Biophys. Acta.*, 1979, **59**, 399-420.
9. S.E. Lowe, M.K. Jain, and J.G. Zeikus, *Micobiol. Rev.*, 1993, **57**, 451-509.

10. H.H. Mantsch, C. Madec, R.N.A.H. Lewis, and R.N. McElhaney, *Biochim. Biophys. Acta.*, 1989, **980**, 42-49.

11. M. Sinensky, *Proc. Natl. Acad. Sci. USA*, 1974, **71**, 522-525.

12. L. Huang, S.K. Lorch, G.G. Smith, and A. Huang, *FEBS Lett.*, 1974, **43**, 1-5.

13. A.F. Esser and K.A. Souza, *Proc. Natl. Acad. Sci. USA,* 1974, **47**, 4111-4115.

14. B. Mycke, F. Narjes, and W. Michaels, *Nature*, 1987, **326**, 126-127.

15. M. Oshima and T. Agriga, *J. Biol. Chem.*, 1975, **250**, 6963-6968.

16. A. Gliozzi, S. Bruno, T.K. Basak, M. de Rosa, and A. Gambacorta, *System. Appl. Microbiol.*, 1986, **7**, 266-271.

17. H. Hauser, *Nature,* 1979, **279**, 536-538.

18. N.C. Johnson and H. Goldfine, *Eur. J. Biochem.*, 1994, **223**, 957-963.

19. R.N. McElhaney, *Biomembranes*, 1984, **12**, 249-278.

20. J.R. Hazel and E.E. Williams, *Prog. Lipid Res.*, 1990, **29**, 167-227.

21. C.A. Abbas and G.L. Card, *Biochim. Biophys. Acta*, 1980, **602**, 469-477.

22. H.-J. Hinz, L. Six, K.-P. Ruess, and M. Liefländer, *Biochemistry*, 1985, **24**, 806-813.

23. B. de Kruijff , *Nature*, 1987, **329**, 587-588.

24. B. de Kruijff, *Nature*, 1997, **386**, 129-130.

25. S.M. Gruner ,1992, in *The Structure of Biological Membranes,* pp. 211-250. (P. Yeagle, ed.), CRC Press, Boca Raton.

26. H. Goldfine, *J. Lipid Res.*, 1984, **25**, 1501-1507.

27. Å. Wieslander, A. Christiansson, L. Rilfors, and G. Lindblom, *Biochemistry*, 1980, **19**, 3650-3655

28. Å. Wieslander, L. Rilfors, L. B.-A. Johanson, and G. Lindblom, *Biochemistry*, 1981, **20**, 730-735.

29. Å. Wieslander, L. Rilfors, and G. Lindblom, *Biochemistry*, 1986, **25**, 7511-7517.

30. Y. Koga and H. Goldfine, *J. Bacteriol.*, 1984, **159**, 597-604.

31. H. Goldfine, N.C. Johnston, J. Mattai, and G.G. Shipley, *Biochemistry*, 1987, **26**, 2814-2822.

32. P. R. Cullis, M.J. Hope, and Colin P.S. Tilcock, *Chem. Phys. Lipids*, 1986, **40**, 127-144.

33. R.G. Griffin, L. Powers, and P.S. Pershan, *Biochemistry*, 1978, **17**, 2718-2722.

34. H. Hauser, I. Pascher, R.H. Pearson, and S. Sundell, *Biochim. Biophys. Acta,* 1981, **650**, 21-51.

35. P.B. Hitchcock, R. Mason, K.M. Thomas, and G.G. Shipley, *Proc. Natl. Acad. Sci. USA*, 1974, **71**, 3036-3040.

36. I. Pasher and S. Sundell, *Chem. Phys. Lipids*, 1977, **20**, 175-191.

37. H. Hauser, I. Pasher, and S. Sundell, *J. Mol. Biol.* 1980, **137**, 249-264.

38. K. Harlos, H. Eibl, I. Pascher, and S. Sundell, *Chem. Phys. Lipids,* 1984, **34**, 115-126.

39. R.H. Pearson and I. Pascher, *Nature,* 1979, **281**, 499-501.

40. I. Pascher, S. Sundell, K. Harlos, and H. Eibl, *Biochim. Biophys. Acta,* 1987, **896**, 77-88.

41. J. Seelig, R. Dijkman, and G.H. de Haas, *Biochemistry,* 1980, **19**, 2215-

42. R.B. Gennis, 1989, *Biomembranes: Molecular Structure and Function*, Springer-Verlag, New York.

43. H.C. Jarrell, J.B. Giziewicz, and I.C.P. Smith, *Biochemistry*, 1986, **25**, 3950-3957.

44. H. Hauser and G. Poupart, "Lipid Structure" , 1991, in *The Structure of Biological Membranes,* pp. 3-71 (P. Yeagle, ed) CRC Press, Boca Raton.

45. S.W. Hui and C.-H. Huang, *Biochemistry*, 1986, **25**, 1330-1335.

46. C.P.S. Tilcock, *Chem. Phys. Lipids*, 1986, **40**, 109-125.

47. J.N. Israelachvili, S. Marcelja, and R.G. Horn, *Q. Rev. Biophys.*, 1980, **13**, 121-200.

48. E.G. Bligh and W.J. Dyer, *J. Biochem. Physiol.*, 1959, **37**, 911-917.

49. T.L. Kaduce, K.C. Norton, and A.A. Spector, *J. Lipid Res.*, 1983, **24**, 1398-1403.

50. S.S. Chen and A.Y. Kou, *J. Chromatogr.*, 1982, **227**, 25-31.

51. G.M. Patton, J.M. Fasulo, and S.J. Robins, *J. Lipid Res.*, 1982, **23**, 190-196.

52. S.U. Rehman, *J. Chromatogr.*, 1991, **567**, 29-37.

53. W. Bernhard, M. Linck, H. Creutzburg, A.D. Postle, A. Arning, I. Martin-Carrera, and K.-Fr. Sewing, *Anal. Biochem.*, 1994, **220**, 172-180.

54. F.C. Phillipis, W.L. Erdahl, J.D. Nedenicek, L.J. Nutter, J.A. Schmit, and O.S. Privett, *Lipids*, 1984, **19**, 142-150.

55. W.W. Christie, *J. Chromatogr.*, 1986, **361**, 396-399.

56. V.K.S. Shukla, *Pro. Lipid. Res.*, 1988, **27**, 5-38.

57. T. Matsubara and A. Hayashi, *Prog. Lipid Res.*, 1991, **30**, 301-322.

58. N.J. Jensen and M.L. Gross, *Mass Spectrom. Rev.*, 1988, **7**, 41-70

59. E. Benfenati and R. Reginato, *Biomed. Mass Spectrom.*, 1985, **12**, 643-651.

60. W.D. Lehmann and M. Kessler, *Biomed. Mass Spectrom.*, 1983, **10**, 220-226.

61. G.R. Fenwick, J. Eagles, and R. Self, *Biomed. Mass Spectrom.*, 1983, **10**, 382-386.

62. B.N. Pramanik, J.M. Zechman, P.R. Das, and P.L. Bartner, *Biomed. Environ. Mass Spectrom.*, 1990, **19**, 164-170.

63. R.C. Murphy and K.A. Harrison, *Mass Spectrom. Rev.*, 1994, **13**, 57-75.

64. K.A. Kayganich and R.C. Murphy, *Anal. Chem.*, 1992, **64**, 2965-2971.

65. D.A. Gage, Z.-H. Huang, and C.C. Sweeley, 1994, in *Mass Spectrometry: Clinical and Biomedical Applications*, Vol 2, (D.M. Desiderio ed.) Plenium Press, New York.

66. Z.-H. Huang, D.A. Gage, and C.C. Sweeley, *J. Am. Soc. Mass Spectrom.*, 1992, **3**, 71-78.

67. M.L. Gross, *Mass Spectrom. Rev.*, 1989, **8**, 165-187.

68. D.N. Heller, R.J. Cotter, C. Fenselau, and O.M. Uy, *Anal. Chem.*, 1987, **59**, 2806-2809.

69. Cole and C.G. Enke, *Anal. Chem.*, 1991, **63**, 1032-1038.

70. R. Wait, 1992, in *Mass Spectrometry in the Biological Sciences: A Tutorial*, pp427-441, Kluwer Academic Publishers, Netherlands.

71. P.B. Smith, A.P. Snyder, and C.S. Harden, *Anal. Chem.*, 1995, **67**, 1824-1830.

72. H.-Y. Kim, T.-C.L. Wang, and Y.-C. Ma, *Anal. Chem.*, 1994, **22**, 3977-3982.

73. J.L. Kerwin, A.R. Tuininga, and L.H. Ericsson, *J. Lipid Res.*, 1994, **35**, 1102-1114.

74. X. Han and R.W. Gross, *Proc. Natl. Acad. Sci. USA*, 1994, **91**, 10635-10639.

75. D.J. Harrey, *J. Mass Spectrom*, 1995, **30**, 1333-1346.

76. J.A. Marto, F.M. White, S. Seldomridge, and A.G. Marshall, *Anal. Chem.*, 1995, **67**, 3979-3984.

77. S. Bradamante, E. Barchiesi, L. Barenghi, and F. Zoppi, *Anal. Biochem.*, 1990, **185**, 299-303.

78. M.L. Sparling, R. Zidovetaki, L. Muller, and S.I. Chan., *Anal. Biochem.*, 1989, **178**, 67-76.

79. G.T. Choi, M. Casu, and W.A. Gibbons, *Biochem. J.*, 1993, **290**, 717-721.

80. M. Kriat, J. Vion-Dury, S. Confort-Gouny, R. Favre, P. Viout, M. Sciaky, and P.J. Cozzone, *J. Lipid Res.*, 1993, **34**, 1009-1019.

81. J. Henke, W. Willker, J. Engelmann, and D. Leibfritz, *Anticancer Res.*, 1996, **16**, 1417-1427.

CHAPTER II

A DYNAMICALLY REGULATED TRANSFORMATION OF THE BILAYER MEMBRANE OF BACTERIA TO A CROSS-LINKED 2-DIMENSIONAL SHEET DURING ADAPTATION TO UNFAVORABLE ENVIRONMENTAL PRESSURES

ABSTRACT

The membrane is a critical molecular matrix of living systems in which several enzymatic catalytic activities are embedded. Molecular motion and dynamics are critical in regulating enzyme activity. For membrane-associated enzymes, this motion is controlled by vibrational / collisional exchanges between these enzymes and the membrane lipid chains. To maintain an optimum dynamic range, membranes of living systems must have the ability to regulate their translational and vibrational motion in the face of environmental changes that might be offset it. The greater adaptability of an organism, the more spectacular the adaptative changes are likely to be. *Sarcina ventriculi* is used as a case study to explore membrane structural reorganizations which allow some organisms to be tolerant or adaptable to environmental extremes. This organism was found to be capable of a variety of unusual and dramatic processes including lipid alkyl chain tail-to-tail coupling. There is also inter-lipid head group transfer or lipid headgroup shuffling to possibly fine tune membrane dynamics. The tail-to-tail coupling activity is capable of joining foreign (exogenously added) hydrocarbon chains to the native chains confirming the assertion that this unpredictable and unusual chemistry does occur. The adaptative processes occur dynamically and instantaneously and render this organism tolerant to low pH, moderately high temperatures, and the presence of organic solvents and a wide spectrum of antibiotics at concentrations as high as 200 μg/mL. The membranes of this and other organism with similar membrane chemistry should exist in a dynamic equilibrium somewhere between bilayers and cross-linked bipolar monolayers. Under very extreme conditions, such membranes should approach highly cross linked,

two-dimensional molecular sheets. These structural reorganizations parallel the same strategies used by organic chemists in their effort to synthesize stabilized monolayers and vesicles. Enzymatic activities in the membranes of this and similar organisms hold much potential for use in stabilizing supramolecular arrays and nano structures.

INTRODUCTION

Membranes are critical components of the cell surface of living organisms and are responsible for maintaining cellular integrity whilst still maintaining contact and communication with the environment and with other cells or organisms. This contact and communication include the passage of metabolites out of the cell and the passage of nutrients in. In addition, it includes the sensing and preliminary responses to stimuli. These functions often require catalytic or structural reorganizational events which require precise and very concerted molecular motion. At the same time, sufficient rigidity is required in order to maintain structural integrity. Membranes, therefore, must possess very sophisticated molecular mechanisms for ensuring fluidity sufficient enough that molecular events can take place in the correct time scale. They must also have sufficient rigidity to preserve cellular integrity. The term "homeoviscous adaptability" has been used to describe the process whereby, after a perturbation which changes membrane viscosity, the membrane chemistry of an organism is immediately altered so as to restore the original viscosity or fluidity [1]. For modest changes in environmental parameters such as temperature, pressure or pH, these changes involve modification of fatty acid chain lengths, degree of unsaturation or modest changes in lipid composition [2,3]. There

are, however, some extremophilic microorganisms which can tolerate much more than modest changes in environmental parameters [4]. Such conditions include high temperatures, high or low pH, high salt concentrations, and the presence of organic solvents and antibiotics. These can all destroy membrane integrity. Organisms which can adjust to, still thrive in or even just survive such conditions must have very dynamic, rapid and efficient means of controlling membrane properties. The bilayer structure with independent lipid species is the generally accepted membrane model. It is normally a reasonable departure point for rationalizing the relationship between membrane structure and function for microorganisms.

Sarcina ventriculi is a Gram-positive bacterium which is tolerant to extremes of pH (2.0 to 10) as well as moderately high temperatures, and the presence of organic solvents [5-7]. In previous studies, we demonstrated that this tolerance was linked to the production of very long, bifunctional fatty acids which, we proposed, spanned the cell membrane and are synthesized by the tail-to-tail joining of membrane lipid chains between the bilayers to form bipolar transmembrane species which stabilize membrane structure [7-9]. The latter conclusion arose from the fact that if one knew the structures and abundances of all of the regular length fatty acids or aldehydes, then the structures and abundances of all of the very long bifunctional fatty acids can be accurately predicted. This was demonstrated by mathematical modeling [8] and by rigorous structural proof [9] of the actual very long chain bifunctional fatty acid species. The synthesis of α,ω-bifunctional fatty acids is not unique to *Sarcina ventriculi*. Similar fatty acids have been reported in *Butyrivibrio* sp. [10-13], *Thermatoga maritima* [14] and

Thermoanaerobacter ethanolicus [15] among others. In the case of *Butyrivibrio* sp., it was suggested that covalent tail-to-tail joining could have occurred and a structure for one transmembrane lipid species was proposed [13]. These organisms are all acclimatized to extreme environmental conditions, from the low pH conditions of the stomach in the case of *S. ventriculi*, to the high pressures and temperatures up to and above 90°C in geothermally active regions at the bottom of the ocean floor in the case of *Thermatoga maritima*. A parallel membrane organization is found in the archaebacteria except that the hydrocarbon chains in these organisms have ether linkages to their head groups and are isoprenoid in nature. Although there has been some debate to the contrary [16], it has been proposed that the transmembrane ether lipids found in the archae might also be formed by tail-to-tail coupling [17,18]. A related adaptative response in which the proportion of transmembrane ether lipids in archae increases with increased growth temperature is also seen in these organisms [19] and supports the tail-to-tail coupling mechanism. Transmembrane lipid synthesis, therefore, is an adaptative mechanism which has been adopted by a large cross section of extremophiles. These are other possible structural modification taking place in the adaptation of membrane structure and dynamics of highly adaptable organisms to changes in head group structure. These modifications result in the conversion of the bilayer to a 2-dimensional cross-linked molecular system with linkages occurring not only between the tails of the lipid chains but between the head groups as well as.

MATERIALS AND METHODS

Bacterial Cultures and Cell Extraction

S. ventriculi was grown and harvested as described previously [7]. The cells were extracted with 600 mL of 1,2-dichloroethane/chloroform/methanol/water (2:1:1:2 ratios in volume) under reflux for 24 h. The organic layer was then concentrated to dryness under a stream of nitrogen and the product re-dissolved in chloroform : methanol (1:1) for further analyses.

Tail-to-Tail Coupling of Foreign Fatty Acids

Cells (200 mL) were cultured anaerobically in the absence of the exogenous fatty acid at 37°C and pH 7. They were then harvested anaerobically by centrifugation, resuspended in 2 mL of oxygen free medium, lysed by French press under anaerobic conditions and hexadecanoic acid (1 mg) and methyl ethyl ketone (0.2 mL) were then added. The mixture was incubated at 45°C for 3 h and then the fatty acid composition was determined by GC/MS after converting them to methyl ester derivatives.

Isolation and Purification of Individual Lipids

Lipids were separated and isolated by preparative thin layer chromatography (TLC) on silica gel using a solvent system composed of chloroform / methanol / ammonia / water (3:3:1:0.1:0.05 by volume). Bands were removed from the layers by

scraping and extracting with chloroform/methanol (1:1). The eluates were brought to dryness under nitrogen and re-dissolved in $CHCl_3$/MeOH (1:1).

Fatty Acid Analyses

The whole cells were methanolyzed with 5% HCl in MeOH at 72°C for 24 h as described previously [9]. After concentration to dryness under nitrogen, samples were partitioned between chloroform and water and the aqueous layer was washed with chloroform. The combined chloroform solutions were brought to dryness and redissolved in chloroform.

Gas Chromatography and Mass Spectrometry

The components were then analyzed by fast atom bombardment mass spectrometry (FAB/MS). FAB mass spectra were recorded on a JEOL HX 110 double focusing mass spectrometer in both positive and negative modes with nitrobenzyl alcohol or glycerol as matrix. Collisionally activated dissociation tandem mass spectrometry (CAD-MS/MS) was conducted by scanning the electric sector and magnetic sector in a fixed ratio (B/E linked scan). Helium was used as the collision gas in a cell located in the first field-free region. The helium pressure was adjusted to reduce the abundance of the precursor ion by 50%. The fatty acid methyl esters were carried out on a gas chromatograph on a 25 m J&W Scientific DB1 Capillary column using helium as the carrier gas and a temperature-programmed from 150°C to 300°C (holding 30 min) at

3°C/min. GC/MS analysis was carried out using a JEOL JMS-AX505H mass spectrometer interfaced with a Hewlett-Packard 5980A gas chromatograph.

NMR Spectroscopy

NMR spectra were recorded on a Varian VXR-500 spectrometer (500 MHz for ^{1}H, 125 MHz for ^{13}C). The NMR solvent system was prepared as a mixture of pyridine-d_5/deuterium chloride in deuterium oxide/methanol-d_4/chloroform-d in a volume ratio of 1:1:2:10, respectively [19]. Chemical shifts are quoted relative to the chloroform resonance taken at 7.24 ppm for proton and 77 ppm for ^{13}C measurements. For the heteronuclear multiquantum coherence (HMQC) experiments, spectral width of the ^{13}C dimension was 3927 Hz. A total of 32 transients were acquired at 1024 points each. A total of 512 data sets were acquired. The total correlated spectroscopy (TOCSY) experiment was performed using a total of 512 data sets with 8 transients at 2048 data points each. A mixing time of 60 ms was used.

RESULTS AND DISCUSSION

Tail-to-Tail Coupling is Independent of New Protein Synthesis

Since formation of transmembrane lipid species is triggered by a perturbation of environmental factors, how quickly the process can be activated and what are the cellular steps leading to its activation were important questions the answers to which meant determining whether the activity was constitutive or whether it required new protein

synthesis or even new fatty acid synthesis. Attempts were therefore made to block the process by inhibiting new fatty acid synthesis with cerulenin and new protein synthesis with several antibiotics which are known to block protein synthesis at different stages. Thus, treatment of cells at pH 7 and 37°C with cerulenin, chloramphenicol, erythromycin, streptomycin, neomycin or tetracycline, followed by a temperature shift to 45°C resulted in no decrease in the tail-to-tail coupling response compared to controls without antibiotics. In fact, the proportion of transmembrane fatty acids synthesized in the presence of antibiotics after the perturbation was much greater than in the controls which lacked antibiotics. These results suggested that, somehow, antibiotics were actually promoting the formation of these transmembrane fatty acid species. This was confirmed by experiments in which the antibiotics were added but the system was not subjected to a temperature shift or any other perturbation. This led to the production of the same family of transmembrane species as was formed by a temperature shift in the absence of antibiotics (Figure 2.1). The levels of antibiotics used were as high as 200 μg/mL. Based on these results, it could be concluded that the formation of the very long bifunctional fatty acids takes place independently of new enzyme and fatty acid synthesis and is triggered by perturbing membrane structure or dynamics. This lack of dependence on new protein or fatty acid synthesis is consistent with the fact that these transmembrane fatty acid species can be detected immediately after the perturbing event. The adaptative process is very general and is triggered not only by pH change, temperature increase and the presence of solvents, but also by the action of any foreign substance which may interact with the cell membrane and tend to destabilize it. This is consistent with results

Figure 2.1: Gas chromatography profiles of the fatty acid methyl ester derivatives of the total membrane fatty acids of *Sarcina ventriculi* cultured at pH 7.0. (A) in the absence of antibiotics, (B) in the presence of streptomycin (100 μg/ml), (C) in the presence of chloramphenicol at the same concentration. The late eluting cluster of peaks in B and C are due to α,ω-bifunctional fatty acid methyl esters and aldehydes ranging from 28 to 36 carbon atoms long.

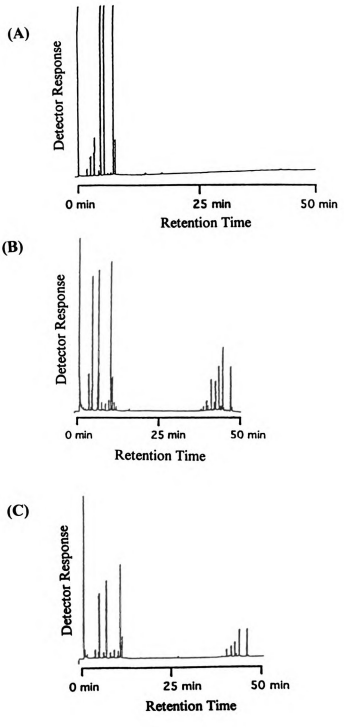
(A)
Detector Response
0 min
25 min
50 min
Retention Time
(B)
Detector Response
0 min
25 min
50 min
Retention Time
(C)
Detector Response
0 min
25 min
50 min
Retention Time

Figure 2.1

from the antibiotics tested here since they are either hydrophobic and neutral (in the case of chloramphenicol) and should partition into and disturb the lipid chains much like alcohols or they are polar and cationic and should bind to the lipid headgroups and disturb their arrangement. Either process should lead to destabilization of the membrane structure creating voids in the lipid packing thus increasing molecular motion and triggering the repair process.

The site-specific and stereospecific coupling of two inactivated alkyl chains is way beyond the realms of ordinary chemistry accomplished in the laboratory and would require a very sophisticated enzymatic system. It is clear from the antibiotic studies described above that the enzymatic activity responsible for this coupling event must be constitutive and an intact viable organism should not even be required.

Cell-Free Coupling Activity

In order to further test the conclusion that no new protein (and possibly no new message) synthesis is involved in the formation of these very long bifunctional fatty acid species and to definitively prove the primary conclusion that they are formed by random, indiscriminate (but enzymatic) tail-to-tail joining of existing fatty acids, we decided to try to demonstrate that foreign, exogenously-added fatty acids could be taken up intact into membrane vesicles of *S. ventriculi* and could be incorporated into the transmembrane lipid species. This is easily conceivable if the foreign fatty acids were incorporated into membrane vesicles to become permanently incorporated by covalent linkage to the tail of an opposing membrane lipid after the perturbation. Addition of heptadecanoic acid which is not normally found in membranes of *S. ventriculi* to a growing culture of that organism

at 37°C, followed by cell lysis by French press and a temperature shift to 45°C resulted in the formation of a family of chimeric fatty acid species with structures one half of which was formed from the foreign fatty acid and the other from a native species (Figure 2.2). In this experiment, methyl ethylketone was added as a final hydrogen acceptor which forms 2-butanol catalyzed by native oxidases to ensure that all of the potential cofactors were always oxidized and able to accept the two hydrogen atoms generated in the coupling process.

Characterization of Membrane Lipids

The important task in this study was to determine the individual lipid components to gain insight into the adaptation at the molecular level. The gas chromatogram of fatty acid methyl esters and their assignments obtained from *S. ventriculi* cells grown at pH 3 are shown in Figure 2.3 and Table 2.1. The previous studies proved that the long chain fatty acids are formed by the tail-to-tail coupling of preexisting fatty acids from opposite sides of the lipid bilayer [7,9]. Previous studies focus on the fatty acids, but no attempts were made to characterize the intact lipids in this bacterium. Proton NMR analysis of the aqueous fraction left after removal of the fatty acids and alkenyl ethers by acid hydrolysis and chloroform extraction from the total lipids of cells grown at pH 7 and 37°C revealed that glycerol, phosphoglycerol and glucose were the only components. ^{1}H-^{31}P correlated NMR spectroscopy of the crude lipid fraction showed cross peaks at 3.86 ppm and 3.92 ppm on the proton axis correlating with a chemical shift of 1.41 ppm on the phosphorous axis and attributable to phosphate in a phosphodiester linkage (data not shown). These

Figure 2.2: The EI mass spectrum of one of the chimeric bifunctional fatty acid dimethyl esters formed by tail-to-tail coupling between an exogenously added fatty acid (heptadecanoic acid) and an hexadecanoic acid residue from an *S. ventriculi* lipid component. The fragmentation pattern is indicated above the spectrum. Detailed discussions of the fragmentation modes for these molecules have been presented earlier [7,9]

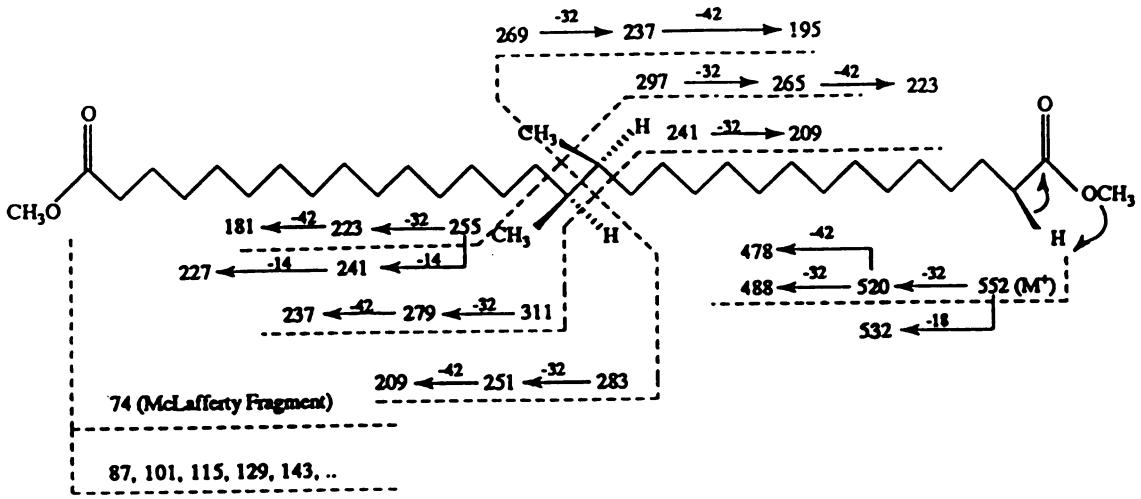
269 -32 237 -42 195
297 -32 265 -42 223
241 -32 209
CH3
H
O
CH3O
OCH3
181 -42 223 -32 255
227 -14 241 -14
237 -42 279 -32 311
209 -42 251 -32 283
74 (McLafferty Fragment)
87, 101, 115, 129, 143, ..
478 -42
488 -32 520 -32 552 (M+)
532 -18

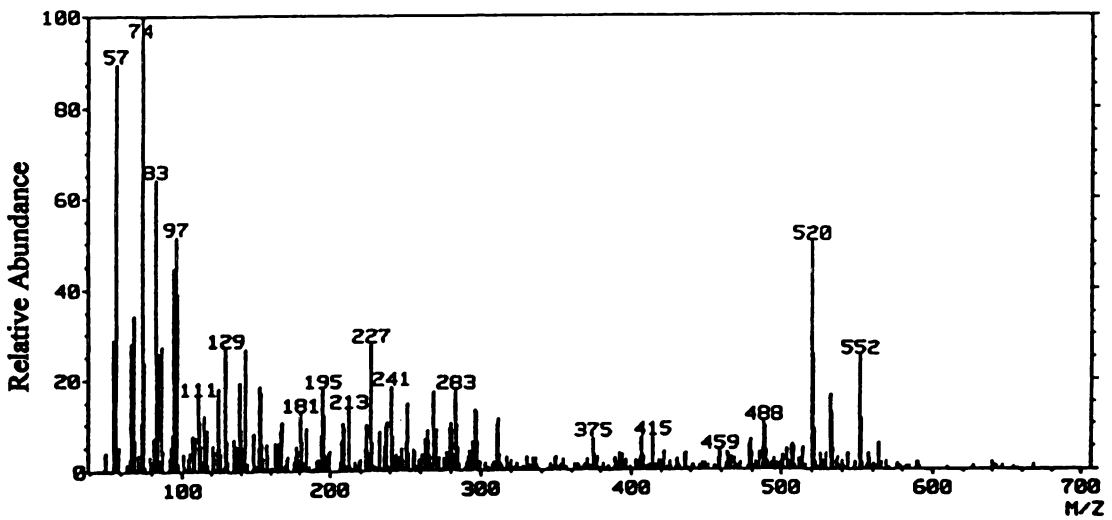
Relative Abundance
M/Z
100
80
60
40
20
0
100
200
300
400
500
600
700
74
57
83
97
129
111
195
181
213
227
241
283
375
415
459
488
520
552

Figure 2.2

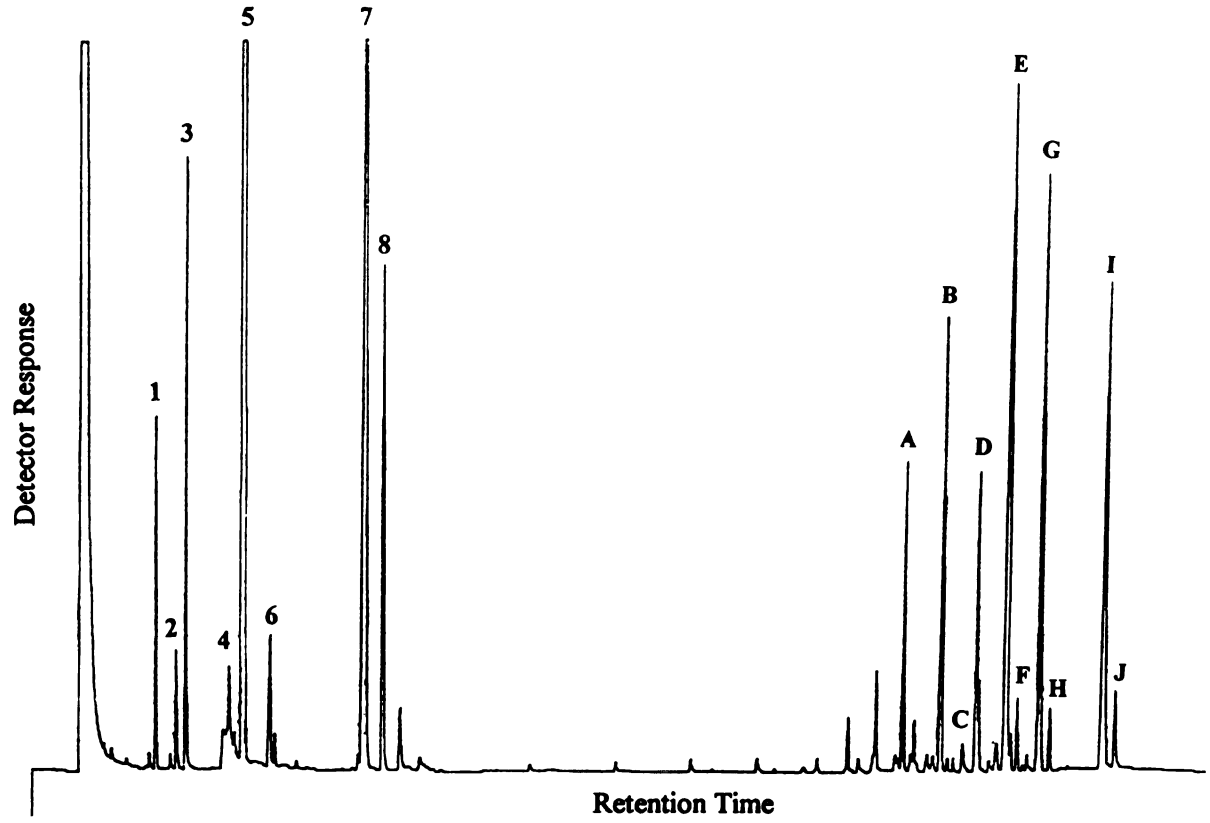

Figure 2.3: GC chromatogram of the total membrane fatty acid methyl esters of *S. ventriculi* cells grown at pH 3. The later eluting cluster of peaks is due to very long chain α,ω-bifunctional fatty acids. See Table 1 for assignments.

Table 2.1: List of fatty acids present in the membrane lipids of *S. ventriculi* cells grown at pH 3.

Peak # Fig. 6	Structure
1	$C_{14:0}$-carboxylic acid methyl ester
2	Octadecene
3	$C_{16:0}$-fatty aldehyde
4	Hexadecanol
5	$C_{16:0}$-carboxylic acid methyl ester
6	Hexadecanoic acid
7	$C_{18:1}$-carboxylic acid methyl ester
8	$C_{18:0}$-carboxylic acid methyl ester
A	$C_{32:0}$-fatty aldehyde
B	$C_{32:0}$-ω-formyl methyl ester
C	$C_{32:1}$-α,ω-dicarboxylic acid dimethyl ester
D	$C_{32:0}$-α,ω-dicarboxylic acid dimethyl ester
E	$C_{34:1}$-ω-formyl methyl ester
F	$C_{34:0}$-ω-formyl methyl ester
G	$C_{34:1}$-α,ω-dicarboxylic acid dimethyl ester
H	$C_{34:0}$-α,ω-dicarboxylic acid dimethyl ester
I	$C_{36:2}$-α,ω-dicarboxylic acid dimethyl ester
J	$C_{36:1}$-α,ω-dicarboxylic acid dimethyl ester

results were confirmed by FAB/MS after isolating the individual lipid components. The predominant components (Figures 2.4A-D) were diacylglycerol (DAG), monoglucosyldiacylglycerol (MGDG), lsyo-phosphatidylglycerol (lyso-PG) and phosphatidylglycerol (PG) containing palmitic acid ($C_{16:0}$), *cis*-vaccenic acid ($C_{18:1}$) and 1-hexadecenyl or 1-octadecenyl ethers as the primary fatty acid or alkyl components. Lesser ions corresponding to lipids containing tetradecanoic acid, other minor fatty acids and alkenyl ethers [8,9] were also observed. The presence of plasmalogen molecular species was also confirmed by FAB-CAD-MS/MS. The FAB-CAD-MS/MS experiment was performed for molecular ion at m/z 731 and compared to linked scan spectrum of molecular ion at m/z 747 (Figure 2.5). For the plasmalogen molecular specie there is only a single carboxylate anion, since the loss of the *sn*-1 position cannot occur as a carboxylate anion. The FAB-CAD-MS/MS spectrum of $[M-H]^-$ ion at m/z 731 gave one carboxylate anion at m/z 281 corresponding to *cis*-vaccenic acid whereas $[M-H]^-$ ion at m/z 747 yielded two carboxylate anions at m/z 255 (16:0) and 281(18:1).

A 2-dimensional ^{1}H-^{13}C HMQC NMR study also confirmed the mass spectrometric identification of the major lipid components from the pH 7 cells and indicated that glucose was present in the β-D-glucopyranosyl form (Figure 2.6A). This was indicated by the presence of a signal for the anomeric carbon of the glycosyl group at 103.5 ppm in the ^{13}C spectrum correlating with another at 4.20 ppm in the proton spectrum. A smaller signal at 104.8 ppm in the ^{13}C spectrum was assigned to a similar β-anomeric carbon appearing at a slightly different chemical shift because of different anisotropic effects caused by differing substituents on the glyceryl residue. This was most

Figure 2.4: FAB mass spectra of the most predominant membrane lipid components of *S. ventriculi* cells grown at pH 7 and 37°C. (A) Positive ion FAB mass spectrum of DAG. The ion at m/z 577 was due to loss of water from the psedomolecular ion as $[M+H-H_2O]^+$ with a hexadecanoyl and a octadecenoyl group. The ions at m/z 523 and 551 were also due to the $[M+H-H_2O]^+$ ions. Sodium adduct ions are designated by an asterisk. (B) Positive ion FAB mass spectrum of MGDG containing a hexadecanoyl and an octadecenoyl chain (m/z 779) and homologous. Similar species containing alkenyl ether groups (plasmalogens) were also observed (m/z 765 and 793). All ions corresponded to the sodium adduct ions. (C) Negative ion FAB mass spectrum of lyso-PG with an octadecenoyl residue (m/z 509). The ion at m/z 297 was due to matrix. (D) Negative ion FAB mass spectrum of PG with a hexadecanoyl group and an octadecenoyl group (m/z 747) and lower homologues. The ion at m/z 731 was from a plasmalogen with the same alkyl chain lengths and unsaturation. Structures were also confirmed by FAB collisionally activated dissociation tandem mass spectrometry (FAB-CAD-MS/MS).

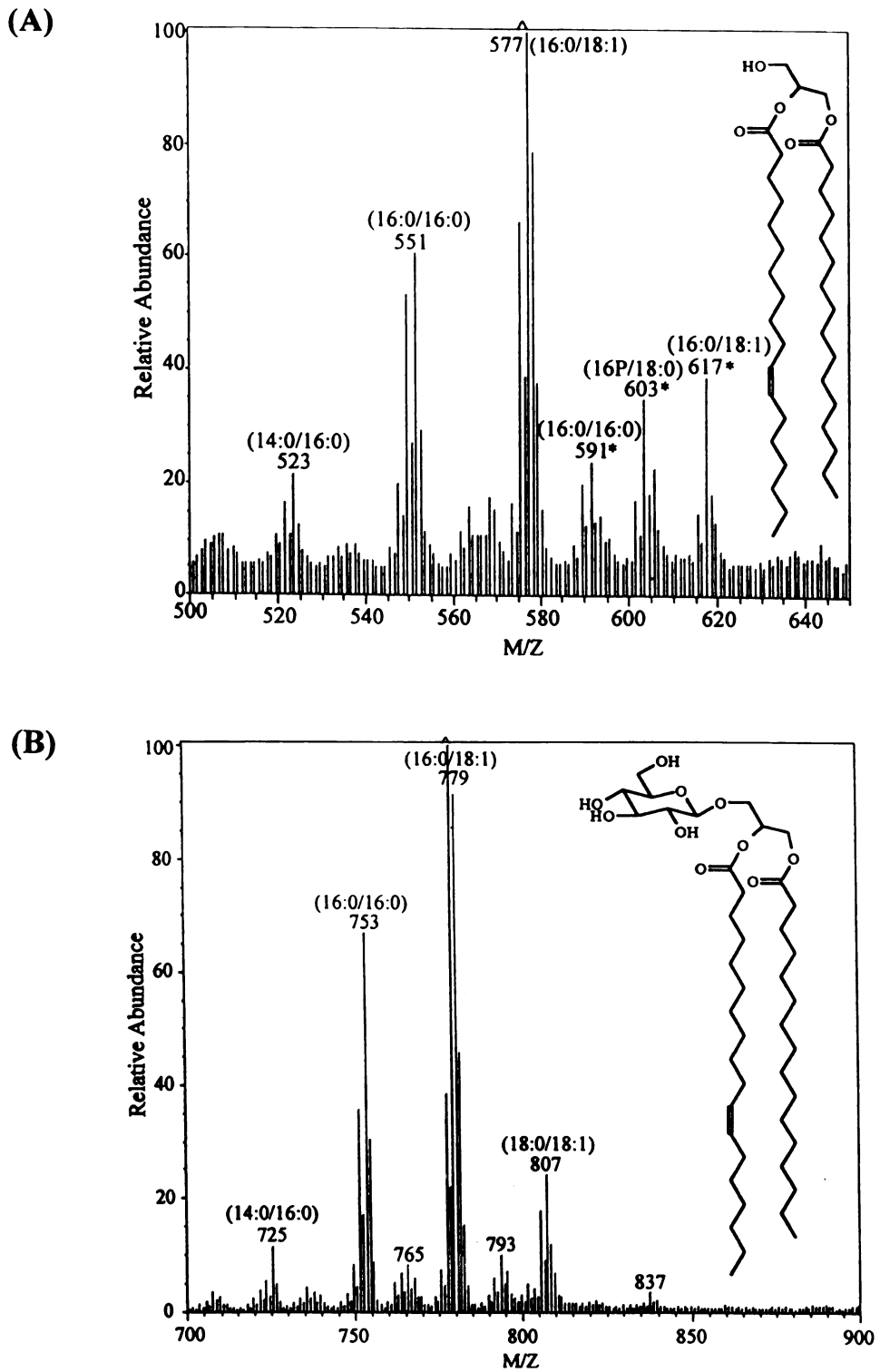
(A)
Relative Abundance
M/Z
577 (16:0/18:1)
(16:0/16:0)
551
(14:0/16:0)
523
(16P/18:0)
603*
(16:0/18:1)
617*
(16:0/16:0)
591*
(B)
Relative Abundance
M/Z
(16:0/18:1)
779
(16:0/16:0)
753
(18:0/18:1)
807
(14:0/16:0)
725
765
793
837

Figure 2.4

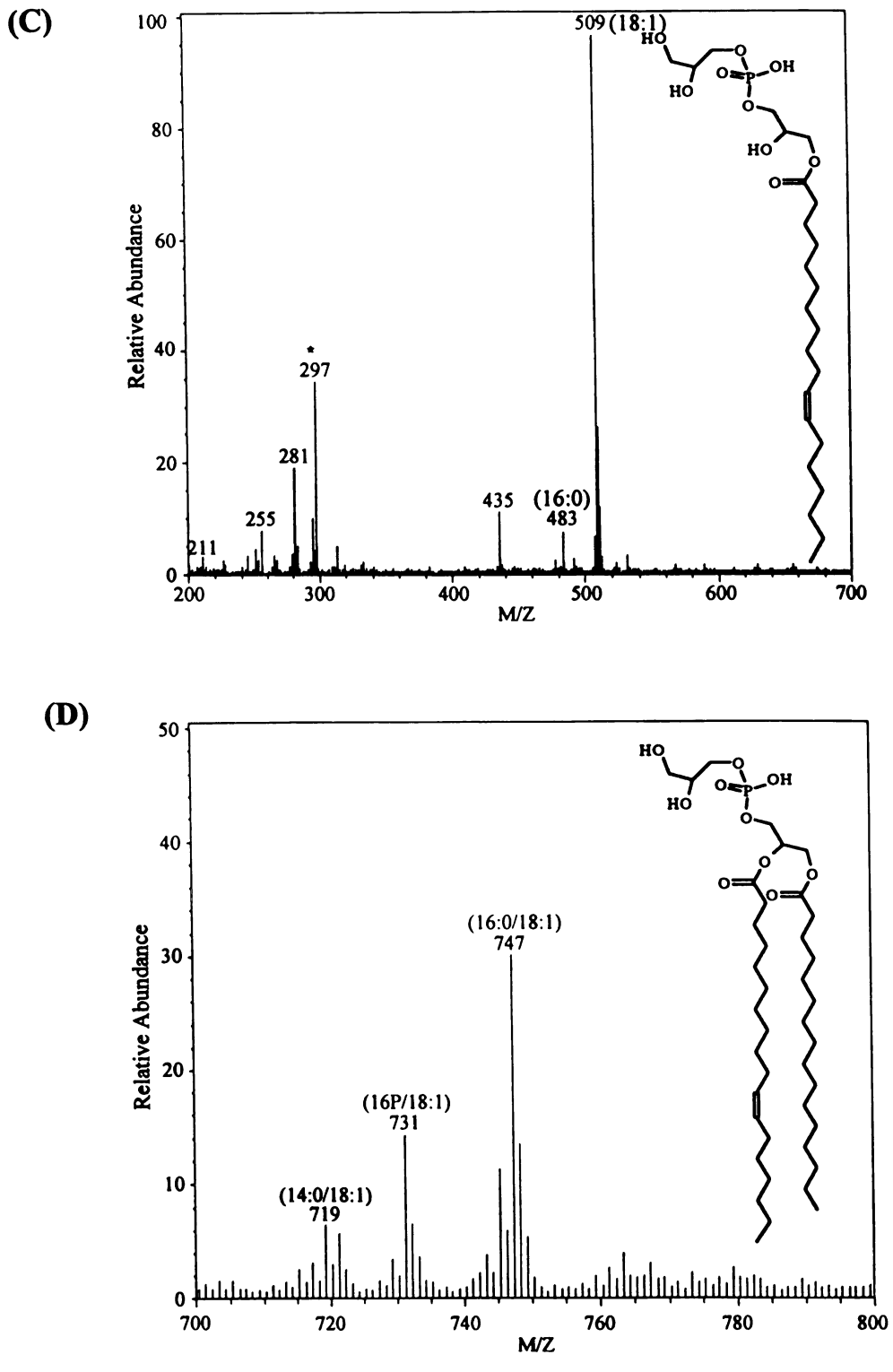

Figure 2.4 (cont'd)

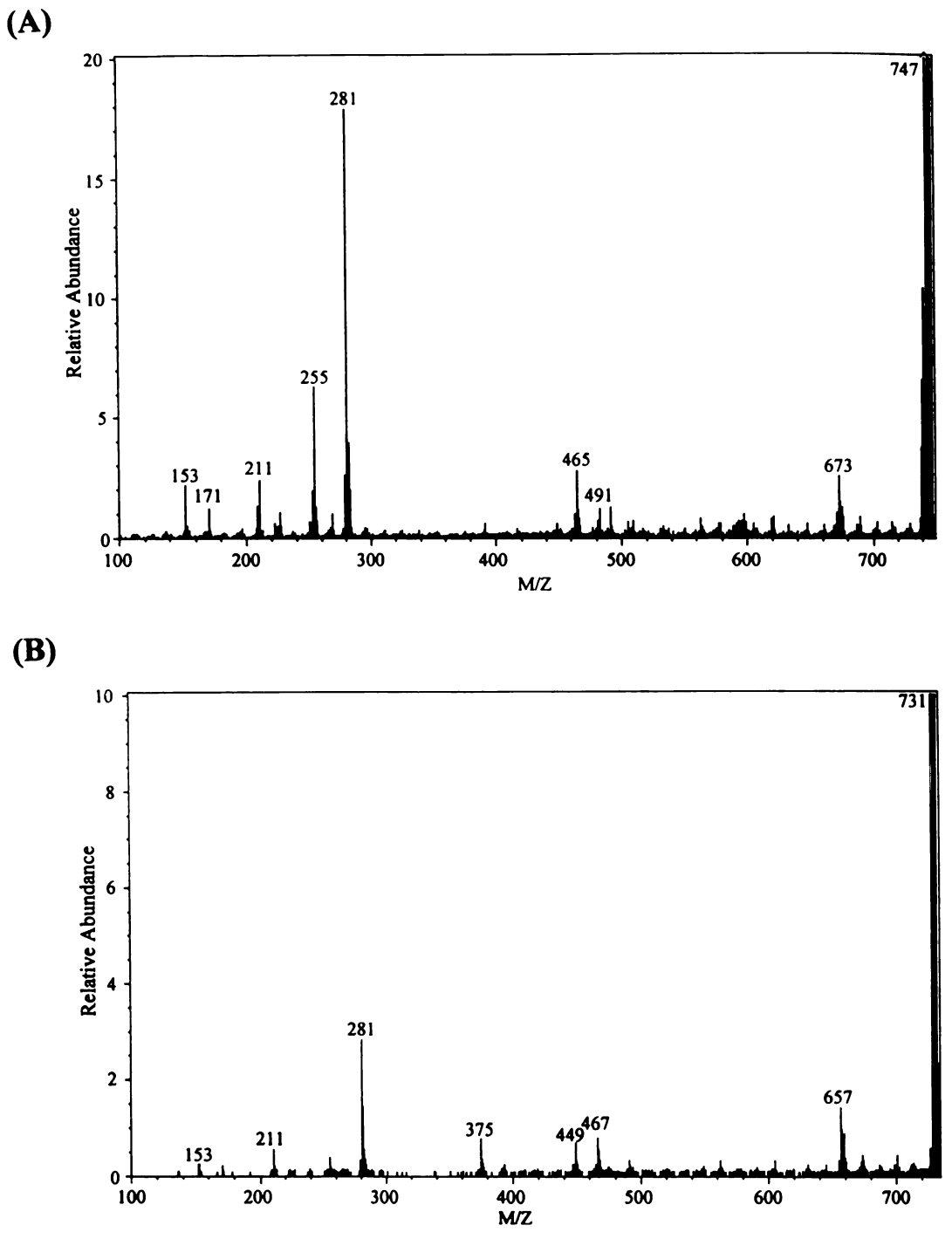

Figure 2.5: Negative ion FAB-CAD-MS/MS spectra of molecular ions of phosphatydyl glycerol. (A) Negative ion FAB linked scan spectrum of the precursor ion at m/z 747. (B) Negative ion FAB linked ion spectrum of the precursor ion at m/z 731.

Figure 2.6: ^{1}H-^{13}C HMQC NMR spectra of the total lipids from *S. ventriculi* cells grown (A) at pH 7 (B) at pH 3. The intense signals in the proton spectra at 49, 77, 126, 142 and 146 ppm were residual signals from the NMR solvent. The first two signals were due to methanol and chloroform, respectively. The others were due to pyrdine.

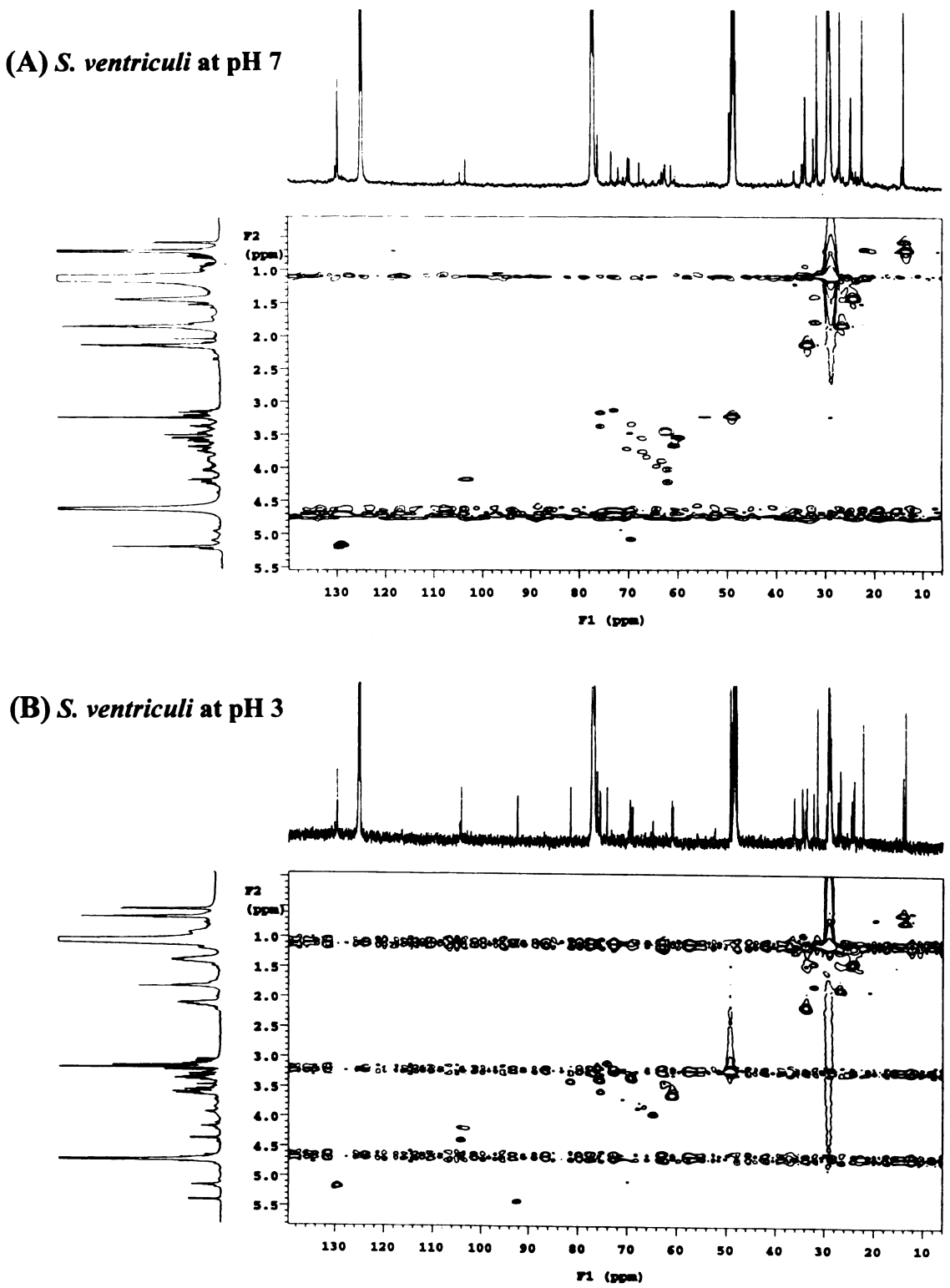
(A) S. ventriculi at pH 7
F2 (ppm)
1.0
1.5
2.0
2.5
3.0
3.5
4.0
4.5
5.0
5.5
130 120 110 100 90 80 70 60 50 40 30 20 10
F1 (ppm)
(B) S. ventriculi at pH 3
F2 (ppm)
1.0
1.5
2.0
2.5
3.0
3.5
4.0
4.5
5.0
5.5
130 120 110 100 90 80 70 60 50 40 30 20 10
F1 (ppm)

Figure 2.6

likely because either alkenyl ether or acyl residues can occur at the 1-position of the glyceryl group. Other signals were mostly attributed to the signals from MGDG and PG. The NMR spectra of the lipids obtained from cells grown at pH 3 showed dramatic differences indicating that major modifications had occurred (Figure 2.6B). The doublet signal at 0.70 ppm in the proton spectrum correlating with the ^{13}C signal at 14.8 ppm was assigned to the vicinal methyl group formed by tail-to-tail coupling of alkyl chains. A new resonance at 104.2 ppm in the ^{13}C NMR spectrum correlated with a doublet (J 8Hz) at 4.40 ppm in the proton spectrum. Two new signals also appeared between 80 and 100 ppm in the ^{13}C spectrum correlating with new signals in the proton spectrum. These new signals were assigned to the signals from the novel glycolipid of this bacterium, β-1-*O*-acyl-β-1,2-diglucosyl glycoside [20]. Perhaps the most important new resonances appeared at 104.0 ppm in the ^{13}C spectrum correlating with a triplet (J 7 Hz) at 4.20 ppm in the proton spectrum. This unusual combination of chemical shifts was readily assignable to an acetal function. The fact that the acetal proton appeared as a triplet with a 7 Hz splitting indicated that it was adjacent to a methylene group. Such an acetal group could only be possible if it were derived from a fatty aldehyde or its equivalent. This conclusion was substantiated by a proton-proton total correlated spectroscopy (TOCSY) experiment (Figure 2.7). Which clearly showed that the signal for the new acetal proton correlated with signals for methylene groups at 1.40 and 1.17 ppm as anticipated. The signal at 1.40 ppm is due to the methylene group adjacent to the acetal proton. Chemical proof of the acyclic acetal linkage came from the fact that the NMR signal corresponding to it was lost on allowing the sample to stand in the presence of traces of acid. A new

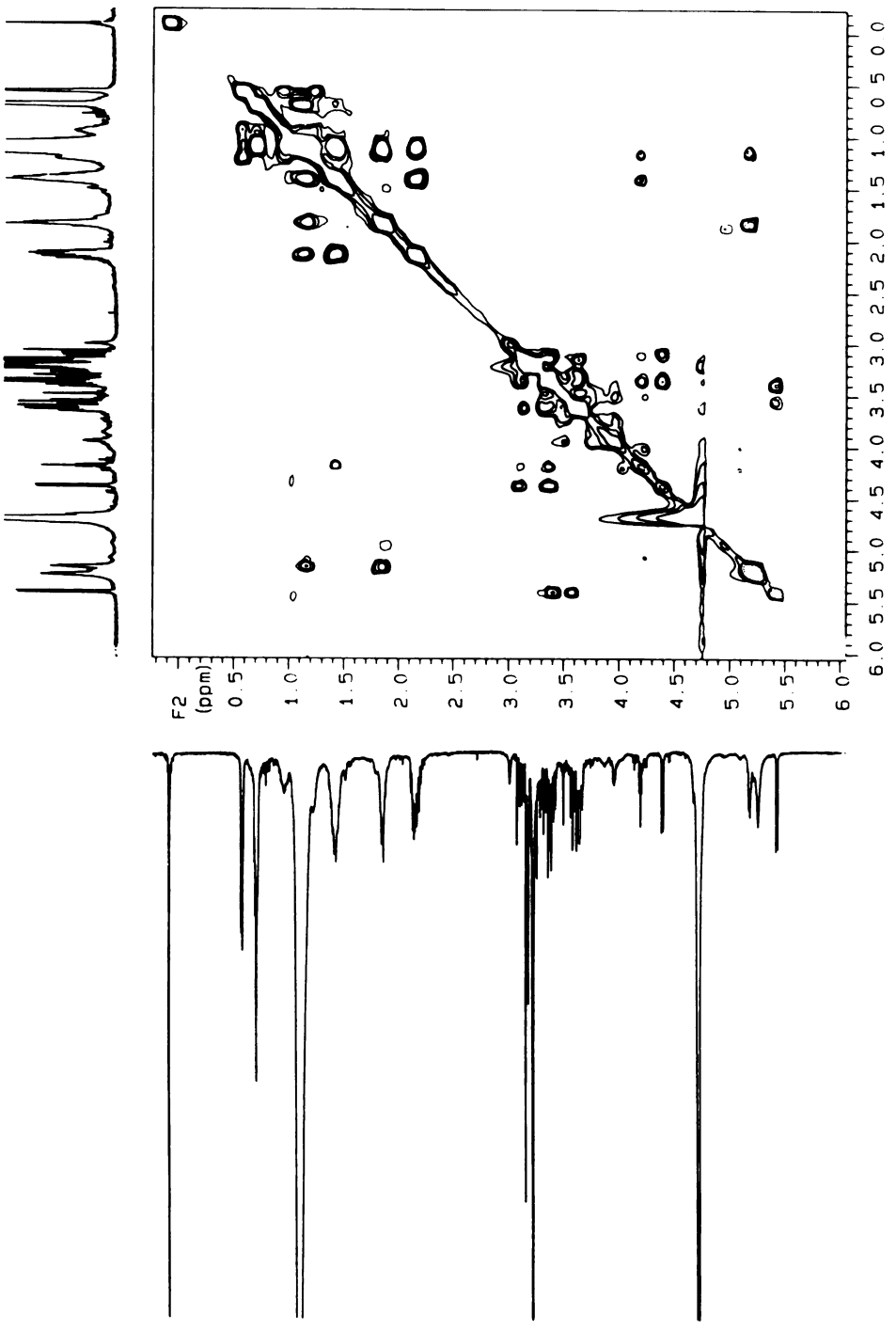

Figure 2.7: TOCSY NMR spectrum of the total lipids from *S. ventriculi* cells grown at pH 3.

signal at 10.4 ppm, corresponding to an aldehyde proton, appeared in the proton NMR spectrum.

A simple chemical mechanism can be advanced to explain how the 2-position of a glucosyl residue of a glycolipid or the free primary alcohol function of glycerol could be involved in the formation of the acetal linkage observed in the membrane lipids of *S. ventriculi*. Acetals can be formed from the addition of alcohols to enol ethers or aldehydes. In this system, such a mechanism would simply involve the nucleophilic attack of a hydroxyl group on the enol ether function of a plasmalogen (1-alkenyl ether lipid) with assistance from either a proton (metal catalyst) or a metal ion as demonstrated in Figure 2.8. This is a very facile process even in laboratory chemistry. The fact that the process is so total, stereospecific and rapid and takes place even in instances when the pH is not lowered indicates that it is probably enzymatic. Such a mechanism indicated that during the adaptation process, head-to-head joining of lipid species might have occurred. An attempt was made to isolate and further characterize some of these unusual lipids by FAB/MS and FAB/MS/MS. These structures included β-1-*O*-acyl and alkyl sophorosides (Figures 2.9A) [20]. The mass spectra also confirmed tail-to-tail and head-to-head joined lipids including DAG/PG, DAG/DAG, DAG/MGDG and MGDG/MGDG molecules. Their FAB mass spectra and proposed structures are presented in Figures 2.9B-E. In this study, data obtained by FAB mass spectrometry provide the structural information of intact transmembrane lipids. The molecular weight of the tail-to-tail joined lipid between PG and DAG having two 16:0, one 18:1 and one 18:0 chains is 1343.0, and that of the form with one 16:0, two 18:1 and one 18:0 chains is 1369.0 (Figure 2.9B).

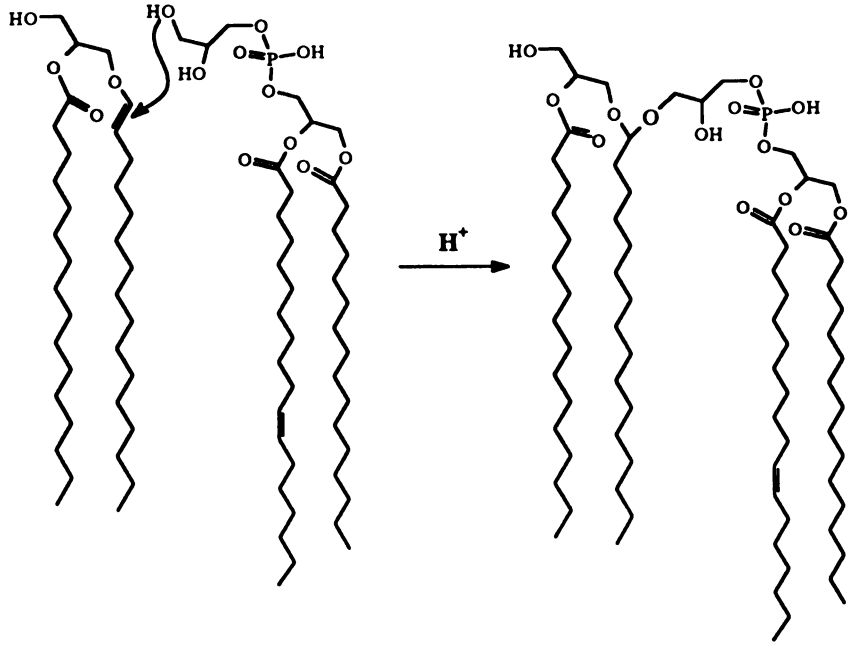

Figure 2.8: Proposed model showing the formation of head-to-head coupled lipids.

Figure 2.9: FAB mass spectra and their general structures of the novel lipid components from *S. ventriculi* cells grown at pH 3. (A) Negative ion FAB mass spectrum and structure of β-1-*O*-acyl and alkyl sophorosides. (B) Positive ion FAB mass spectrum and structure of a family of tail-to-tail coupled lipids of DAG molecule and PG molecule. Small amounts of some head-to-head coupled lipids were also present. (C) Positive ion FAB mass spectrum and structure of tail-to-tail and head-to-head coupled lipids of two DAG molecules. The ions corresponded to $[M+H-H_2O]^-$ ions (D) Positive ion FAB mass spectrum and structure containing a cluster ions corresponding to the sodium adducts of tail-to-tail and head-to-head coupled DAG molecule and MGDG molecule. (E) Negative ion FAB mass spectrum showing a cluster ions of a family of tail-to-tail and head-to-head coupled MGDG with a variety of fatty acyl and fatty alkenyl chains.

(A)

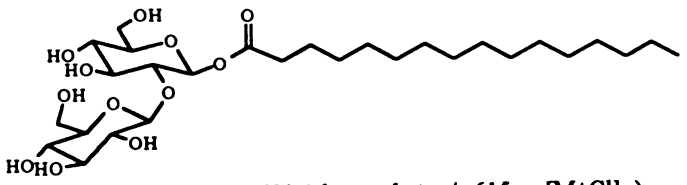

MW=580 (observed at m/z 615 as [M+Cl]$^-$)

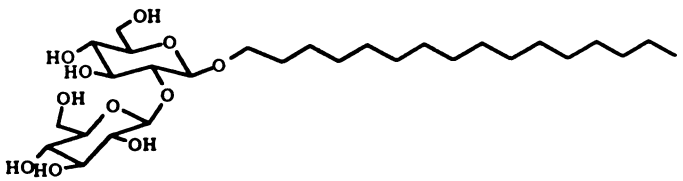

MW=566 (observed at m/z 601 as [M+Cl]$^-$)

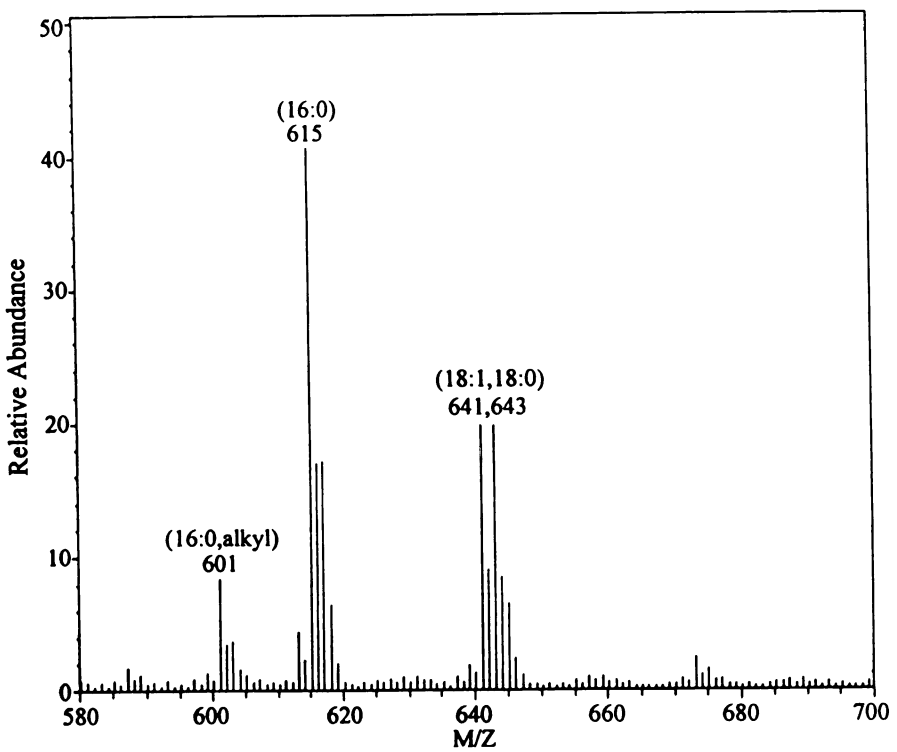

Figure 2.9

(B)

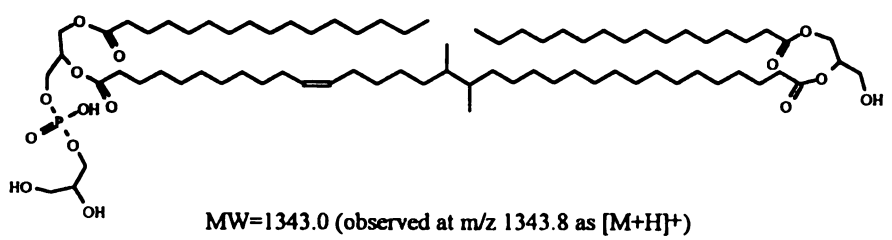

MW=1343.0 (observed at m/z 1343.8 as $[M+H]^+$)

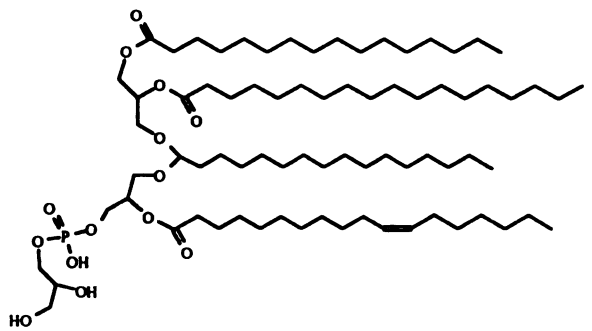

MW=1327.0 (observed at m/z 1327.8 as $[M+H]^+$)

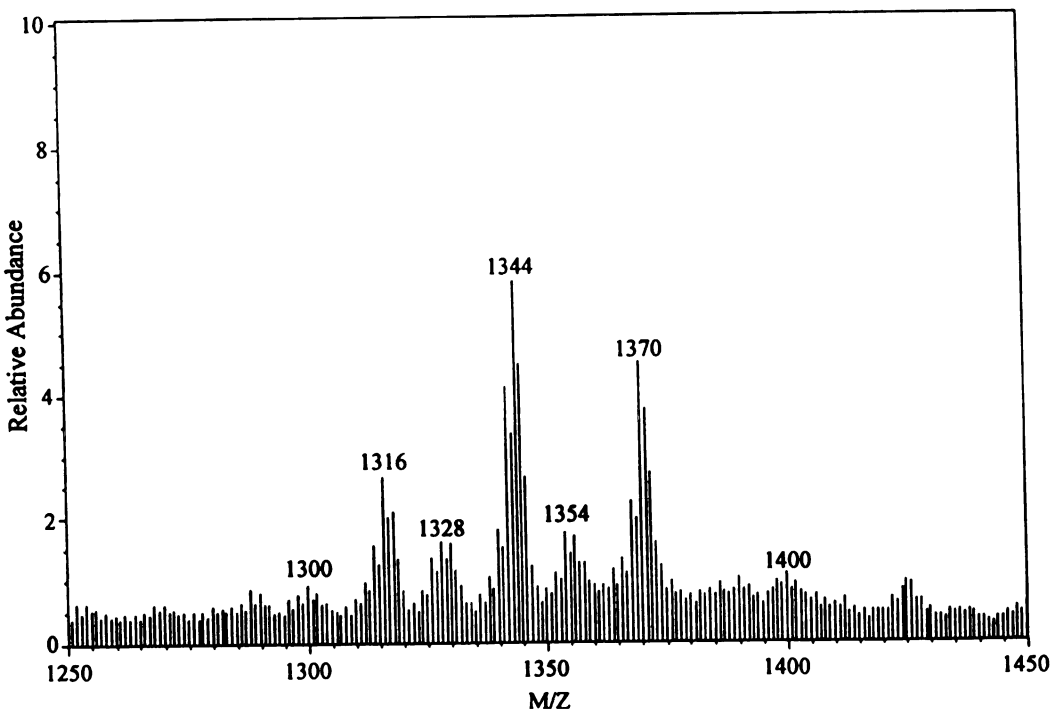

Figure 2.9 (cont'd)

(C)

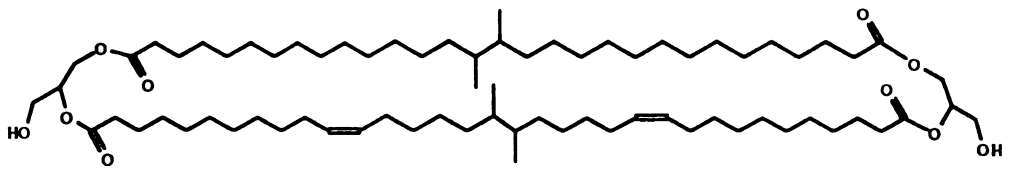

MW=1184 (observed at m/z 1167 as $[M+H-H_2O]^+$)

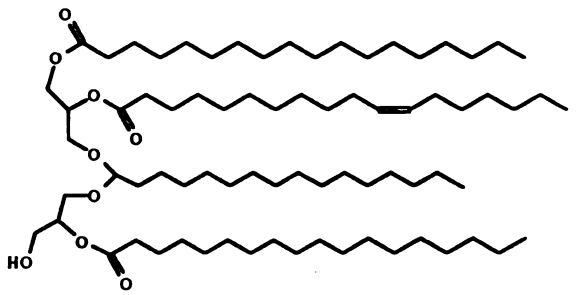

MW=1202 (observed at m/z 1185 as $[M+H-H_2O]^+$)

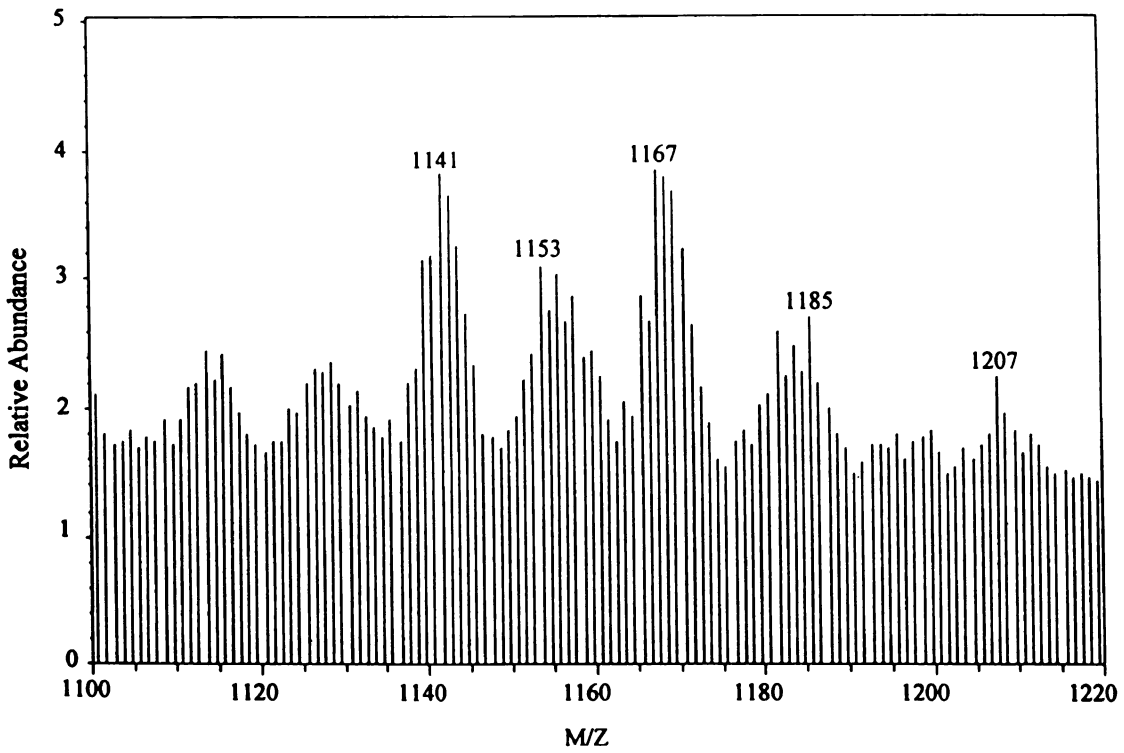

Figure 2.9 (cont'd)

(D)

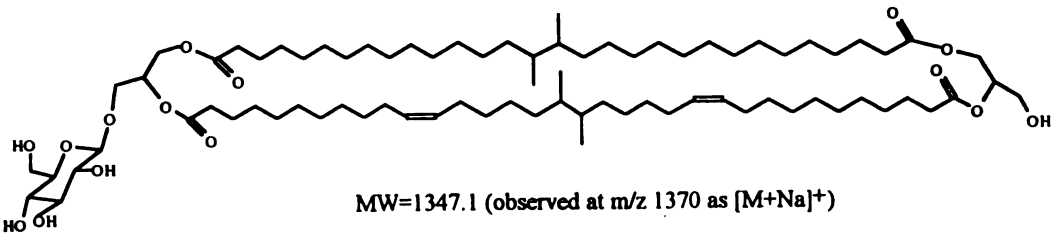

MW=1347.1 (observed at m/z 1370 as $[M+Na]^+$)

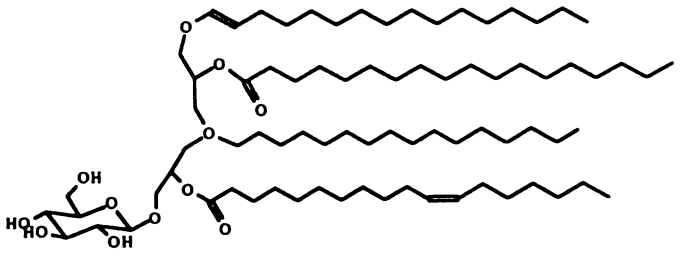

MW=1321.0 (observed at m/z 1344 as $[M+Na]^+$)

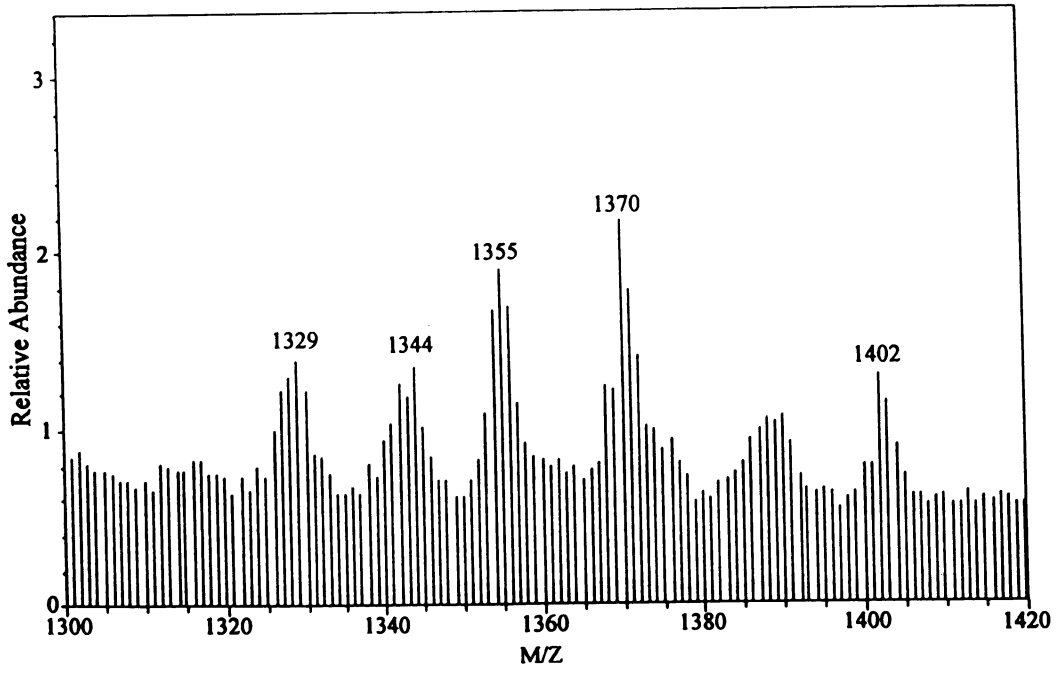

Figure 2.9 (cont'd)

(E)

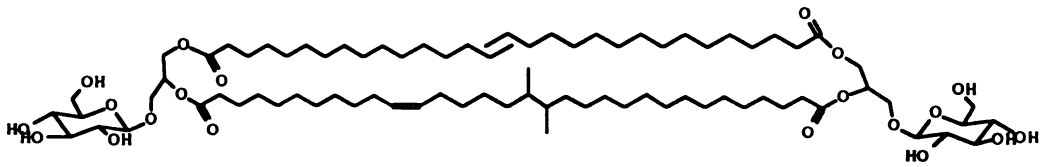

MW=1485.1 (observed at m/z 1484 as [M-H]$^-$)

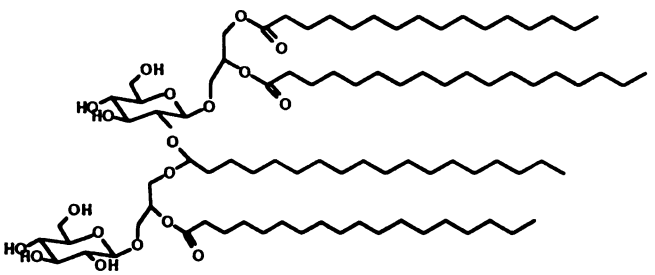

MW=1501.0 (observed at m/z 1500 as [M-H]$^-$)

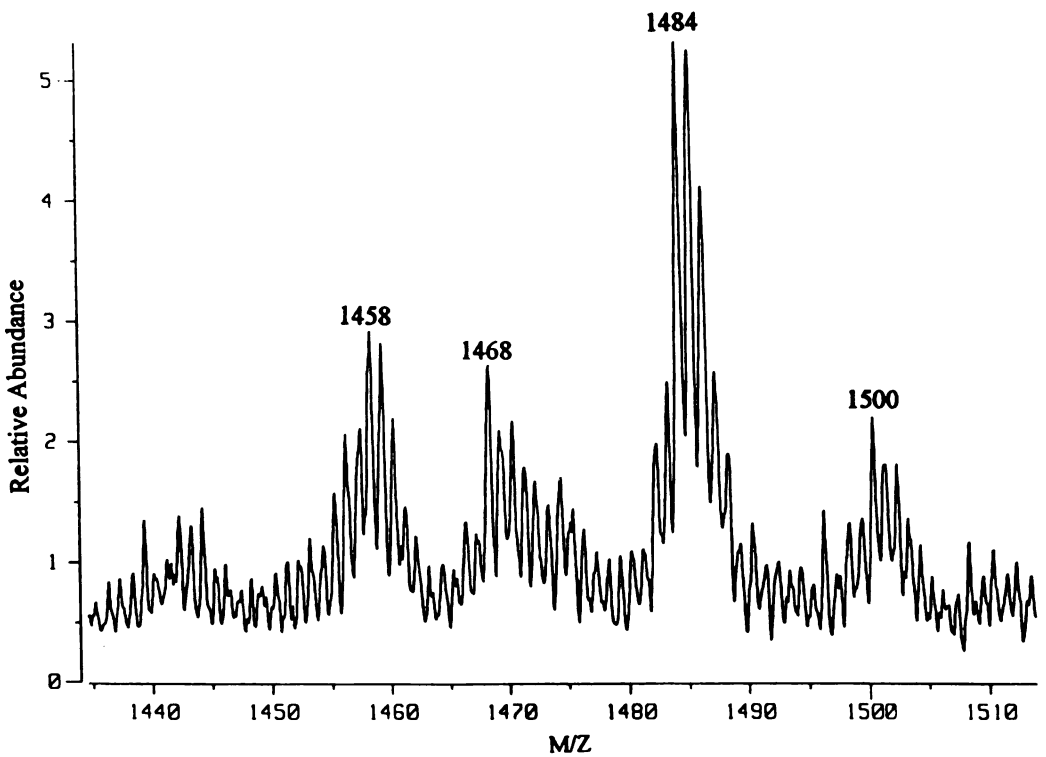

Figure 2.9 (cont'd)

The FAB mass spectrum obtained in the positive mode gave m/z 1343.8 and 1369.8 as psedomolecular ions $[M+H]^+$. Ion at m/z 1327.8 corresponded to the head-to-head joined lipid between PG (16P/8:1) and DAG (16:0/18:1) molecules. The mass spectrum also confirmed the head-to-head coupling phenomenon since peaks corresponding to two head-to-head coupled lipids were present in the sample giving rise to the ion at m/z 1327. As demonstrated in the positive FAB mass spectrum of DAG, the protonated molecular ions $[M+H]^+$ of a family of head-to-head and tail-to-tail coupled DAG molecules were absent. The highest ions corresponded to the loss of water from the psedomolecular ions (Figure 2.9C). In some cases the molecular masses derived from the head-to-head coupled lipids could not be distinguished from those ions of equivalent masses derived from the tail-to-tail coupled lipids. Additionally, the fatty acid chains of the molecular ions were proposed arbitrarily due to the equivalent masses of different combinations of fatty acid chains and tail-to-tail couplings of one or two leaflets. The FAB-CAD-MS/MS may provide a means to distinguish between the tail-to-tail or head-to-head coupled lipids. In this study, a large amount of lipids formed at low pH or under other stress conditions were intractable. They were difficult to separate and to obtain spectra. This coupled with their chromatographic properties indicate that they were larger oligomeric or polygomeric structures.

CONCLUSION

Membrane lipid chemistry has always been somewhat of an enigma because of its structural complexity and, seemingly, excessive heterogeneity. This work provides a

rationale for the existence and function of very long bifunctional fatty acids and ethers [7,21] found in the membrane lipids of bacteria which are adapted to a wide variety of extreme environmental conditions. It also explains the formation, presence and significance of the unusual acetal lipids which have been observed in some of these extremophiles [22,23]. The structure of one of these unusual acetal molecules [22], for instance, can now be rationalized simply by head-to-head coupling between two phosphatidyl ethanolamine plasmalogens followed by phospholipase C activity at one of the phosphate groups. The structure of another known lipid acetal, a head-to-head dimer, could be easily explained by the coupling between phosphatidyl glycerol and the plasmalogen form of phosphatidyl ethanolamine [23]. In one organism, head-to-head trimers have been tentatively identified [24]. A layer of finer adaptative control involving phospholipase and glycosidase activities that allow the disconnection of head-to-head crosslinks thus affording a high degree of tunability is evident. The formation of head-to-head and tail-to-tail cross-links is a formidable formula for adaptation to environmental extremes which essentially cross-links the membrane lipids. This process is the key to membrane stability for bacteria as different as *Clostridia* which generate large amounts of organic acids and alcohols, *Sarcina ventriculi* which is adapted to the very low pH conditions inside of the stomach and to acidic peat bogs as well as being resistant to a large cross section of antibiotics, and *Thermatoga maritima* which can thrive in high salinity and the extremely high pressures and temperatures of the geothermally active ocean floor. The formation of these cross-links is, as shown here in the case of *S. ventriculi*, also a swift, effective, universal, and dynamically regulated adaptative response which is immediately activatable without requiring new protein or lipid

synthesis. Such processes are the ultimate in adaptability. Since they do not require intact organism for their action, it is very possible that their use can be extended to stabilizing membranes, monolayers and vesicles in laboratory and industrial applications.

REFERENCES

1. M. Sinensky, *Proc. Natl. Acad. Sci. USA.*, 1974, **71**, 522-525.
2. L.O. Ingram and N.S. Vreeland, *J. Bacteriol.*, 1980, **144**, 481-488.
3. D.A. deMendoza, A.K. Ulrich , and J.E. Cronan, Jr, *J. Biol. Chem.*, 1983, **258**, 2098-2101.
4. S.E Lowe, M.K. Jain, and J.G. Zeikus, *Microbiol. Rev.*, 1993, **57**, 451-509.
5. S. Goodwin and J.G. Zeikus, *J. Bacteriol.* 1987, **169**, 2150-2157.
6. S.E Lowe and J.G. Zeikus, *Arch. Microbiol.* 1991, **155**, 325-329.
7. S. Jung, S.E. Lowe, R.I. Hollingsworth, and J.G. Zeikus, *J. Biol. Chem.* 1993, **268**, 2828-2835.
8. S. Jung and R.I. Hollingsworth, *J. Theoret. Biol.*, 1995, **172**, 121-126.
9. S. Jung and R.I. Hollingsworth, *J. Lipid Res.*, 1994, **35**, 1932-1945.
10. G.P. Hazlewood and R.M.C. Dawson, *J. Gen. Microbiol.*, 1979, **112**, 15-27.
11. R.A. Klein, G.P. Hazlewood, P. Kemp, and R. M. C. Dawson, *Biochem. J.*, 1979, **183**, 691-700.
12. H. Hauser, G.P. Hazlewood, and R.M.C. Dawson, *Nature*, 1979, **279**, 536-538.
13. N.G. Clarke, G.P. Hazlewood, and R.M.C. Dawson, *Biochem. J.*, 1980, **191**, 561.
14. R. Huber and T.A. Langworthy, H. Konig, M. Thomm, C.R. Woese, U.B. Sleytr, and K.O. Stetter, *Arch. Microbiol.*, 1986, **144**, 324-333.
15. S. Jung, J.G. Zeikus, and R.I. Hollingsworth, *J. Lipid Res.*, 1994, **35**, 1057-1065.

16. Y. Koga, M. Nishihara, H. Morii, and M.A. Matsushita, *Microbiol. Rev.*, 1993, **57**, 164-182.

17. H. Morii, M. Nishihara, and Y. Koga, *Agric. Biol. Chem.*, 1988, **52**, 3149-3156.

18. M. Nishihara, H. Morii, and Y. Koga, *Biochemistry*, 1989, **28**, 95-102.

19. Y. Wang and R.I. Hollingsworth, *Anal. Biochem.* 1995, **225**, 242-251.

20. J. Lee and R.I. Hollingsworth, *Tetrahedron*, 1996, **52**, 3873-3878.

21. G.D. Sprott, M. Meloche, and J.C. Richards, *J. Bacteriol.*, 1991, **173**, 3907-3910.

22. M. Matsumoto, K. Tamiya, and K. Koizumi, *J. Biol. Chem.* (Tokyo), 1971, **69**, 617-620.

23. N.C. Johnston and H. Goldfine, *Biochim. Biophys. Acta*, 1988, **961**, 1-12.

24. N.C. Jhonson and H. Goldfine, *Eur. J. Biochem.*, 1994, **223**, 957-963.

CHAPTER III

ISOLATION AND CHARACTERIZATION OF A β-1-*O*-ACYL & ALKYL-β-1,2-DIGLUCOSYL GLYCOSIDE FROM THE MEMBRANES OF A GRAM-POSITIVE BACTERIUM *SARCINA VENTRICULI*

ABSTRACT

The major glycolipids of a highly adaptable Gram-positive bacterium, *Sarcina ventriculi* were isolated and characterized by 2-D NMR spectroscopy and mass spectrometry. The structure of one of these glycolipids were identified as β-1-*O*-acyl-β-1,2-diglucosyl glycoside containing predominantly hexadecanoic acid, octadecanoic acid and octadecenoic acid. Another glycolipid was β-1-*O*-hexadecyl-β-1,2-diglucosyl glycoside. Their levels are regulated by environmental conditions such as pH and temperature. This paper also describes a relatively simple procedure for the synthesis of β-1-*O*-hexadecyl-β-1,2-diglucosyl glycoside (β-1-*O*-hexadecyl-sophoroside).

INTRODUCTION

Synthetic O-glycosides and O-glycosides from natural sources are extremely important molecules for many applications. The simplest commercially important O-glycosides are the 1-alkyl glycosides used as emulsifiers in paint formulations and for the large scale purification or stabilization of proteins. Octyl glucoside is the most commonly used glycoside for the latter application. Another potential use of simple O-glycosides is as non-ionic surfactants for laundry applications. Long chain alkyl glycosides have been extensively studied from the standpoint of their crystal structure and conformational properties and their ability to form liquid crystalline phases [1-3]. One glycoside that has risen to some prominence recently is sulfoquinovosyl diacylglycerol. This is a very

important candidate as an anti-aids drug [4].

Amphiphilic molecules tend to form organized structures and are thus always interesting prospects for the preparation of liquid crystalline materials. One obvious way of controlling the properties of glycosides is to alter the hydrophilicity of the polar headgroup. Hence disaccharide-containing alkyl glycosides should have different physical properties, such as critical micelle concentration, for instance, when compared to the corresponding monosaccharide derivatives. Acyl glycosides are relatively unknown compared to long chain alkyl glycosides. From a synthetic standpoint, they represent much more of challenge. Simple alkyl glycosides can be prepared by a Fischer acid-catalyzed reaction between an alcohol and a monosaccharide carbohydrate to give, in the case of glucosides, the β-anomer. This will not work with acylations since the other hydroxyl groups will also react under these conditions. A relatively elaborate scheme of protecting all of the hydroxyl groups on the carbohydrate molecule, with benzyl groups for example, activating the reducing end with a bromo functionality and doing an *sn*-2 type displacement with a carboxylate followed by catalytic hydrogenolysis would have to be followed. Acyl and alkyl glycosides with disaccharide head groups, especially those with unusual linkages and anomerically pure, are more problematic and naturally occurring ones are immediately interesting.

We have been studying the changes in membrane chemistry that accompany the adaptation of certain bacteria to extreme changes in environment [5-8]. Such changes include pH, temperature and the presence of organic solvents or antibiotics. Among the many fascinating modifications that occur is the chemical linking of hydrocarbon chains

from opposite ends of the membrane bilayer to form transmembrane bifunctional fatty acid species that span the bilayer. These changes are important for maintaining the optimum dynamic range of molecular motion and energy transfer [9,10]. There are also several modifications to membrane lipid head group structure. We report here on the structure of an unusual β-1-*O*-acyl-disaccharide and β-1-*O*-acyl-disaccharide with an unusual β-1,2-linkage (Structure **1** and **2**) that is formed in the membranes of the Gram-positive organism *Sarcina ventriculi* under low pH conditions. Even though a few 1-*O*-acyl-D-glucoses have been found in nature this represents the first report of this class of molecules in bacteria.

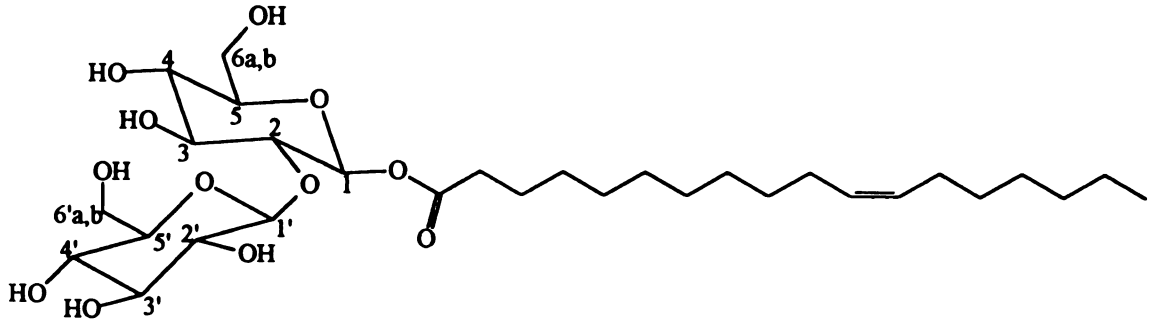

1

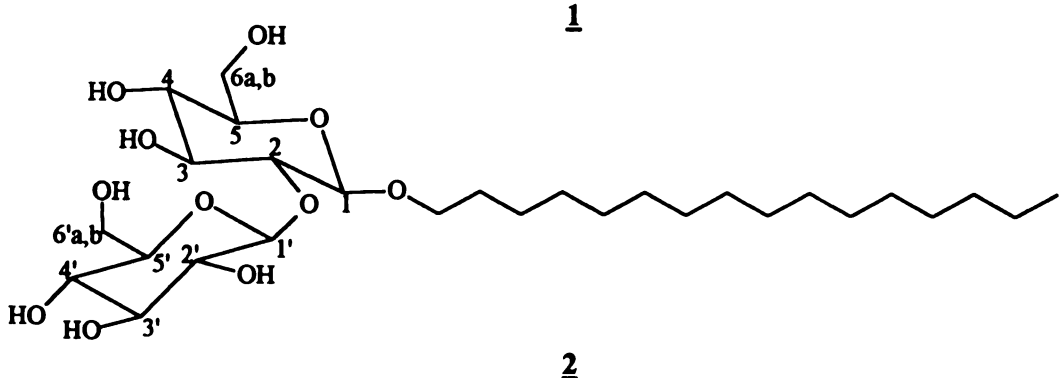

2

MATERIALS AND METHODS

Isolation and Purification of Glycolipids

Bacterial cells were grown under the control of pH, harvested and extracted as described earlier [5]. One batch of cells was grown and the pH adjusted to 3 at the mid-exponential phase and harvested 3 h later (pH-shocked cells). Another batch of cells was cultured with the pH controlled at 3 throughout growth (pH-3 cells). The acyl glycoside was purified by preparative TLC on silica gel plates eluted with a mobile phase system consisting of chloroform / methanol / ammonia / water (3.3:1.0:0.1:0.05 by volume).

Separation of Alkyl Glycoside

This formed a gel which separated from the total extract of pH-3 cells. It was recovered by filtration and washed with chloroform several times. The gel was then subjected to alkaline hydrolysis using 5 mL of 10 % K_2CO_3 in methanol to remove contaminating acyl glycosides. The mixture was stirred for 4 h at room temperature, filtered and passed through C18 Sep-Pak cartridge. The cartridge was eluted sequentially with 3 mL each water, 5:1 MeOH-water, and finally MeOH. The fractions of 5:1 MeOH-water were collected and subjected to further analyses.

Synthesis of β-1-*O*-Hexadecylsophoroside

The reaction scheme for the synthesis of β-1-*O*-hexadecyl-β-1,2-diglucosyl glycoside is summarized in Figure 3.1. α-Acetobromosophorose was prepared by the

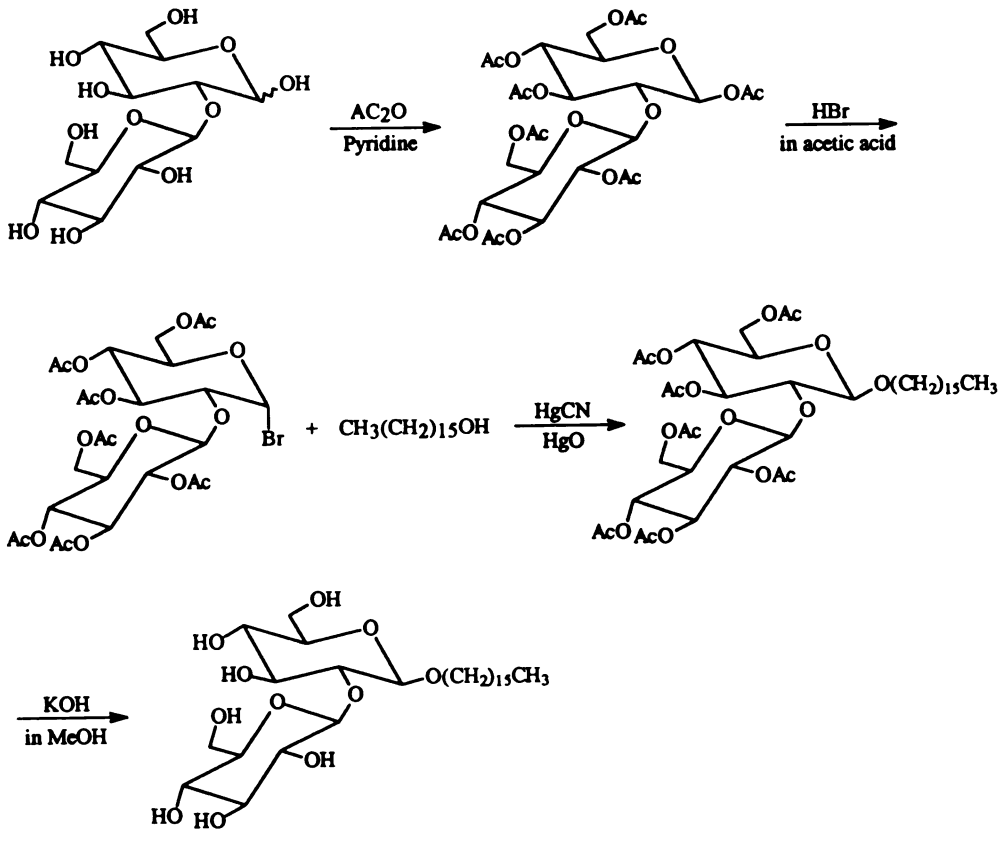

Figure 3.1: Reaction scheme for the synthesis of β-1-*O*-hexadecyl-β-1,2-diglucosyl glycoside.

reaction of octaacetyl β-sophorose with HBr in glacial acetic acid. Octaacetyl β-sophorose was prepared by suspending sophorose (20 mg) in acetic anhydride (0.25mL) and pyridine (1.25 mL) and stirring at room temperature for 24 h. The reaction mixture was then blown under a stream of nitrogen to dryness. The octaacetyl β-sophoroside was dissolved in acetic anhydride (0.3 mL) and added 30 % HBr in acetic acid (1.5 mL). After 6 h, the reaction mixture was slowly poured onto 100 g of ice in a separatory funnel. After 15 min, the reaction mixture was extracted with dichloromethane. The dichloromethane layer was washed 1 time with H_2O and 3 times with cold, saturated sodium bicarbonate with the last wash had pH>7. The dichloromethane layer was then washed 3 times with water and dried over $MgSO_4$ for 2 h. Hexadecanol (80 mg), α-acetobromosophorose (30 mg), and mercury(II) cyanide (30 mg), and mercuric oxide (yellow) (7 mg) were added to 2 mL of anhydrous benzene/nitromethane (1:1 volume) [12]. The mixture was stirred at room temperature for 12 h and then heated to 50°C for 12 h. The mixture was then filtered to remove salts, concentrated. Hexadecylsophoroside peracetate was subjected to alkaline hydrolysis by stirring for 1 h with methanolic KOH (10 mg/mL). The reaction mixture was purified on a C18 Sep-Pak cartridge which was eluted sequentially with water, methanol/water (5:1), methanol as eluents. The methanol/water (5:1) fraction contained pure β-1-*O*-hexadecylsophoroside.

NMR Spectroscopy

NMR spectra of the purified sample for the β-1-O-acyl sophoroside were obtained in a solvent system consisting of chloroform/ methanol/pyridine/37 % HCl in the ratio

10/2/1/1 as described earlier [13] and referenced relative to the $CDCl_3$ at 7.24 ppm. NMR spectra of the gel and synthetic alkyl glycoside samples were acquired in deuterated methanol with chemical shifts being referenced relative to CD_3OD signal at 3.3 ppm. Proton spectra were measured at 500 MHz and ^{13}C spectra were measured at 125 MHz. Double quantum filtered J-correlated spectroscopy (phase sensitive mode) and heteronuclear multiquantum coherence spectroscopy (HMQC) [14] experiments were performed using a total of 256 real data sets.

Derivatization

The samples were subjected to hydrolysis by 2M trifluoroacetic acid and partitioning between chloroform-water. The chloroform extract was subjected to methanolysis using 2% HCl in methanol thus converting the fatty acids to methyl ester derivatives [5]. The aqueous fraction was concentrated to dryness and redissolved in water and reduced with sodium borohydride. The alditols so formed were acetylated with acetic anhydride and pyridine and subjected to GC/MS analysis. The fatty acid methyl esters were subjected to gas chromatography analysis on a 25m J & W DB1 Capillary column with a temperature of 150°C - 250°C at 3°C/min.

Mass Spectrometry

The electrospray ionization (ESI) mass spectra were acquired on a Fisons Platform I instrument operating in the negative mode. The samples were dissolved in 1:2 chloroform/methanol and introduced into the ESI source at a flow rate of 10 μL/min

using a syringe pump. The electrospray needle was operated at 3.2 kV, and nitrogen was used as the nublization gas.

RESULTS AND DISCUSSION

Growth of *Sarcina ventriculi* under pH-shocked condition led to the formation of a new slow-moving component on thin layer chromatography. Gas chromatography and GC/MS indicated that the compound contained fatty acids, predominantly hexadecanoic acid ($C_{16:0}$), octadecanoic acid ($C_{18:0}$) and octadecenoic acid ($C_{18:0}$), and glucose. The ^{1}H-NMR spectrum contained signals between 0.5 ppm and 2.4 ppm characteristic of fatty acid groups as well as some between 3.0 ppm and 3.6 ppm characteristic of carbohydrate groups (Figure 3.2). A triplet at 5.14 ppm that was partially obscured by the water line but readily visible in the water-suppressed ^{1}H-NMR spectrum was assigned to the vinyl protons of unsaturated fatty acids. A multiplet at 1.82 ppm was assigned to the methylene groups adjacent to these unsaturations. Signals for the methylene groups adjacent to the carbonyl functions of fatty acid groups appeared as a multiplet at 2.14 ppm. The signals for the terminal methyl groups of fatty acid chains appeared at 0.67 ppm. Two signals of equal intensity at 5.40 and 4.36 ppm were attributed to two anomeric proton resonances. They appeared as doublets and displayed large coupling constants of 8 Hz. The large chemical shift of the one at 5.40 ppm indicated that the position was substituted by an electron withdrawing function such as an acyl group. Further proton signal assignments were accomplished through the spin connectivities in the DQF-COSY spectrum. The anomeric proton resonance at 5.40 ppm showed a cross peak with the signal at 3.36 ppm.

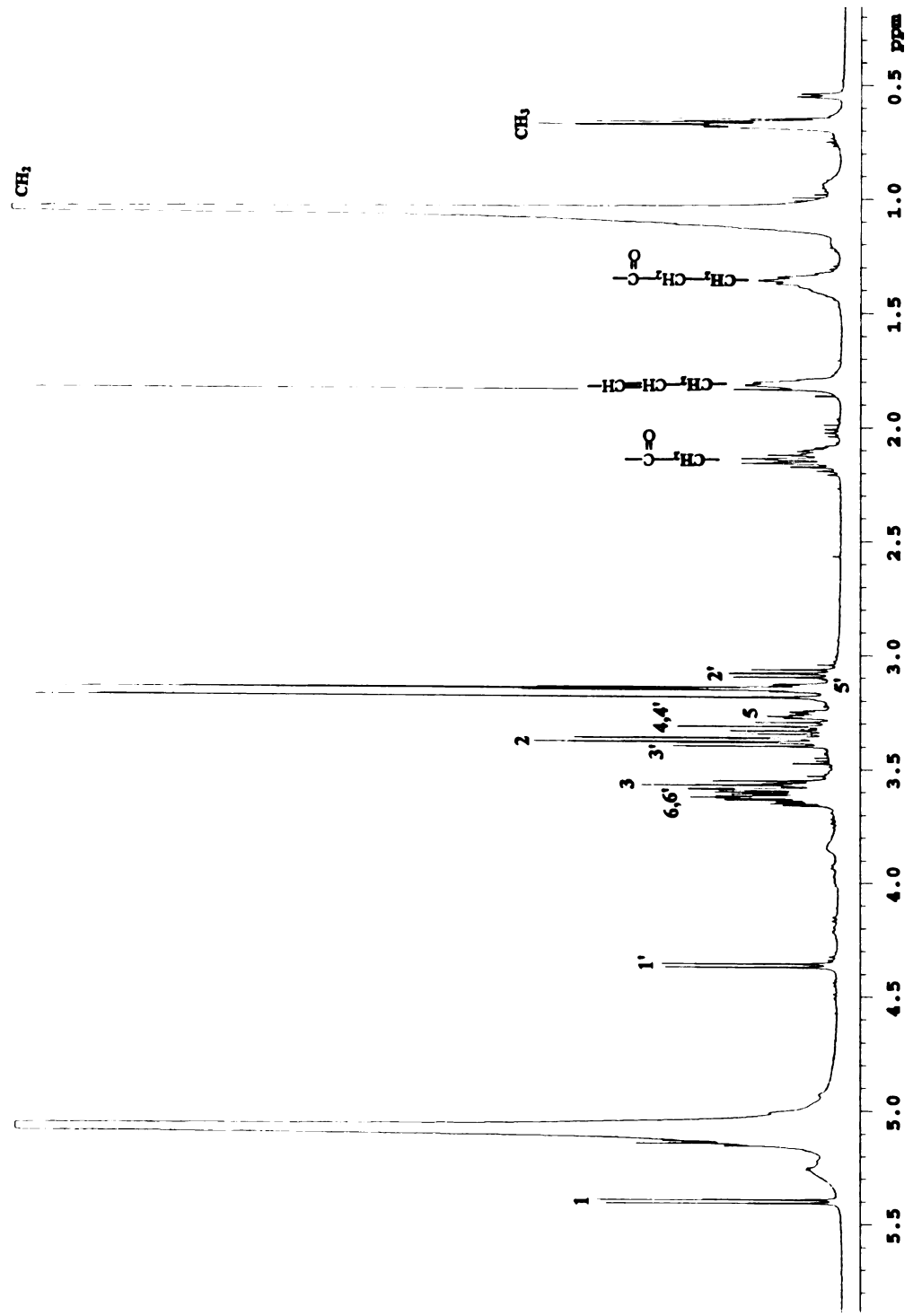

Figure 3.2: ^{1}H NMR spectrum of β-1-*O*-acyl-β-1,2-diglucosyl glycoside from *Sarcina ventriculi*.

This signal was, therefore, assigned to H-2. The H-2 signal for the other glycosyl residue was assigned in a similar fashion. It was possible to make most of the proton assignments from the COSY cross peaks (Figure 3.3) and a consideration of the multiplicities and coupling constants of the signals. The complete proton and carbon assignments are given in Table 3.1. The ^{1}H-^{13}C-HMQC NMR spectrum (Figure 3.4) confirmed the assignments in the ^{1}H-spectrum. The proton signal at 5.40 ppm showed a cross peak with a ^{13}C signal at 92.5 ppm. As noted earlier, the large proton chemical shift of H-1 indicated that the anomeric position at C-1 was probably acylated by a fatty acid group. This was confirmed by the ^{13}C spectrum since the corresponding chemical shift appeared at a much more upfield position quite close to that of a free anomeric carbon. The other anomeric proton signal correlated with a ^{13}C signal at 104.4 ppm as is expected for β-glycosides. The next most downfield ^{13}C signal appeared at 81.9 ppm and correlated with the proton signal at 3.36 ppm which was earlier assigned to H-2 of the glucose residue bearing the acyl group. This carbon position is, therefore, involved in the linkage of two glucosyl residues as indicated by its large ^{13}C chemical shift. The signal assignments from DQF-COSY and HMQC results therefore revealed that the two glucosyl residues were linked at the 2-position and the reducing end was acylated. The other signals in the ^{13}C-NMR spectrum were also in agreement with the proposed structure (Table 3.1). The reported chemical shift of the non-reducing anomeric carbon of β-sophorose (a β-1,2-linked disaccharide of D-glucopyranose) is 103.9 Hz [16], quite consistent with our value.

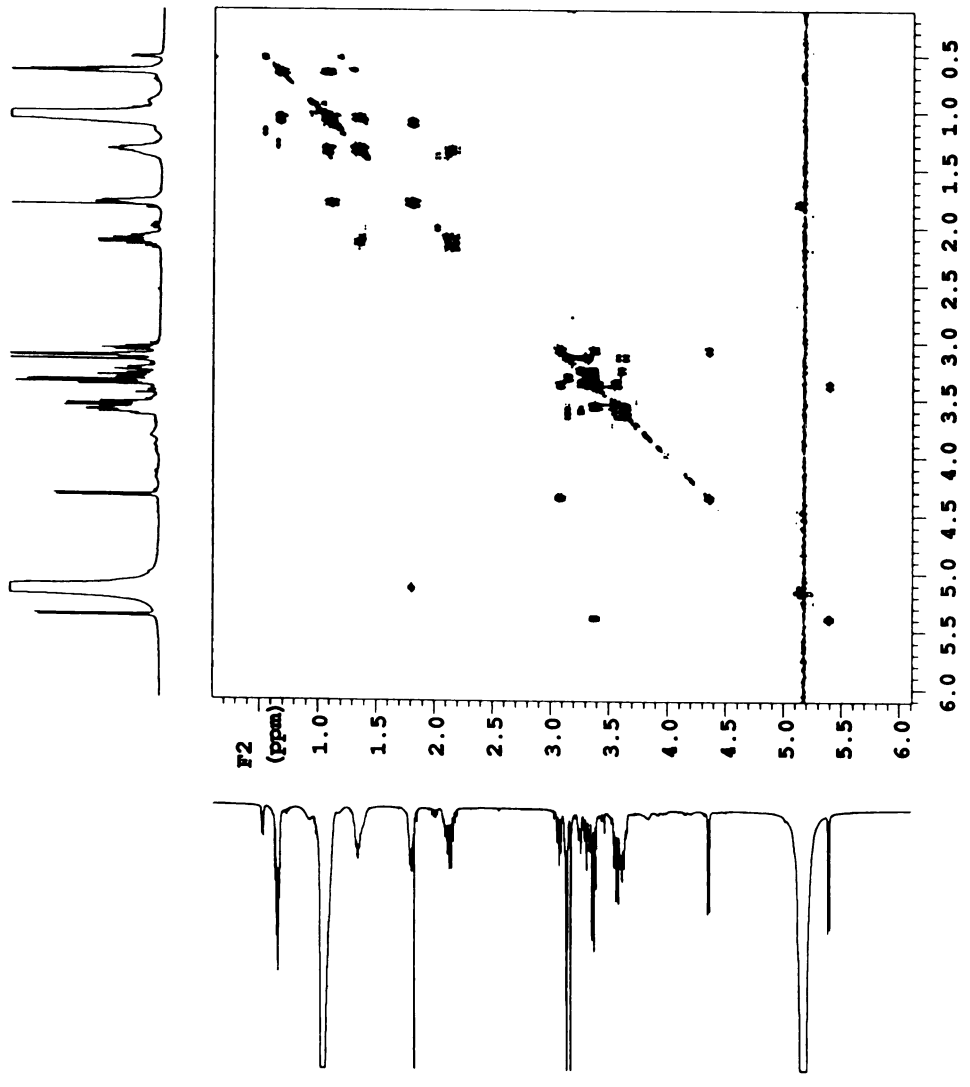

Figure 3.3: Proton-proton double quantum filtered COSY (DQF-COSY) NMR spectrum of the β-1-*O*-acyl sophoroside.

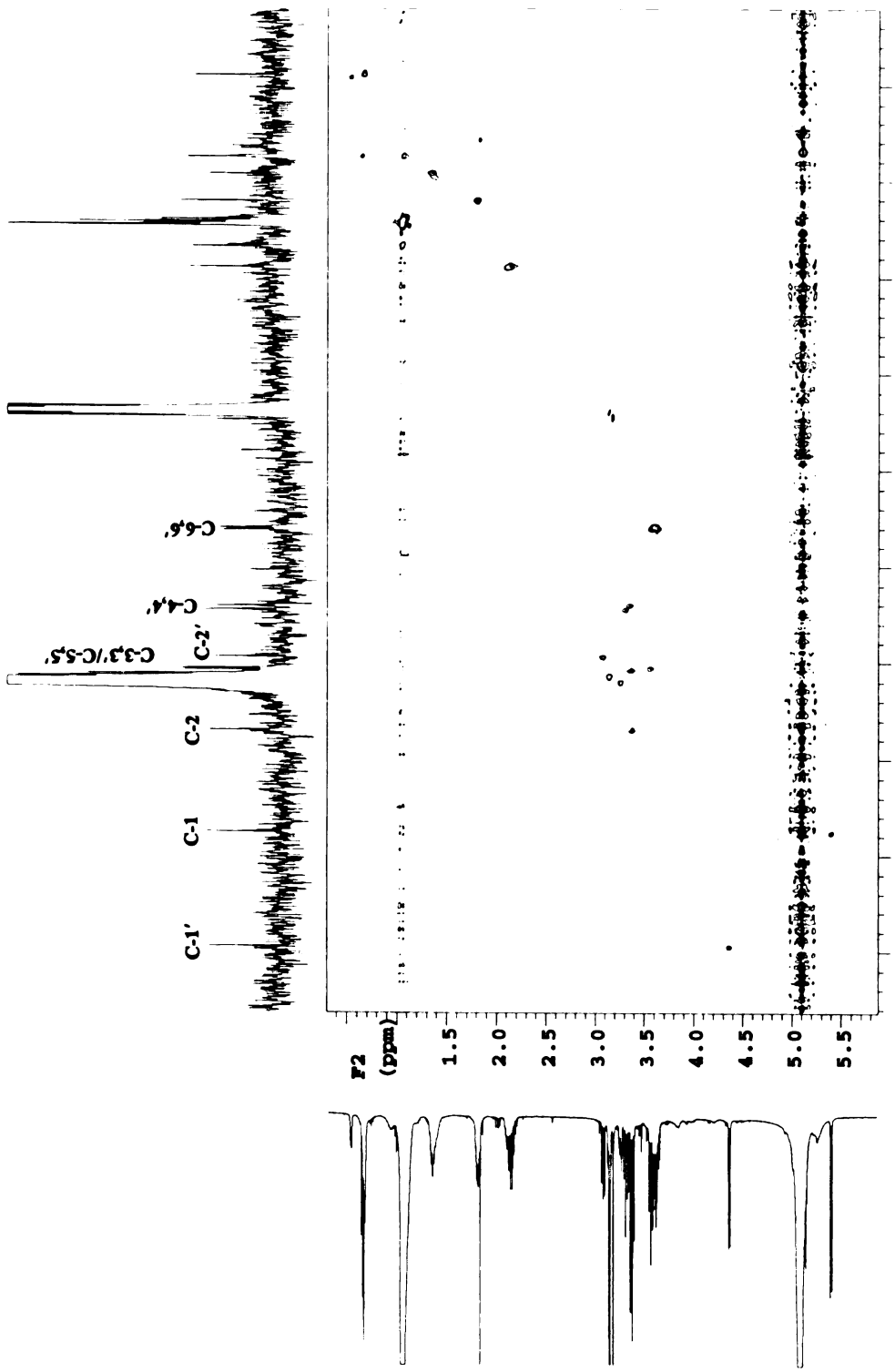

Figure 3.4: 2-D proton-carbon heteronuclear multiquntum coherence (HMQC) NMR spectrum of the β-1-*O*-acyl sophoroside.

Table 3.1: ^{1}H and ^{13}C chemical shifts of the disaccharide residue of β-1-*O*-acyl-β-1,2-diglucosyl glycoside.

^{1}H (ppm)	H-1	H-2	H-3	H-4	H-5	H-6
Glu-1	5.40	3.36	3.57	3.34	3.26	3.64,3.75
Glu-1′	4.36	3.08	3.38	3.31	3.13	3.59,3.62
^{13}C (ppm)	C-1	C-2	C-3	C-4	C-5	C-6
Glu-1	92.5	81.9	75.5	69.0	76.7	61.1
Glu-1′	104.4	74.3	75.7	69.4	76.1	60.8

The negative ion ESI mass spectrum contained signals for molecular ions species as chloride adducts $(M+Cl)^-$ at m/z 587, 615, 641, and 643 (Figure 3.5). The assignments were in agreement with ions at m/z 575, 603, 629, and 631 as $(M+Na)^+$ ions in the positive ion mode (data not shown). These masses were fully consistent with the presence of four species with the general assigned structure but differing in their fatty acid chains. In addition to these peaks, the fragments showed diagnostic ions at m/z 341, 323, 281, 263, 221, 179, and 162. These ions were associated with fragment ions from the disaccharide residue [17]. The abundant ions corresponding to carboxylate anions appeared at m/z 255($C_{16:0}$), 281($C_{18:1}$) and 283($C_{18:0}$). GC and GC/MS analyses revealed that the ratio of hexadecanoic acid, octadecanoic acid and octadecenoic acid was 2.4:2.7:1.0, respectively. Also, the position and configuration of double bond of octadecenoic acid were confirmed as *cis*-11-octadecenoic acid in a previous study [7]. A signal in the mass spectrum indicating a minor amount of tetradecanoate was visible at m/z 277. Based on the NMR and MS analyses, the molecule under investigation was

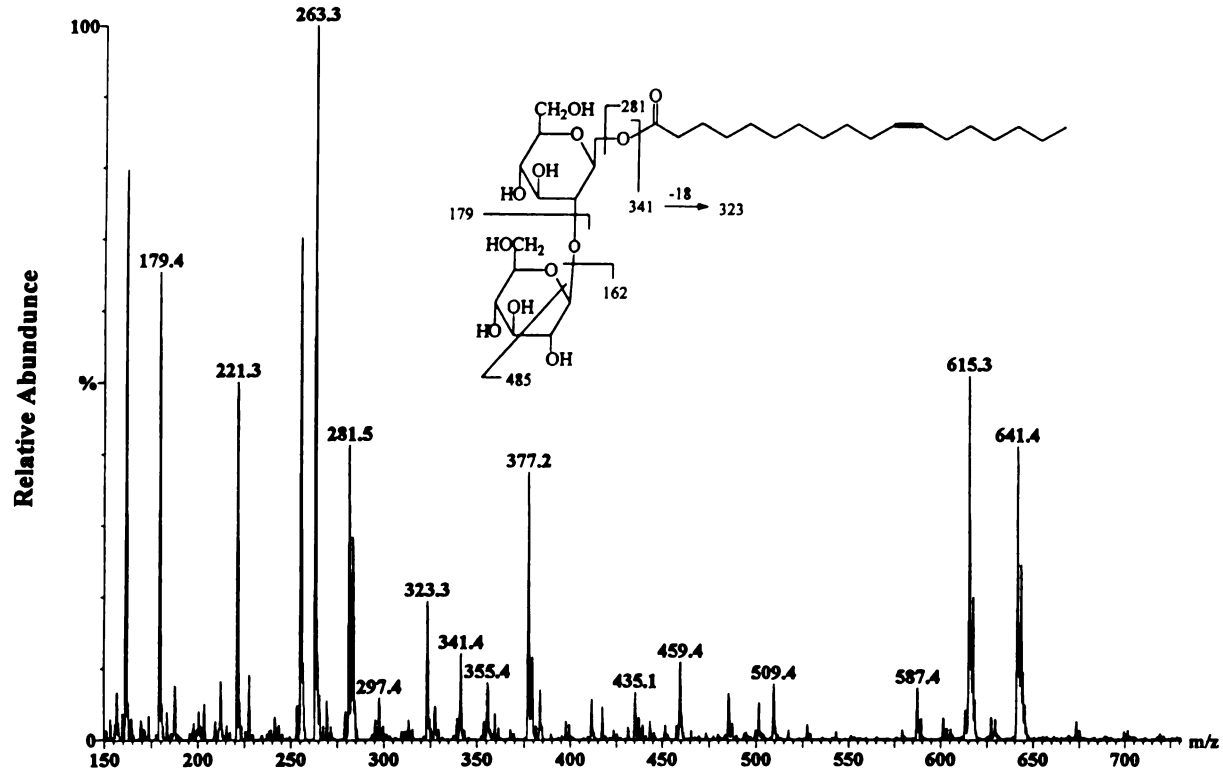

Figure 3.5: Negative ion electrospray ionization (ESI) mass spectrum of the β-1-*O*-acyl sophoroside.

clearly a family of β-1-*O*-acyl-β-1,2-diglucosyl glycoside containing predominantly hexadecanoic acid, octadecanoic acid and octadecenoic acid.

Quite unexpectedly, a gel was formed in total lipid extracts of pH-3 cells. This prompted us to separate and examine the gel further. A thin-layer chromatography of the gel showed the band with the same R_f value as that of pH-shocked cells. However the ^1H and ^{13}C NMR spectra indicated the presence of another glycolipid in addition to the β-1-O-acyl sophoroside (Figure 3.6). Two doublets at 5.60 and 4.56 ppm (in CD_3OD solvent) were due to the β-anomeric protons from the acyl sophoroside as described earlier. Two doublets at 4.39 ppm and 4.59 ppm with coupling constants (J 8Hz) indicated the presence of two β-anomeric protons. The negative ion ESI mass spectrum gave peaks at m/z 565 and 601 in addition to m/z 615, 641, and 643 which corresponds to the β-1-*O*-acyl sophorosides (Figure 3.7). The ions at m/z 565 and 601 corresponded to the psedomolecular ions $[M-H]^-$ and $[M+Cl]^-$, respectively. To further characterize the sample, it was hydrolyzed by potassium carbonate to cleave ester linkages, thus destroying the acyl glycosides. The occurrence of only hexadecanol from this purified glycolipid was demonstrated by GC/MS of the methanolysis products. These data taken together were strong evidence for β-1-*O*-hexadecyl sophoroside. Further evidence was obtained by NMR studies with synthetic β-1-*O*-hexadecylsophoroside. The ^1H NMR spectrum of the purified glycoside was identical to that of the synthetic β-1-*O*-hexadecylsophoroside (Figure 3.8). The proton signal assignments were accomplished by the DQF-COSY (Figure 3.9) and TOCSY (Figure 3.10) NMR experiments. The two doublets at 4.39 and 4.59 ppm were assigned to the H-1 and H-1′ resonances of

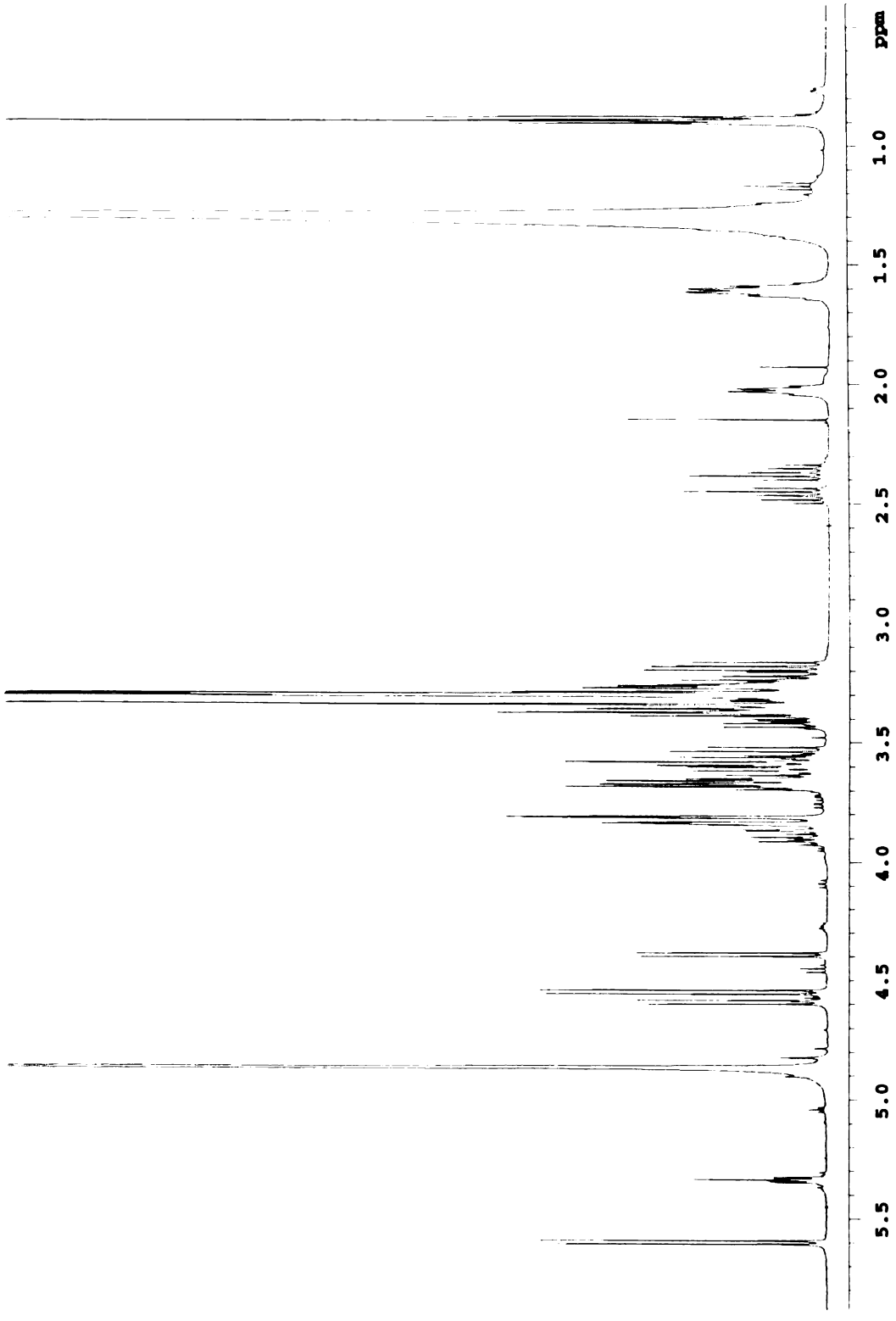

Figure 3.6: ^{1}H NMR spectrum of the gel purified from total lipid extracts of *S. ventriculi* grown at pH 3.

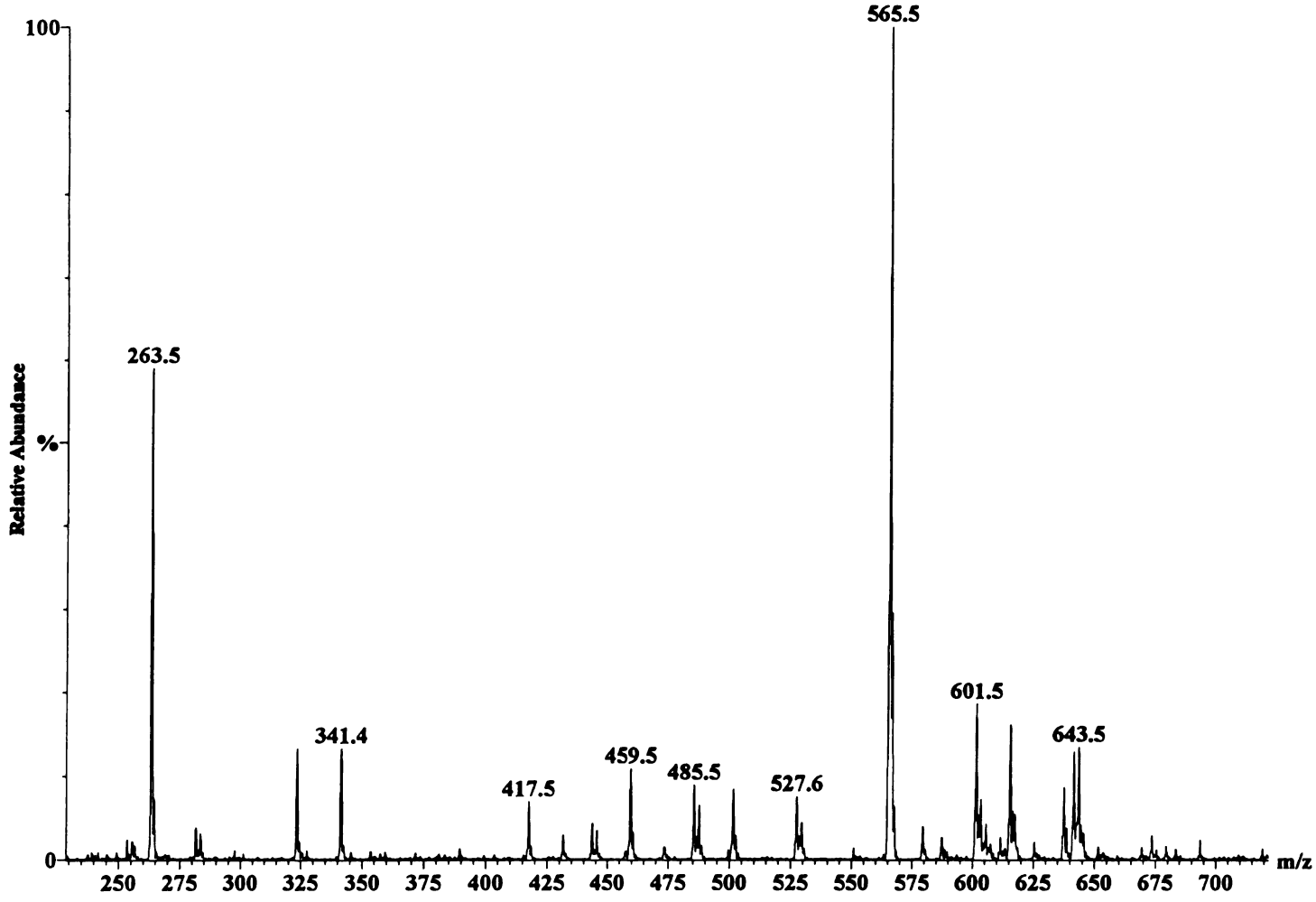

Figure 3.7: Negative ion ESI mass spectrum of the gel.

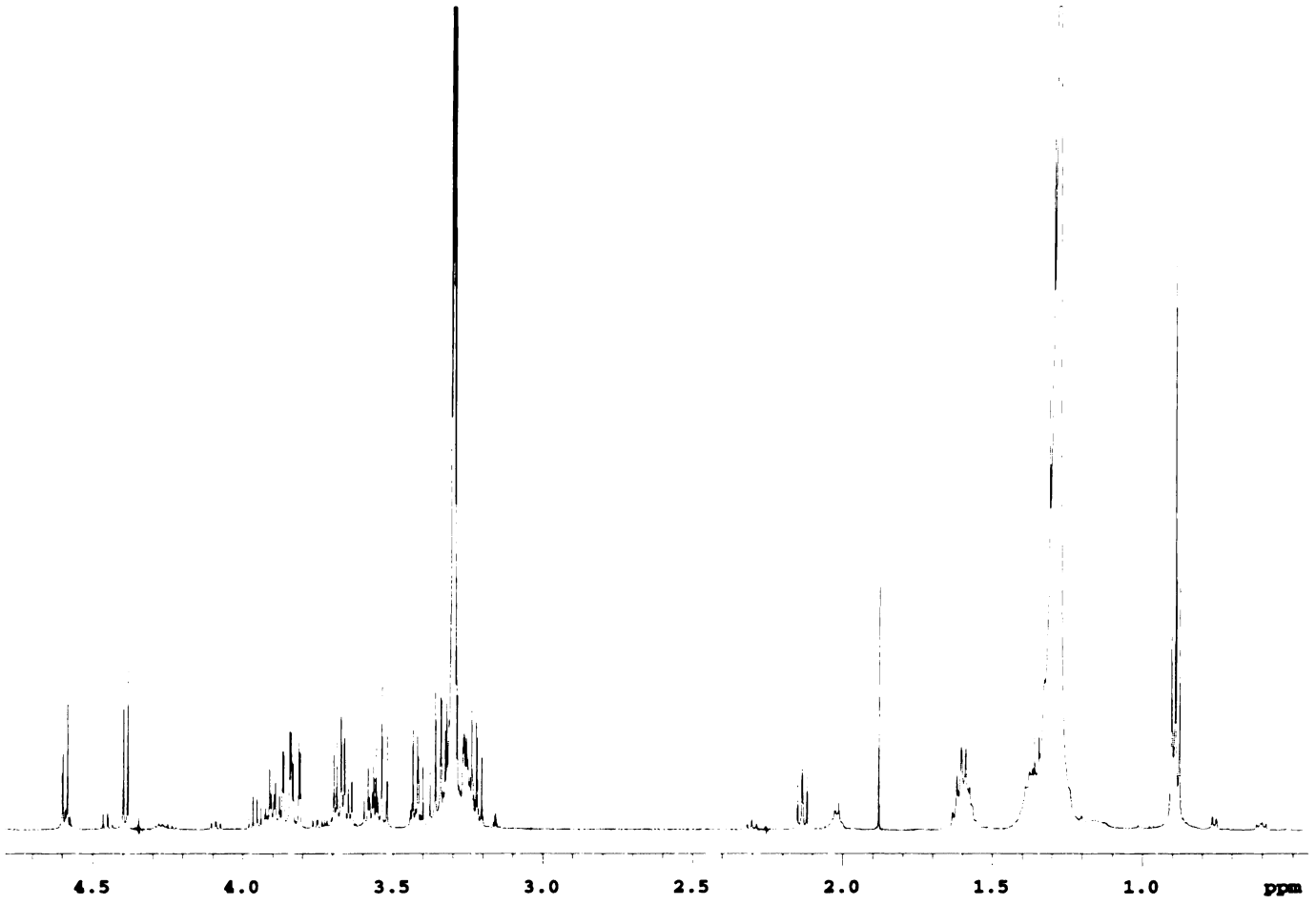

Figure 3.8: ^{1}H NMR spectrum of the glycolipid separated from the gel after alkaline hydrolysis.

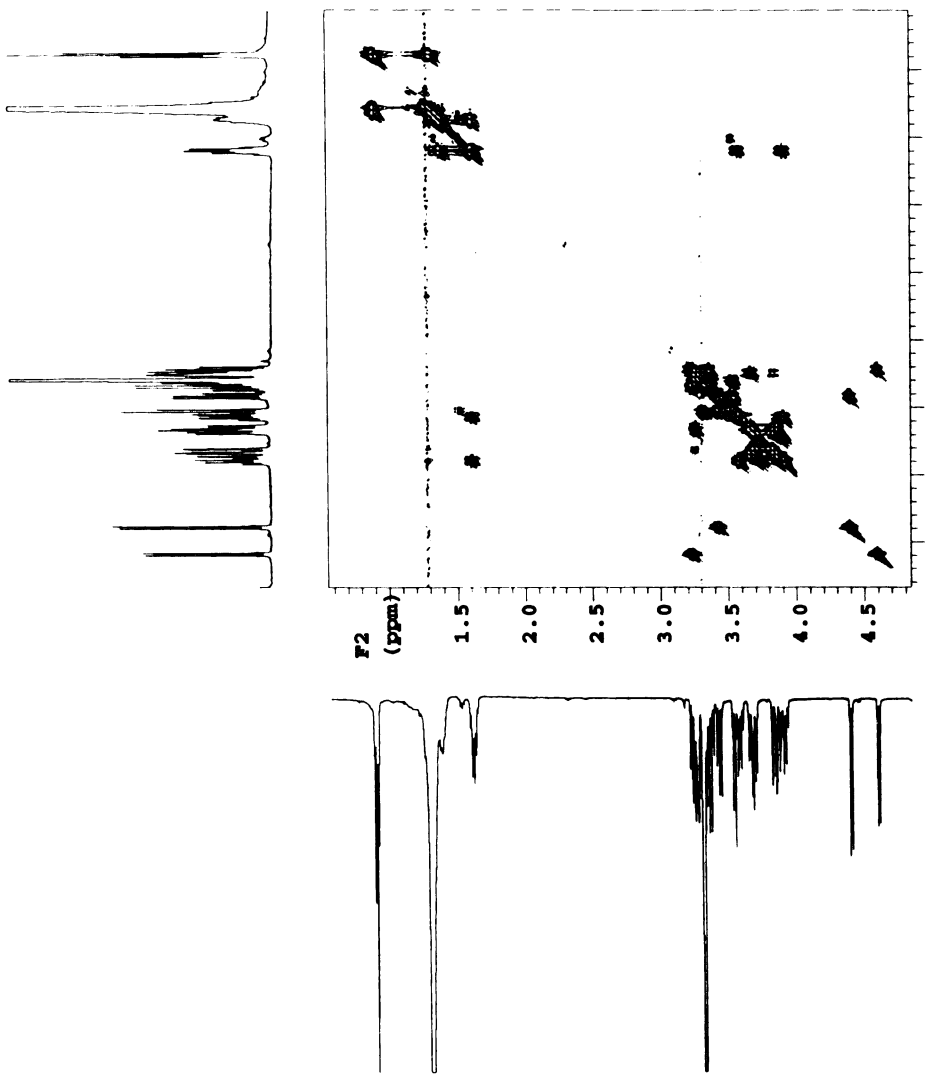

Figure 3.9: ^{1}H-^{1}H DQF-COSY NMR spectrum of the β-1-*O*-hexadecyl sophoroside.

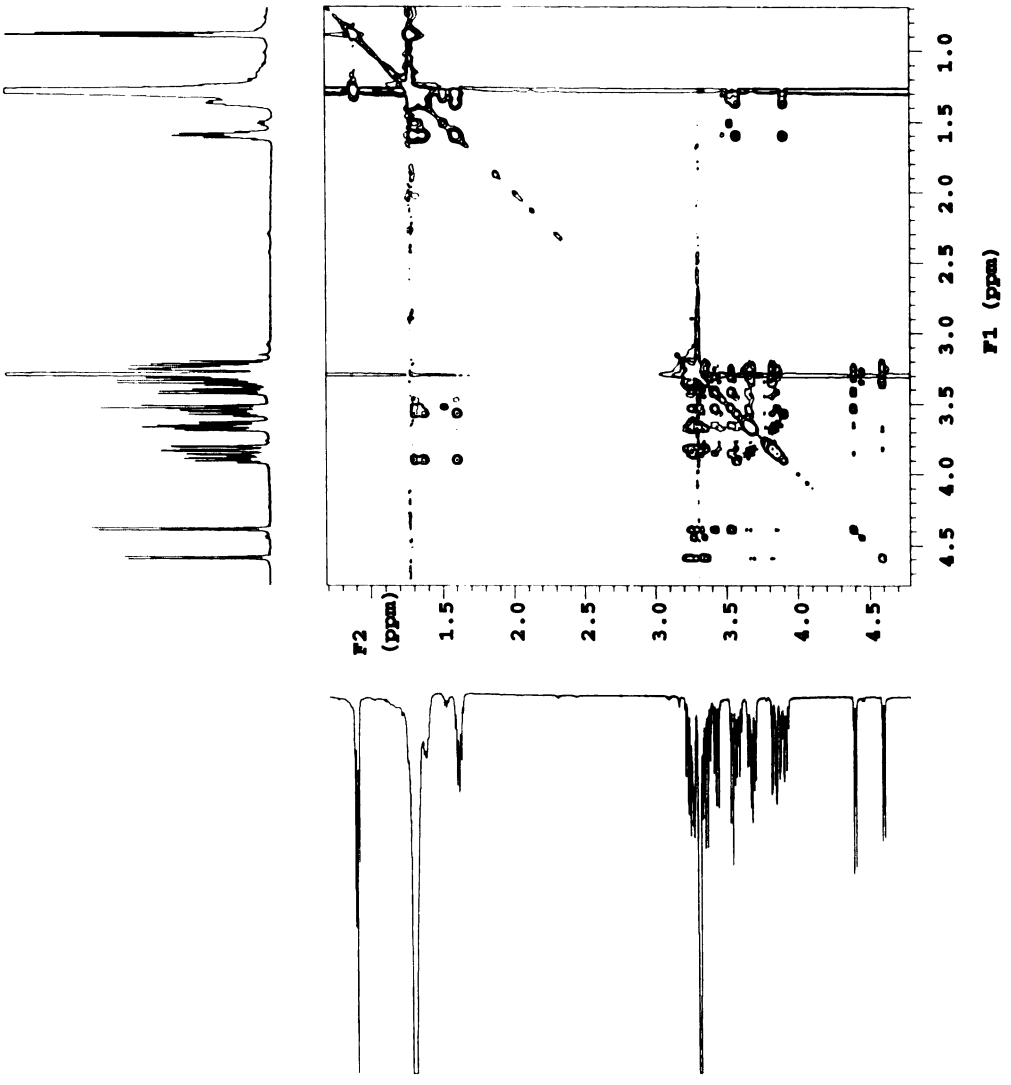

Figure 3.10: TOCSY NMR spectrum of the β-1-*O*-hexadecyl sophoroside.

sophorose moiety. The anomeric proton resonance at 4.39 ppm gave a cross peak with the H-2 resonance at 3.42 ppm, which in turn gave a cross peak with the H-3 resonance at 3.54 ppm. The H-3 resonance showed a cross peak with the H-4 resonance at 3.32 ppm. Likewise, the resonances of H-5 and H-6 were identified at 3.25 and 3.75 ppm, respectively. Similarly, the chemical shifts of the proton resonances of the other glucosyl unit were determined. The H-1′ through H-6′ resonances were found at 4.59, 3.22, 3.36, 3.26, 3.25, and 3.74 ppm, respectively. The assignments of ^{1}H NMR signals agreed well with the ^{13}C NMR signals, as demonstrated by the ^{1}H-^{13}C HMQC NMR spectrum (Figure 3.11). The ^{13}C signals can be assigned easily by ^{1}H-^{13}C correlated pairs in the HMQC spectrum. The resonance at 104.9 ppm represented the C1 of sophoroside β-linked to hexadecanol. The second anomeric resonance at 103.0 ppm corresponded to the C1′ of non-reducing glucose β-linked to the C2 of glucose in the sophorose moiety. The ^{1}H and ^{13}C signals of β-1-*O*-hexadecylsophoroside are listed in Table 3.2.

Table 3.2: ^{1}H and ^{13}C chemical shifts of the disaccharide residue of β-1-*O*-hexadecyl-β-1,2-diglucosyl glycoside.

^{1}H (ppm)	H-1	H-2	H-3	H-4	H-5	H-6
Glu-1	4.39	3.42	3.54	3.32	3.25	3.65,3.84
Glu-1′	4.59	3.22	3.36	3.26	3.25	3.67,3.81
^{13}C (ppm)	C-1	C-2	C-3	C-4	C-5	C-6
Glu-1	103.0	82.8	77.9	71.5	77.8 or 78.3	62.8
Glu-1′	104.9	75.9	77.6	71.5	77.8 or 78.3	62.8

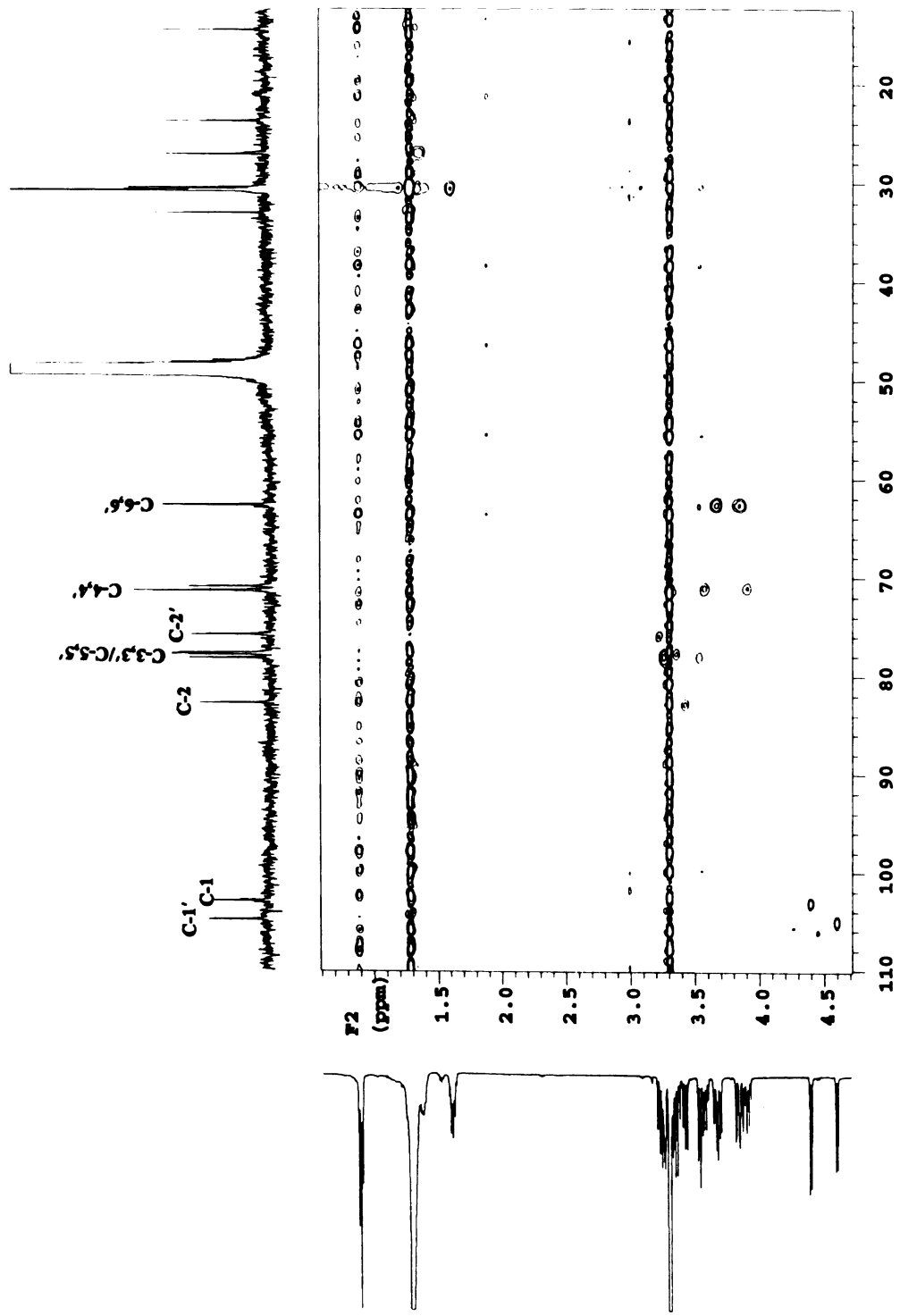

Figure 3.11: 2-D ^{1}H-^{13}C HMQC NMR spectrum of the β-1-*O*-hexadecyl sophoroside.

Because of the problematic nature of their synthesis, 1-*O*-acyl glycosides, especially of disaccharides, have not been available for study in the many areas in which alkyl glycosides have been used. *Sarcina ventriculi* and related organisms may prove to be a very valuable source of them in the future. This unusual family of glycosides represents the major proportion of the chloroform-methanol extractable lipids formed by this organism at low pH. The order, phase behavior and other properties of these glycosides should prove very interesting since they are synthesized in the ordered environment of a biological membrane. The study of the detergent-sensitive activity of membrane proteins especially in cytochrome *c* oxidase demonstrated that its activity in laruryl maltoside most closely approaches that of the physiological state [18]. It also indicated that the conformation of the sugar moiety as the critical factor in influencing the ability of the detergent to form micelles. The occurrence of these glycolipids in biological membranes might contribute to the membrane fluidity, stability, and the activity of membrane-associated proteins for *S. ventriculi* at low pH. Their biological activity and ability to preserve the conformational integrity of membrane proteins and other macromolecules should also be interesting. The fact that they separate out as a gel from the general bulk of the membrane indicates that they may form separate domains or islands of specific fluidity within the functioning membrane system. This would provide a richer variety of micro-environments. They may also off-set the rigidifying effect of the tail-to-tail cross linking.

REFERENCES

1. G.A. Jeffrey and Y. Yeon, *Carbohydr. Res.*, 1987, **169**, 1-11.

2. Y.J.Chung and G.A. Jeffrey, *Biochim Biophys. Acta*, 1989, **985**, 300-306.

3. H.M. van Doren and L.M. Wingert, *Mol. Cryst. Liq. Cryst.*, 1991, **198**, 381-391.

4. K.R. Gustafson, J.H. Cardellina, R.W. Fuller, O.S. Weislow, K.M. Kiser, K.M. Snader, G.M.L Patterson, and M.R. Boyd, *J. Natl. Cancer Inst.*, 1989, **81**, 1254-1258.

5. S. Jung, S.E. Lowe, R.I. Hollingsworth, and J.G. Zeikus, *J. Biol. Chem.*, 1993, **268**, 2828-2835.

6. S. Jung and R.I. Hollingsworth, *J. Theoret. Biol.*, 1995, **172**, 121-126.

7. S. Jung and R.I. Hollingsworth, *J. Lipid Res.*, 1994, **35**, 1932-1945.

8. S. Jung, J.G. Zeikus, and R.I. Hollingsworth, *J. Lipid Res.*, 1994, **35**, 1057-1065.

9. L.R. Bérubé and R.I. Hollingsworth, *Biochemistry*, 1995, **34**, 12005-12011.

10. R.I. Hollingsworth, *J. Phys. Chem.*, 1995, **99**, 3406-3410.

11. C.G. Jeremias, G.B. Lucas, and C.A. Mackenenzie, *J. Am. Chem. Soc.*, 1948, **70**, 2598-2590.

12. N. Weber and H. Benning, *Chem. Phys. Lipids*, 1982, **31**, 325-329.

13. Y. Wang and R.I. Hollingsworth, *Anal. Biochem.*, 1995, **225**, 242-251.

14. R.R. Earnst, G. Bodenhansen, and A. Wokaun, 1987, *Principles of Nuclear Magnetic Resonance in One and Two Dimensions*, pp 431-440, Oxford University Press, Oxford.

15. A. Bax and S. Subramanian, *J. Magn. Reson.*, 1986, **67**, 565-569.

16. K. Bock and H. Thogersen, *Ann. Rep. NMR Spectroscopy*, 1982, **13**, 1-57.

17. D. Garozzo, G. Impallomeni, E. Spina, B.N. Green, and T. Hutton, *Carbohydr. Res.*, 1991, **221**, 253-257.

18. P. Rosevear, T. VanAken, J. Baxter, and S. Ferguson-Miller, *Biochemistry*, 1980, **19**, 4108-4115.

CHAPTER IV

A TRI AND HEXASACCHARIDE β-GLUCAN WITH UNUSUAL LINKAGES FROM *SARCINA VENTRICULI*

ABSTRACT

The structure of a family of unusual glucans from *Sarcina ventriculi* has been characterized by NMR spectroscopy, methylation analysis, and mass spectrometry. One is a trisaccharide containing a β-1,3 and a β-1,4-linkage. The other is a hexasaccharide that is simply a β-1,4-linked dimer of the trisaccharide unit. This is the first report of β-glucan biosynthesis in a Gram-positive organism. Their occurrence in these organisms support an even more general link between their synthesis and the adaptability of bacteria.

INTRODUCTION

Beta-1,2-linked glucans are regular glucose oligomers that have been found thus far only in Gram-negative bacteria. The levels produced are affected by the osmotic balance and their synthesis is known to occur in the periplasm, the space between the inner and outer membranes. The absence of these glucans in Gram-positive bacteria, which have no periplasm, supports this idea. β-1,2-Glucans have been found in members of the family *Rhizobiaceae,* notably *Rhizobium* [1,2] *and Agrobacterium* [3,4], that can adapt to surviving intracellularly in plants. They have also been found in a few other Gram-negative genera including *Xanthamonas* (plant pathogens) [5], *Brucella* sp. (mammalian pathogens) [6], *Alcaligenes* [7], and *Acetobacter xylinium* [8]. In *Rhizobium* and *Agrobacterium* they are typically between 14 and 25 glucosyl residues in length and

are usually cyclic in structure [9]. There are instances where they are acyclic (linear) ranging from 6 to 42 glucose units in *Acetobacter* [8] or 6 to 19 units in some strains of *Rhizobium* [10]. Linear glucans ranging from 8 to 20 glucosyl units have been isolated from *Xanthamonas* species [5]. These β-1,2-glucans are related to those with mixed linkages found in *E. coli* and known generally as membrane-derived oligosaccharides [11]. They are thought to function in maintaining the osmolality of the periplasm, thus protecting the organism from osmotic stress [12-15]. As such, they have never before been found in Gram-positive organisms. *Rhizobium, Xanthamonas* and *Agrobacterium* are plant symbionts or pathogens and, since they must survive intracellularly inside the host cell, should be capable of readily adapting to differences in osmotic pressures. A role for the regulated synthesis of a molecule that might facilitate this is expected. In fact, bacterial mutants that are incapable of synthesizing these glucans are impaired in their ability to infect and live intracellularly in host plants. *Brucella* is a mammalian pathogen and the same is true of these species.

Sarcina ventriculi is an anaerobic, Gram-positive organism that is adaptable to a very wide range of environmental conditions including pH values ranging from 3 to 10 [16] and in the presence of a wide variety of organic solvents [17]. During normal growth, the pH of the medium becomes quite acidic and can drop to under 4 [16]. Recently, a family of fatty acylated β-1,2-linked glucose disaccharides were isolated from such cultures [18]. This indicated that *Sarcina ventriculi* was one Gram-positive organism in which the synthesis of β-glucans might be demonstrated. This would expand the link that had already been established between adaptability and β-glucan biosynthesis

[12-15]. Here we describe the isolation and characterization of two such glucans, a trisaccharide and a hexasaccharide from this anaerobic, Gram-positive organism.

MATERIALS AND METHODS

Isolation and Purification of Oligosaccharides

Sarcina ventriculi was cultured as previously described [16]. Cells were extracted by treating a suspension in a buffer consisting of 25 mM EDTA and 50 mM TRIS-HCl (1:1) with lysozyme (50,000 units) and protease (7 units) at 37°C for 5 h. The slurry was then extracted with n-propanol. The propanol-water solution was concentrated to dryness and chromatographed on a C18 column (30 × 2.5cm) using water, water/methanol (1:1), methanol, methanol/chloroform (1:1), and chloroform as eluents. The water fractions were pooled and chromatographed on a Bio-Gel P4 column (200 × 2cm) using water as an eluant. Fractions of 6 mL were collected and assayed for carbohydrate by the phenol - sulfuric acid method [19]. Sugar-containing fractions were pooled and further purified on a silica gel column using a solvent system composed of 2-propanol:ammonia:water in the ratio 6:4:1. Fractions were assayed by the orcinol-sulfuric acid method [20].

Isolation and Purification of β -1,2-Glucan

Agrobacterium tumefaciens strain C58 was cultured as previously reported [21]. Cells were extracted twice with a mixture of water, methanol and chloroform (3:1:5). The aqueous layer was recovered, concentrated to a syrup and chromatographed on a

Sepharose 4B column (75cm × 6cm) in 1% aqueous acetic acid. Column fractions were monitored for carbohydrate using the phenol - sulfuric acid assay [20]. The last eluting peak containing the glucan was then subjected to chromatography on a Bio-Gel P2 column (100cm × 2cm) in water. This fraction was lyophilized and then subjected to limited hydrolysis in 0.2M trifluoroacetic acid at 100°C for use as a standard in thin layer chromatography. This was carried out on silica plates using a solvent system composed of 1-butanol:ethanol:water in the ratio of 5:3:2.

Methylation Analysis

To differentiate between a 3- and 4-substituted reducing end the samples of the trisaccharide and hexasaccharide (each ~100 μg) were reduced with $NaBD_4$ (~100 μg) in water (100 μL) for 2 h before methylation. The solutions were treated with HOAc (50 μL) to decompose excess reducing agent and then concentrated to dryness. Methanol (0.5 mL) was added and the solutions were evaporated to dryness. Four more 0.5 mL of MeOH were added and the solutions again concentrated to dryness after each addition to remove boric acid. The mixtures were treated with 500 μL of a 1.5 M solution of sodium methylsulfinyl anion in dry Me_2SO [22]. The mixtures were stirred for 24 h at room temperature and then treated 100 μL of iodomethane. The resulting suspensions were stirred for 1 h and then diluted to 3 mL of water and passed through C18 Sep-Pak cartridge. The cartridge was eluted sequentially with 3 mL each water, 1:1 MeOH-water, and finally MeOH. The fractions of MeOH-water and MeOH were collected separately and subjected to acid hydrolysis with 2M trifluoroacetic acid (1.5 h, 120°C). The

hyrolyzates were reduced with $NaBH_4$ as described earlier and then acetylated with dry pyridine (200 μL) and Ac_2O (100 μL) for 24 h at room temperature and then dried under N_2. The acetylated products were partitioned between water and $CHCl_3$. The chloroform fraction was removed and dried under N_2 at room temperature. The partially methylated, acetylated alditols were analyzed by GC-MS.

Mass Spectrometry

The fractions corresponding to a single peak by the silica column were pooled and analyzed by fast atom bombardment (FAB) mass spectrometry. Negative ion FAB mass spectra were recorded using a JEOL HX-110 double-focusing mass spectrometer with glycerol as a matrix. Collisionally activated dissociation tandem mass spectrometry (CAD-MS/MS) was conducted by scanning the electric sector and magnetic sector in a fixed ratio (B/E linked scan) [23]. Helium was used as the collision gas in a cell located in the first field-free region. The helium pressure was adjusted to reduce the abundance of the precursor ion by 30%. GC/MS analyses of the partially methylated alditol acetates were performed on a Hewlett-Packard 5995C GC/MS, equipped with a Supelco DB-225 fused-silica capillary column using a temperature program of 170°C (3 min) - 230°C at 2°C/min. Helium was used as the carrier gas.

NMR Spectroscopy

All NMR spectra were measured in D_2O at 500 MHz for ^1H or 125 MHz for ^{13}C with a Varian VXR 500 spectrometer. For the heteronuclear multiquantum coherence

(HMQC) experiments, a spectral width of 7114 Hz was employed for the ^{13}C dimension. A total of 32 transients were required at 1024 points each. A total of 512 data sets were acquired. The Double quantum filtered J-correlated spectroscopy (DQF-COSY) spectrum was obtained using a total of 512 data sets (16 transients at 2048 data points each).

RESULTS AND DISCUSSION

Thin layer chromatographic analysis of a polar fraction of a propanol-water extract of *Sarcina ventriculi* cells indicated the presence of carbohydrates in several components. Most of these corresponded to glycosides but some were much more polar and behaved like free oligosaccharides. The fastest moving of these components had an R_f value, a ^1H NMR spectrum and mass spectrum identical to the previously characterized β-1-*O*-acyl-sophorose. The FAB mass spectra of two slower moving components indicated that they were a trisaccharide and a hexasaccharide, respectively. Gas chromatography of alditol acetate derivatives indicated that glucose was the only component in both molecules. The negative ion FAB mass spectrum of the trisaccharide (Figure 4.1) contained a signal for the pseudomolecular ion, $[M-H]^-$ at m/z 503. The negative ion FAB mass spectrum of the hexasaccharide (Figure 4.2) contained the $[M-H]^-$ ion at m/z 989. The series ions at m/z 827, 665, and 503 corresponded to the sequential loss of glucose units from the pseudomolecular ion. A TLC analysis of the polar fraction from *S. ventriculi* and oligosaccharides of a partially hydrolyzed sample of *Agrobacterium tumefaciens* β-1,2-glucan as a standard was performed (Figure 4.3). This

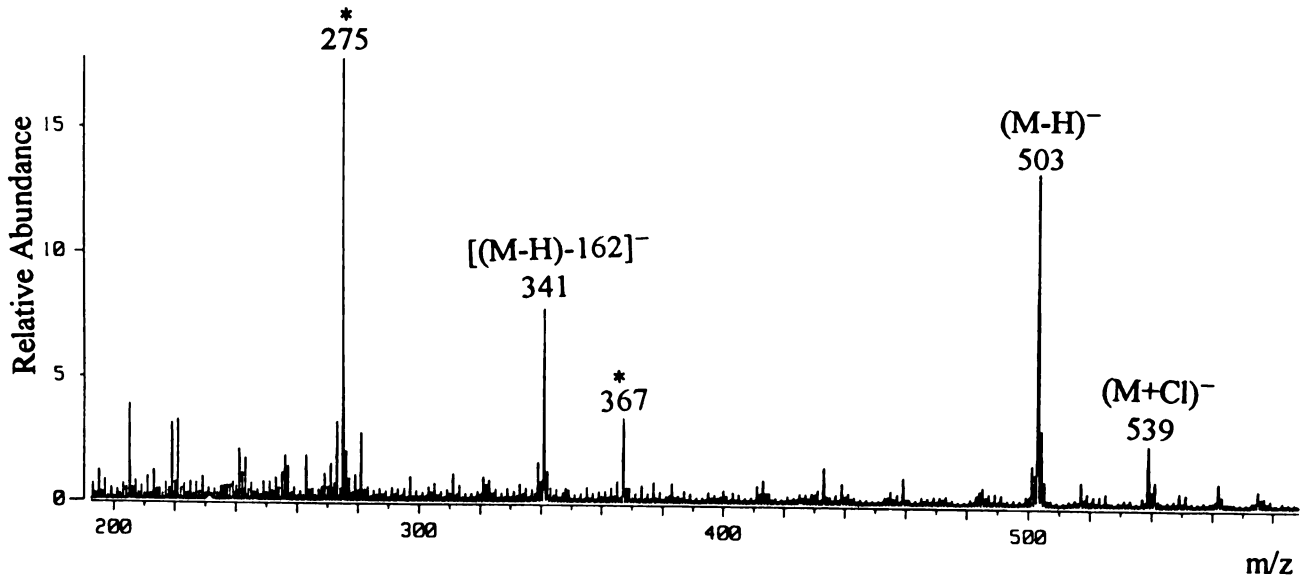

Figure 4.1: Negative ion FAB mass spectrum of the trisaccharide. Glycerol matrix peaks are designated by an asterisk.

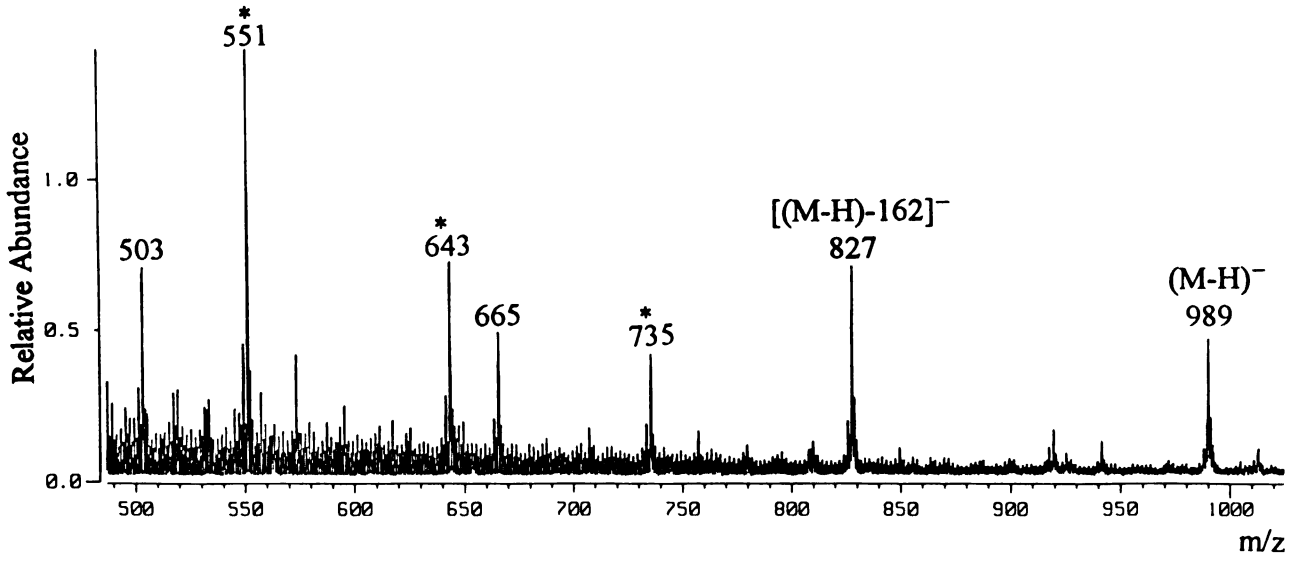

Figure 4.2: Negative ion FAB mass spectrum of the hexasaccharide.

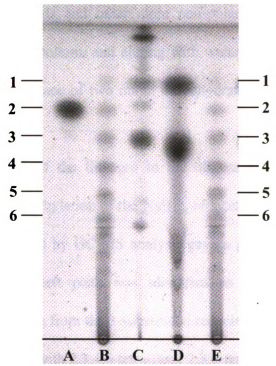

Figure 4.3: Thin layer chromatogram of sophorose (A), a partial acid hydrolysate of *Agrobacterium tumefaciens* β-1,2-glucan as a standard (B and E), a polar fraction of cell extracts of *S. ventriculi* (C), and water fraction from the C18 column of cell extracts of *S. ventriculi* (D). Numbers in the figure represent degree of polymerization.

also supported the chain lengths indicated by the mass spectra and the purity of the samples.

A more quantitative determination of the relative amounts of these oligosaccharides present and sufficient quantity to allow a rigorous structural characterization were obtained by gel filtration chromatography of the eluant after adsorbing out the glycolipids and other more non-polar components in the *Sarcina ventriculi* extract on a C18 column and eluting with water. Colorimetric analysis of the fractions indicated the presence of two major carbohydrate-containing peaks and a few minor ones.

A definitive study of the linkages in the oligosaccharides was performed by methylation analysis. Permethylation of the $NaBD_4$-reduced trisaccharide and conversion into alditol acetates followed by GC-MS analysis gave a profile containing three major peaks (Figure 4.4). The first peak was identified as 1-deuterio-1,2,4,5,6-penta-*O*-methylglucitol acetate arising from the 3-substituted reducing end. The later eluting peaks had mass spectra consistent with 2,3,4,6-tetra-, and 2,3,6-tri-*O*-methylglucitol derivatives. These results indicated that the trisaccharide was linear and contained a 1,3 and 1,4-linkage. The hexasaccharide yielded 1-deuterio-1,2,4,5,6-penta-, 2,3,4,6-tetra-, 2,4,6-tri-, and 2,3,6-tri-*O*-methyl-glucose in the ratio of 1:1:1:3. These results indicated that the hexasaccharide was probably a 1,4-linked dimer of the trisaccharide unit (Figure 4.5).

The positions and configurations of the glycosidic linkages were estabilished by 2-dimensional NMR spectroscopy experiments. In the ^1H NMR spectrum of the trisaccharide (Figure 4.6) four anomeric signals were observed at 4.36 ppm, 4.52 ppm, 4.60 ppm, and 5.09 ppm. Two signals at 5.09 ppm (J 3.8Hz) and 4.52 ppm (J 8.0 Hz)

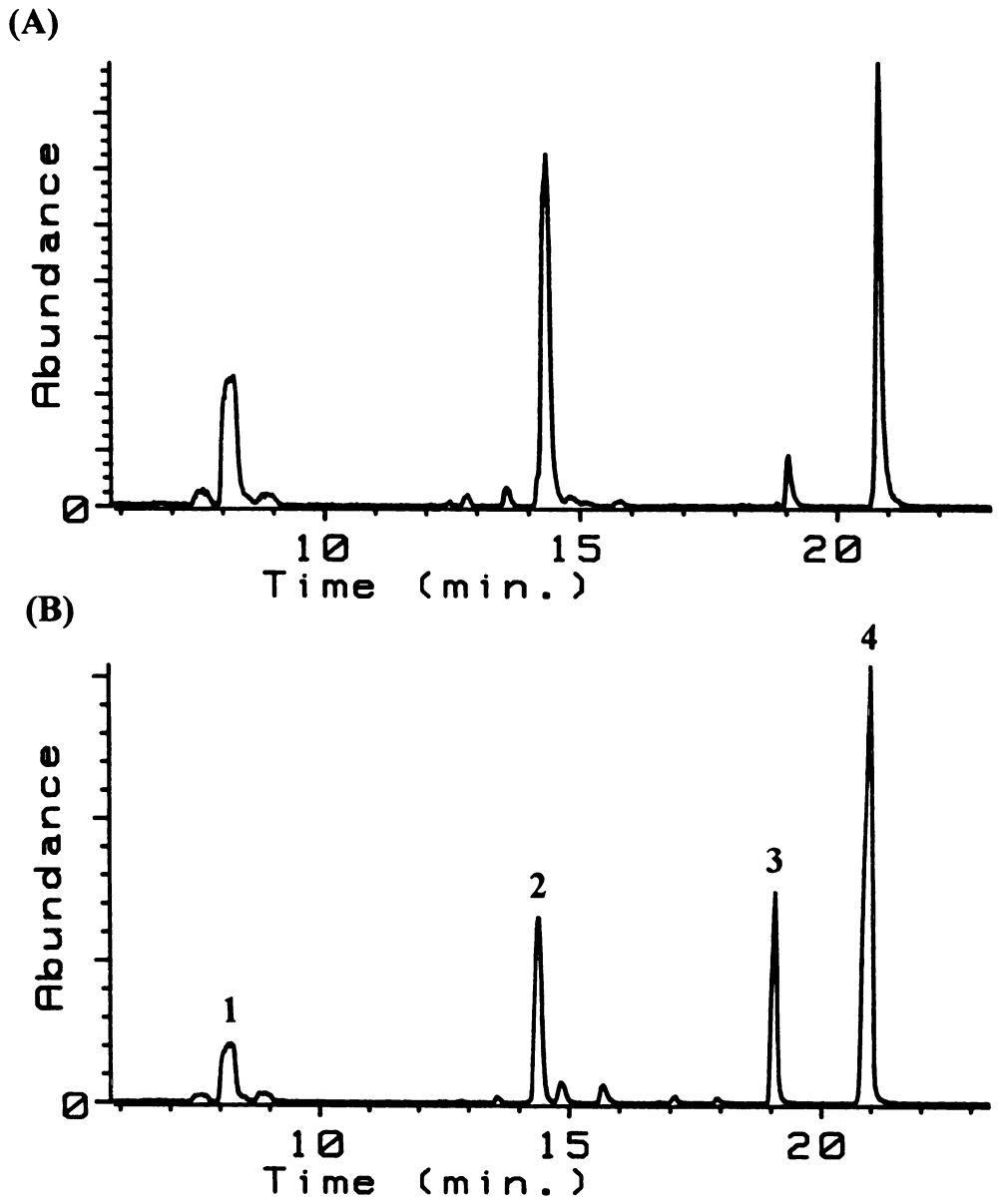

Figure 4.4: GC/MS total ion chromatograms of the partially methylated alditol acetates of the trisaccharide (A) and the hexasaccharide (B).

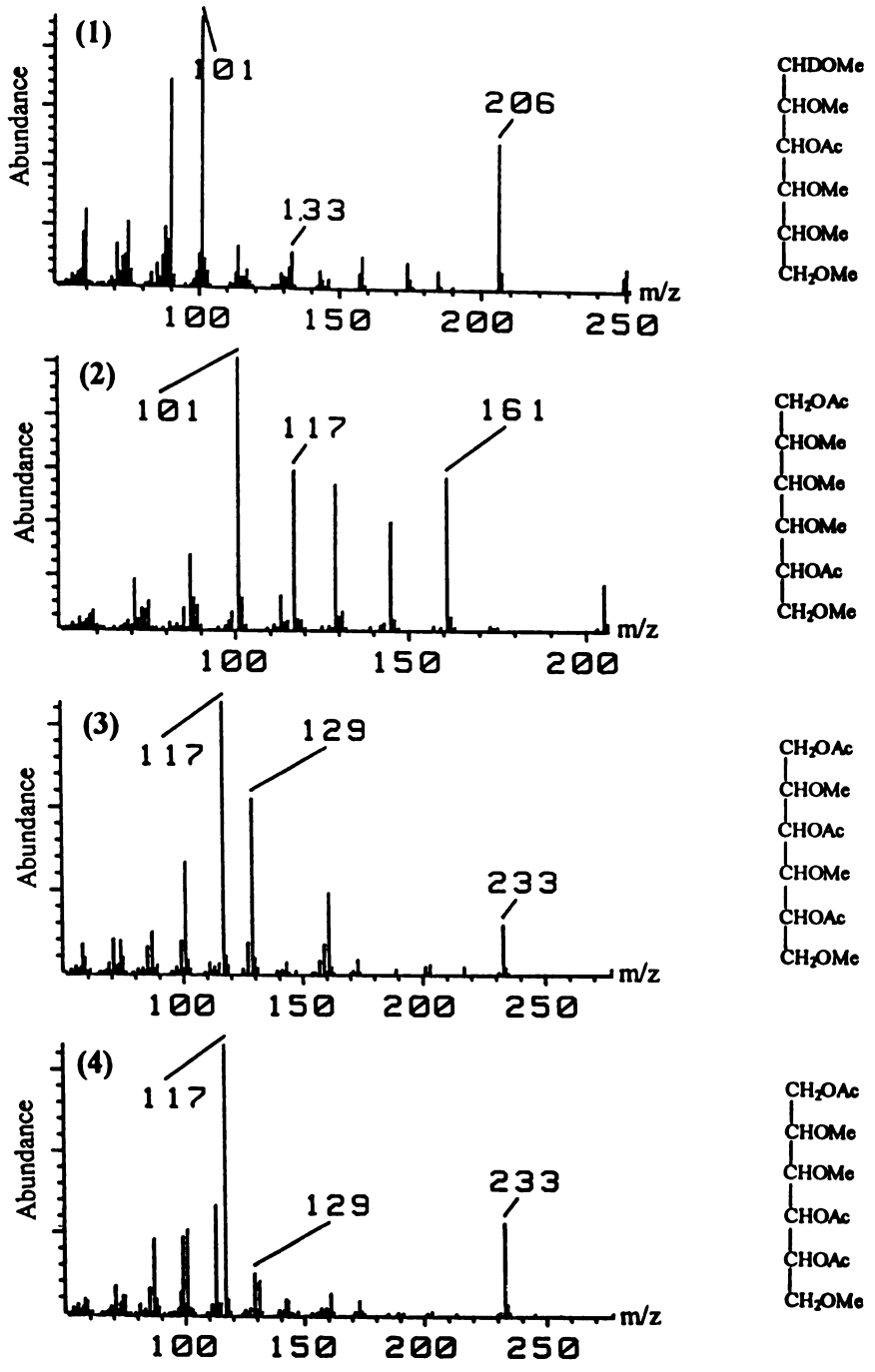

Figure 4.5: Mass spectra and structures of the partially methylated alditol acetates. of the hexasaccharide (peak 1 through 4 in Figure 4.4).

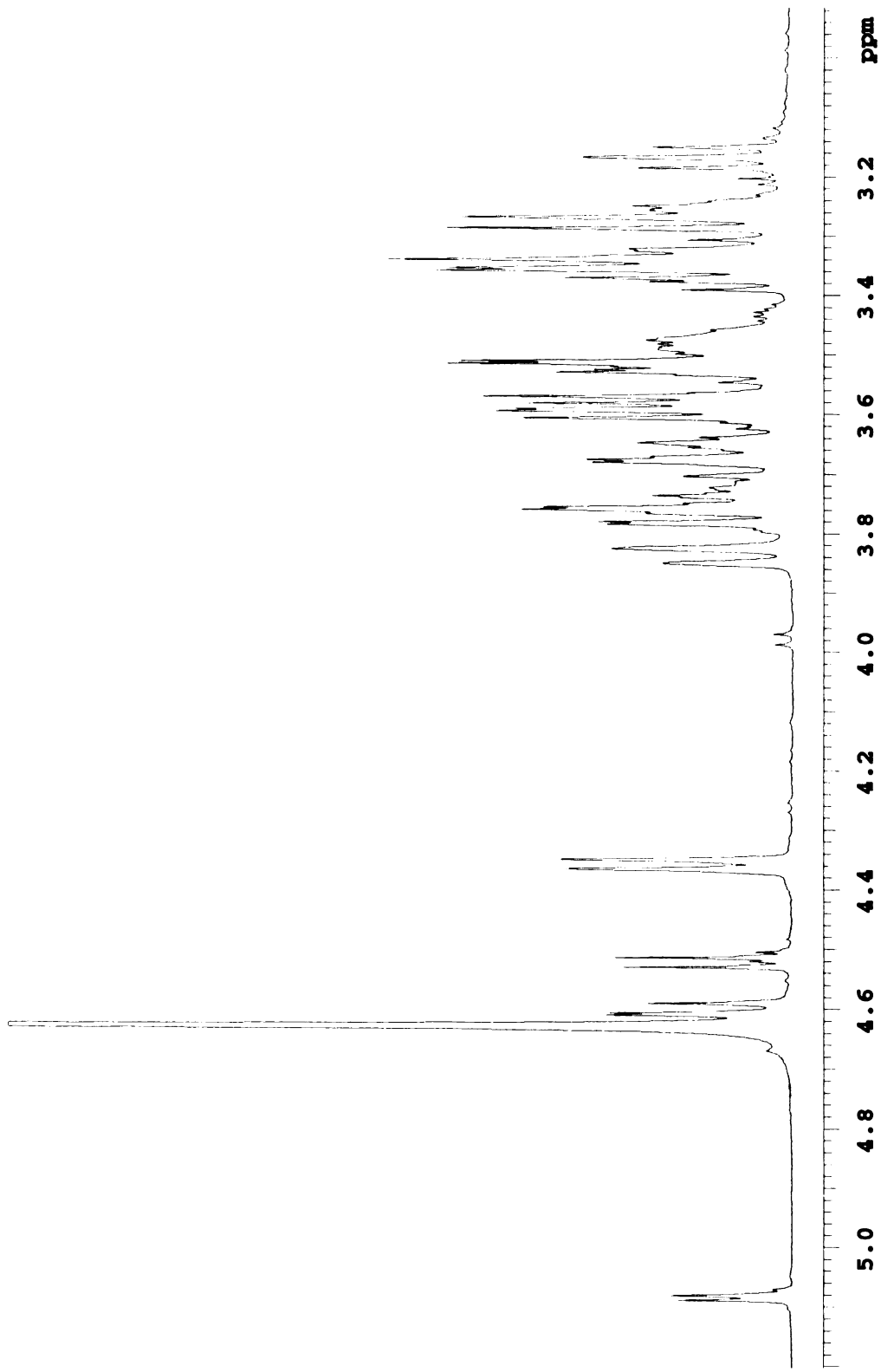

Figure 4.6: ^{1}H NMR spectrum of the trisaccharide.

were assigned to the α- and β-anomeric proton signals, respectively, of the reducing end. The signals at 4.36 ppm and 4.60 ppm were assigned to the two β-glucopyranosyl residues. The following structure was deduced for the trisaccharide : β-glucopyranosyl-(1→4)-β-glucopyranosyl-(1→3)-glucopyranose (Figure 4.7A).

The proposed structure of the hexasaccharide is shown in Figure 4.7B. The complete assignments for ^{1}H and ^{13}C NMR signals of the hexasaccharide are given in Table 4.1. The ^{1}H NMR spectrum of the hexasaccharide showed anomeric proton resonances in the region of 4.3~5.1 ppm. In the ^{1}H-^{13}C HMQC spectrum (Figure 4.8) a doublet at 5.09 ppm (J 4Hz) was correlated with the a ^{13}C signal at 92.9 ppm and was assigned to the α-anomeric proton of the reducing end. A doublet at 4.52 ppm (J 8Hz) was assigned to the β-anomeric proton of the reducing end. The anomeric proton signal at 4.60 ppm (J 8Hz) corresponded to the 1,3-linked β-anomeric proton of the second glucose residue (residue B) seen before in the trisaccharide spectrum. The doublet at 4.36 ppm was assigned to the nonreducing terminal group (residue F) using the same reasoning. These two anomeric signals displayed the same chemical shifts as those of the similar residues in the trisaccharide. The HMQC and DQF-COSY spectra (Figure 4.9) strongly indicated the presence of two anomeric proton signals at ~ 4.6 ppm where one of the signals partially overlapped with the solvent signal. The signal at 4.63 ppm was assigned to the anomeric proton engaged in the 1,3-linkage. The second 3-*O*-linked glucose residue could now either be residue C or D. This was determined by mass spectrometry. FAB-CAD-MS/MS has been used to determine the linkage position and sequence of underivatized disaccharides and oligosaccharides [24]. In the last cited study

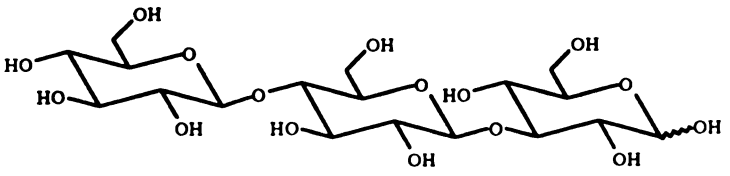

(A)

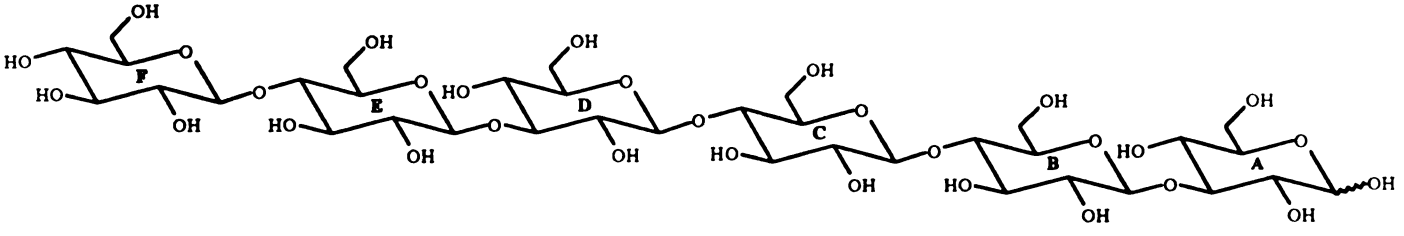

(B)

Figure 4.7: Structures of β-glucan observed in *Sarcina ventriculi*: (A) the trisaccharide (B) the hexasaccharide.

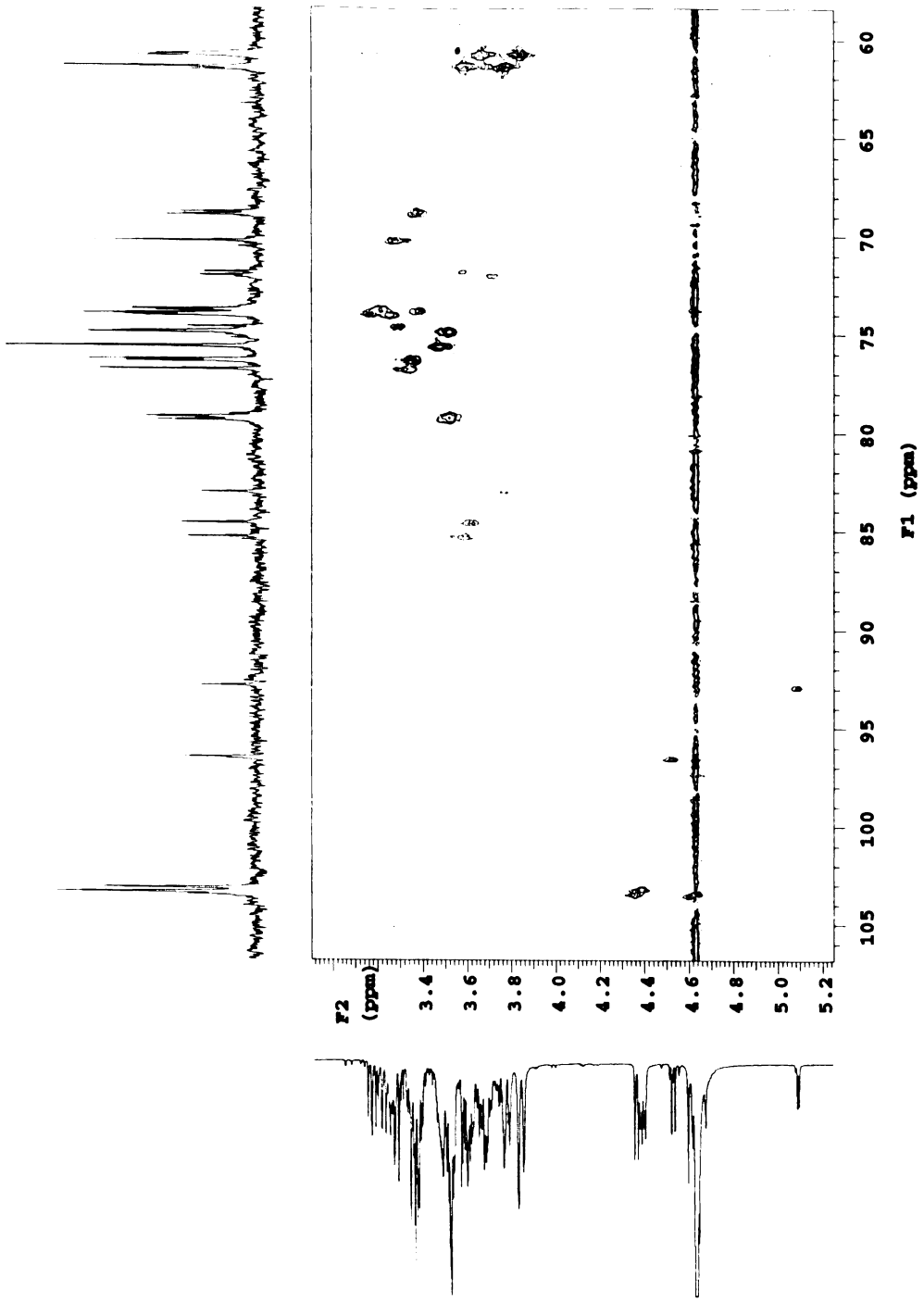

Figure 4.8: ^{1}H-^{13}C-HMQC spectrum of the hexasaccharide.

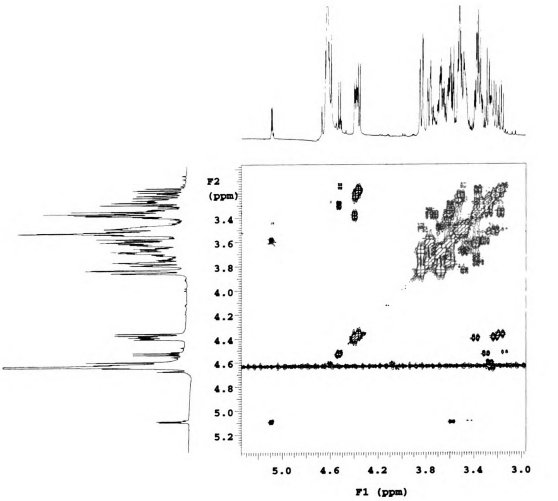

Figure 4.9: DQF-COSY spectrum of the hexasaccharide.

Table 4.1: ^{1}H and ^{13}C NMR chemical shifts of the hexasaccharide.

		Residues					
		A-α	A-β	B, E	C	D	F
1	H	5.09	4.525	4.601, 4.63	4.385	4.393	4.360
	C	92.9	96.5	103.4	103.2	103.2	103.4
2	H	3.59	3.29	3.26, 3.25	3.21	3.38	3.17
	C	71.9	74.7	74.1	73.8	73.8	74.0
3	H	3.79	3.60	3.52	3.51	3.63	3.36
	C	83.1	85.4	75.0	75.0	84.7	76.3
4	H	3.39	3.36	3.53	3.52	3.38	3.27
	C	69.0	69.0	79.2	79.4	68.8	70.3
5	H	3.73	3.37	3.48	3.50	3.37	3.34
	C	72.1	76.4	75.7	75.7	76.4	76.8
6	H	3.60/3.77	3.60/3.77	3.68/3.84	3.68/3.84	3.60/3.77	3.60/3.77
	C	61.4	61.4	60.8	60.8	61.4	61.4

the fragmentation patterns of 1,3- vs. 1,4-linkages were clearly delineated. This was confirmed by comparing the linked scan B/E mass spectra of the trisaccharide (βGlc1 → 4βGlc1 → 3Glc) obtained from this study and cellotriose (βGlc1 → 4βGlc1 → 4Glc) (data not shown). The linked scan B/E mass spectrum of cellotriose showed peaks at m/z 383, 425, and 443 which are characteristic ions of the 1,4-linkage to the reducing sugar. For the trisaccharide, only an intense ion at m/z 411 (loss of 92 amu) was present. The fragmentation pattern due to cleavage between the non-reducing and the middle glucose residues for both cases showed the same characteristic ions for the 1,4-linkage at m/z 161, 179, 221, 263, and 281. The linked scan B/E mass spectrum (Figure 4.10A) of the hexasaccharide ion at m/z 989 showed the characteristic loss of 92 amu indicating that the reducing sugar was linked by a 1,3-linkage. The ion at m/z 827 is attributable to the pentasaccharide formed by elimination of the reducing sugar (residues B-F). The linked scan B/E spectrum of the ion at m/z 827 showed the ions at m/z 707, 749, and 767 and not a simple loss of 92 amu indicating a 1,4-linkage between residues B and C (Figure 4.10B). The presence of peaks at m/z 545, 587, and 605 confirmed that the linkage between residues C and D was a 1,4-linkage. Thus, the second 3-*O*-linked glucose was assigned to residue D. The assignments for the other proton and ^{13}C signals were readily made and were consistent with the methylation analysis and the CAD-MS/MS spectra. The assignments were also consistent with those of model oligosaccharides such as laminaribiose and cellotriose. The other signals at 4.38~4.41 ppm (J 8Hz) in the NMR spectrum of the hexasaccharide corresponded to the two anomeric proton signals of the other internal residues engaged in the 1,4-linkages (residues C and D). The cross peaks

(A)

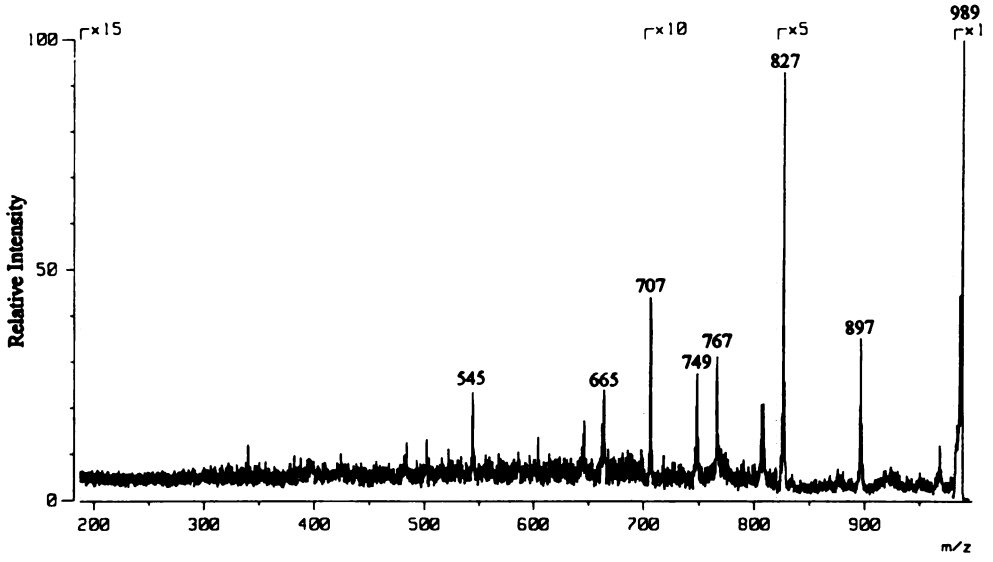

(B)

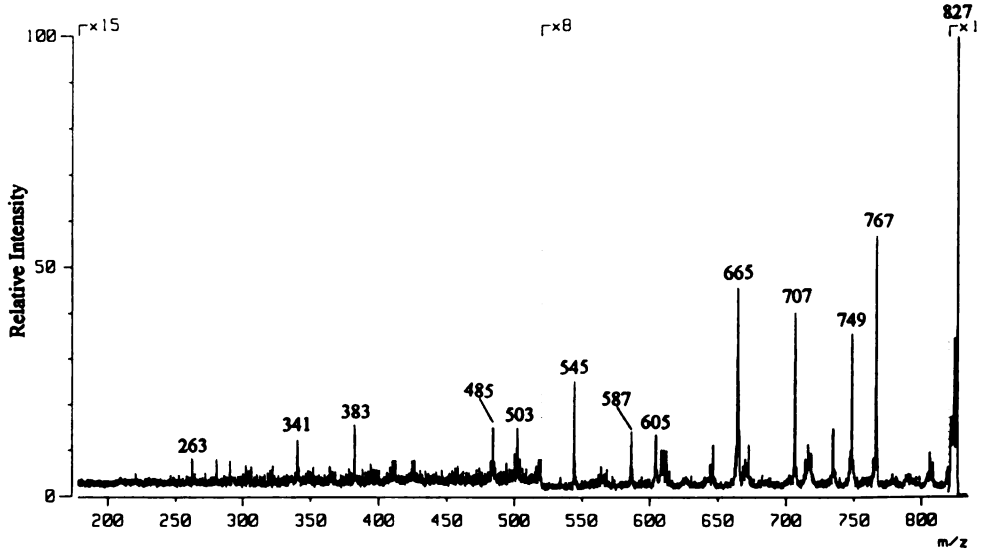

Figure 4.10: Negative ion B/E linked scans FAB mass spectra of the hexasaccharide:(A) psedomolecular ion at m/z 989 (B) ion at m/z 827.

between 79.2~85.4 ppm in the proton-carbon HMQC spectrum were assigned to the carbons involved in linkages. These signals are typically 10 ppm downfield of the other carbon signals. The signals for protons at carbon atoms involved in the linkages were readily identifiable through correlation with the corresponding ^{13}C signals in the HMQC spectrum. The α-anomeric proton of residue A showed three cross peaks at 3.39, 3.59, and 3.79 ppm in the HOHAHA spectrum (data not shown). The α-anomeric proton at 5.09 ppm was coupled to the H-2 proton of residue A at 3.59 ppm in the DQF-COSY spectrum. The H-2 signal of residue A showed a cross peak with H-3 at 3.79 ppm. The latter proton signal was correlated with a ^{13}C signal at 83.1 ppm indicating that C-3 was a linkage site. The HOHAHA-traces for the β-anomeric proton of residue A (4.525 ppm) showed connectivities with three signals at 3.29, 3.36, and 3.60 ppm. In the DQF-COSY spectrum, the β-anomeric proton of residue A was coupled to the H-2 proton signal at 3.29 ppm. The H-2 proton signal was also correlated with a signal at 3.60 ppm (H-3). The latter signal at 3.60 ppm showed a cross peak with in the HMQC spectrum with a ^{13}C chemical shift of 85.4 ppm. The assignments of ^{13}C chemical shifts of residue A were in good agreement with those of the reducing end of laminaribiose [25]. The H-1 signal of residue B was coupled to the H-2 signal at 3.26 ppm. The H-1 signal of residue E showed a cross peak with a signal at 3.25 ppm (H-2). The H-2 signals of residue B and E was coupled to the H-3 signal at 3.52 ppm. The remaining ^{1}H and ^{13}C signals of residue B and E showed the same chemical shifts. The H-1 signals of residue C was correlated with the H-2 signals at 3.21 ppm and was, in turn, coupled to the H-3 signal at 3.51 ppm. These three H-3 signals of residues B, C, and E were correlated with H-4 signals which, in the

HMQC spectrum, had cross peaks with ^{13}C chemical shift between 79.4 and 79.2 ppm indicating that residues B, C and E were the sites of 1,4-linkage. The H-1 signal of the 1,3-linked residue D was coupled to the H-2 signal at 3.38 ppm. The H-2 signal was coupled to the H-3 signal at 3.63 ppm. In the HMQC spectrum, the H-3 signal was correlated with the ^{13}C signal at 84.7 ppm confirming the 1,3-linkage. The assignments of ^{13}C chemical shifts for residue C and F were consistent with those of the internal residue and non-reducing group of cellotriose, respectively [26].

REFERENCES

1. M. Hisamatu, *Carbohydr. Res.*, 1992, **231**, 137-146.
2. M.W. Breedveld and K.J. Miller, *Microbiol. Revs.*, 1994, **58**, 145-161.
3. F.C. McIntire, W.H. Peterson, and A.J. Riker, *J. Biol. Chem.*, 1942, **143**, 491-496.
4. M. Hisamatsu, A. Amemura, T. Matsuo, H. Matsuda, and T. Harada, *J. Gen. Microbiol.*, 1982, **128**, 1873-1879.
5. A. Amemura and J. Cabrera-Crespo, *J. Gen. Microbiol.*, 1986, 132, 2443-2452.
6. D.R. Bundle, J.W. Cherwonogrodzky, and M.B. Perry, *Infect. Immun.*, 1988, **56**, 1101-1106.
7. T. Harada, *Biochem. Soc. Symp.*, 1983, **48**, 97-116.
8. A. Amemura, T. Hashimoto, K. Koizumi, and T. Utamura, *J. Gen. Microbiol.*, 1985, **131**, 301-307.
9. W.S. York, M. McNeil, A.G. Darvil, and P. Albersheim, *J. Bacteriol.*, 1980, **142**, 243-248.
10. A. Amemura, P. Footrakul, K. Koizumi, T. Utamura, and H. Taguchi, *J. Ferment. Technol.*, 1985, **63**, 115-120.

11. E.P. Kennedy, 1987, *Escherichia coli and Salmonella typhimurium: Cellular and molecular biology,* Vol. 1, pp 672-679, American Society for Microbiology, Washington D.C..

12. K.J. Miller, E.P. Kennedy, and V.N. Reinhold, *Science*, 1986, **231**, 48-51.

13. E.P. Kennedy and M.K. Rumley, *J. Bacteriol.,* 1988, **170**, 2457-2461.

14. J. Quandt, A. Hillemann, K. Niehaus, W. Arnold, and A. Puhler, *Mol. Plant-Microb. Interact.,* 1992, 5, 420-427.

15. O. Geiger, F.D. Russo, T.J. Silhavy, and E.P. Kennedy, *J. Bacteriol.,* 1992, **174**, 1410-1413.

16. E.S. Lowe, H.S. Pankratz, and J.G. Zeikus, *J. Bacteriol.*, 1989, **171**, 3775-3781.

17. S. Jung, E.S. Lowe, R.I. Hollingsworth, and J.G. Zeikus, *J. Biol. Chem.*, 1993, **268**, 2828-2835.

18. J. Lee and R.I. Holligsworth, *Tetrahedron,* 1996, **52**, 3873-3878.

19. M. Dubois, K.A. Gilles, J.K. Hamilton, P.A. Rebers, and F. Smith, *Anal Chem.*, 1956, **28**, 350-356.

20. R.B. Kesler, *Anal. Chem.*, 1967, **39**, 1416-1422.

21. Y. Zhang, R.I. Hollingsworth, and U.B. Priefer, *Carbohydr. Res.*, 1992, **231**, 261-271.

22. S. Hakomori, *J. Biochem. (Tokyo)*, 1964, **55**, 205-208.

23. K.R. Jennings and R.S. Mason, 1983, in *Tandem Mass Spectrometry Utilizing Linked Scanning of Double Focusing Instruments* (F.W. McLafferty ed.) Wiley, New York.

24. D. Garozzo, M Giuffrida, G. Impallomeni, A. Ballistreri, and G. Montaudo, *Anal. Chem.*, 1990, **62**, 279-286.

25. K. Bock, C. Pedersen, and H. Pedersen, *Adv. Carbohydr. Chem. Biochem.*, 1984, **42**, 193-225.

26. J.C. Gast, R.H. Atalla, and R.D. McKelvey, *Carbohydr. Res.*, 1980, **84**, 137-146.

CHAPTER V

CONFIRMATION AND COMPLETE ^{1}H-^{13}C NMR SPECTROSCOPY ASSIGNMENT OF THE STRUCTURE OF PEPTIDOGLYCAN FROM *SARCINA VENTRICULI*

ABSTRACT

The structure of peptidoglycan extracted from the Gram-positive bacterium *Sarcina ventriculi* grown at pH 3 was characterized by amino acid analysis, mass spectrometry, and 2-dimensional NMR spectroscopy. The basic muropeptide subunit consisted of a *N*-acetylglucosamine-β-1,4-*N*-acetylmuramic acid disaccharide substituted with an oligopeptide with the sequence Ala-*iso*Gln-A_2pm(-Gly)-Ala. The dimeric muropeptide was also characterized. It was a cross-linked bis-disaccharide-penta-hexapeptide with the structure GlcNAc-MurNAc-Ala-*iso*Gln-A_2pm(-Gly)-Ala → GlcNAc-MurNAc-Ala-*iso*Gln-A_2pm(-Gly)-Ala-Ala. This is completely consistent with a structure proposed based on enzymatic degradation and chemical modifications but with no use of spectroscopic information [O. Kandler, D. Claus, and A. Moore, *Arch. Mikrobiol.*, 82 (1972) 140-146]. The cell wall in this organism is very tightly cross-linked and is much more rigid than in most other Gram-positive bacteria. There is, however, a large degree of conservation in the general structure compared to peptidoglycan in other bacteria that are not well adaptable to extremes indicating that the membrane does play a more important role in adaptation.

INTRODUCTION

Peptidoglycan is a uniquely bacterial macromolecule that forms the rigid cell wall of both Gram-negative and Gram-positive bacteria. It consists of a glycan backbone of

alternating units of *N*-acetylglucosamine (GlcNAc) and *N*-acetylmuramic acid (MurNAc) of the linkage type [GlcNAcβ1→4MurNAc] with a short peptide chain (typically 3-5 amino acids long) linked to the lactyl moiety of muramic acid. There is crosslinking between the tetrapeptides of adjacent glycan strands usually involving the carboxyl of a C-terminal D-alanine of one peptide and the ω-amino group of a diamino acid. Peptide cross-linking bonds between amino acid residues located on different glycan chains lead to the formation of a complex three-dimensional macromolecule surrounding the cell [1]. Although the nature of the oligopeptides and the peptide bridge are both variable among bacterial groups [2], the general structure of a rigid arrangement of polymeric glycan crosslinked by peptides has been well conserved.

The muropeptides obtained by muramidase digestion have been isolated by reverse phase high performance liquid chromatography (HPLC) [3, 4]. Monomeric muropeptides have been characterized by fast-atom bombardment MS (FABMS) [5, 6, 7, 8], tandem mass spectrometry (FABMS/MS) [9, 10, 11], plasma desorption MS (PDMS) [12, 13], and specific enzymatic degradation [14]. The latter method has been used to support a proposed structure for the peptidoglycan of *Sarcina ventriculi* [15]. This structure has not been confirmed by spectroscopic methods.

Sarcina ventriculi is a highly adaptable Gram-positive organism that can be cultured under a variety of conditions including pH values ranging from 3 to 10 [16] and in the presence of a wide variety of organic solvents [17]. During normal growth, the pH of the medium becomes quite depressed and can drop to under 4 [16]. The specific adaptation of plasma membrane components of *Sarcina ventriculi* cells grown at low pH

has been studied and the formation of unusual transmembrane lipid species identified as a key adaptative response [17, 18]. These lipids span the membrane, thus stabilizing it. Whether the peptidoglycan has any unusual structural features in cells grown under these conditions is unknown. It is known that peptidoglycan structure might be sensitive to environmental conditions [19]. Here we describe the isolation and characterization of muropeptides of *Sarcina ventriculi* from cells grown at pH 3 by a combination of mass spectrometry and NMR spectroscopy in an effort to determine whether there are any unusual modifications. This study is also a critical step in providing NMR spectroscopy data that will allow the characterization of the 3-dimensional structure of the *Sarcina ventriculi* peptidoglycan by nuclear Overhauser effect measurements and angular constraints.

MATERIALS AND METHODS

Isolation and Purification of Muropeptides

Sarcina ventriculi was cultured as previously described [14]. Cells were extracted by treating a suspension in a buffer consisting of 25 mM EDTA and 50 mM TRIS-HCl (1:1) with lysozyme (50,000 units) and protease (7 units) at 37°C for 5 h. The slurry was then extracted with n-propanol. The propanol - water solution was concentrated to dryness and chromatographed on a C18 column (30 × 2.5 cm) which was eluted sequentially with water, water/methanol (1:1), methanol, methanol/chloroform (1:1), and chloroform as eluents. The aqueous fractions were pooled and chromatographed on a Bio-

Gel P4 column (200 × 2 cm) using water as the eluant. Fractions of 6 mL were collected. These were assayed for carbohydrate by the phenol sulfuric acid method [20]. The early eluting fractions belonging to the same peak were pooled.

Mass Spectrometry

The fractions were pooled and analyzed by FAB mass spectrometry with an instrument setting for mass range from m/z 0 to 2250. FAB mass spectra were recorded using a JEOL HX-110 double-focusing mass spectrometer with dithiothreitol (DTT) and thioglycerol (TG) mixture in the ratio of 1:2 as a matrix [21]. The accelerating voltage was 10 kV and the resolution was set at 1000. The desalting of the samples was done by using cation exchange resin (Bio-Rad AG 50W-X8). For this, several particles of resin were added into the aqueous samples containing 2% trifluoroacetic acid. The suspension was then vortexed for several minutes. In order to determine the number of free carboxyl groups, the sample was methylated with excess diazomethane in ether for 20 min. at room temperature. The collisionally activated dissociation tandem mass spectrometry (CAD-MS/MS) was conducted by scanning the electric sector and magnetic sector in a fixed ratio (B/E linked scan) [22]. Helium was used as the collision gas in a cell located in the first field-free region. The helium pressure was adjusted to reduce the abundance of the parent ion by 50%. Matrix-assisted laser desorption ionization (MALDI) mass spectrometry was performed in the positive-ion mode on a PerSeptive Biosystems Voyager Elite laser desorption time-of-flight instrument with a nitrogen UV laser. 2,5-Dihydroxybenzoic acid was used as matrix. For carbohydrate analysis, the sample was

hydrolyzed with 2M trifluoroacetic acid, reduced with sodium borohydride and then acetylated with acetic anhydride and pyridine. GC/MS analysis of the alditol acetates was performed on a Hewlett-Packard 5995C GC/MS, equipped with a Supelco DB-225 fused-silica capillary column using a temperature program of 170°C (3 min.) - 230°C at 2°C/min. Helium was used as the carrier gas.

Amino Acid Analysis

Aliquots of muropeptides were hydrolyzed in 6N HCl (24 h, 100◦C), derivatized with phenylisothiocyanate, and subjected to amino acid analysis by HPLC (Waters) equipped with a C18 column (3.8 × 250 mm) and Waters 440 UV detector (λ=254 nm).

NMR Spectroscopy

All NMR spectra were measured in D_2O at 500 MHz for ^{1}H or 125 MHz for ^{13}C with a Varian VXR 500 spectrometer. For the heteronuclear multiquantum coherence (HMQC) experiments [23], spectral width of 23202 Hz was employed for the ^{13}C dimension. A total of 64 transients were acquired at 1024 points each. A total of 512 data sets were acquired. The ge-DQFCOSY (phase sensitive mode) was obtained using a total of 512 data sets (32 transients at 2048 data points each). The proton homonuclear Hartman-Hahn (HOHAHA) experiments [24] were performed using a total of 1024 data sets with 64 transients at 2048 data points each. A mixing time of 80 ms was used. The heteronuclear multiple-bond correlation (HMBC) experiments were carried out with a spectral width of 23202 Hz for the ^{13}C dimension. A total of 256 data sets were acquired

with 32 scans and 1024 data points each.

RESULTS AND DISCUSSION

The separation profile of muropeptides by size exclusion chromatography on a Bio-Gel P4 column is shown in Figure 5.1. Samples from the peaks labeled I, II, III, and IV were subjected to acid hydrolysis followed by amino acid analysis. The amino acids found in all fractions were alanine, glutamic acid or glutamine, diaminopimelic acid, and glycine but in varying proportions between peaks. GC/MS analyses of the alditol acetate derivatives revealed the occurrence of GlcNAc and traces of glucose. The ^{1}H NMR spectra of fractions I, II, III, and IV revealed essentially the same features, indicating that the fractions corresponded to muropeptides of different size. The separation was good enough to permit further analysis. The ^{1}H NMR spectrum of Fraction IV (the lowest molecular size component) showed the least complexity and was expected to give the most information on the basic that it might be a monomeric subunit although some heterogeneity was expected.

The FAB/MS spectrum confirmed this heterogeneity. It indicated the presence of several components in fraction IV. Ions observed at m/z 718, 1018, and 1089 were assigned to sodiated molecular species. The sodium ions were removed with concomitant increase in sensitivity [2,13] by treating the samples with cation exchange resin (H^{+} form). The positive ion FABMS spectrum of muropeptides so treated showed mostly intense protonated molecular ions but still showed weak sodium adduct ions (Figure 5.2) allowing the molecular weights to be determined. A signal for an isotope +1 amu higher

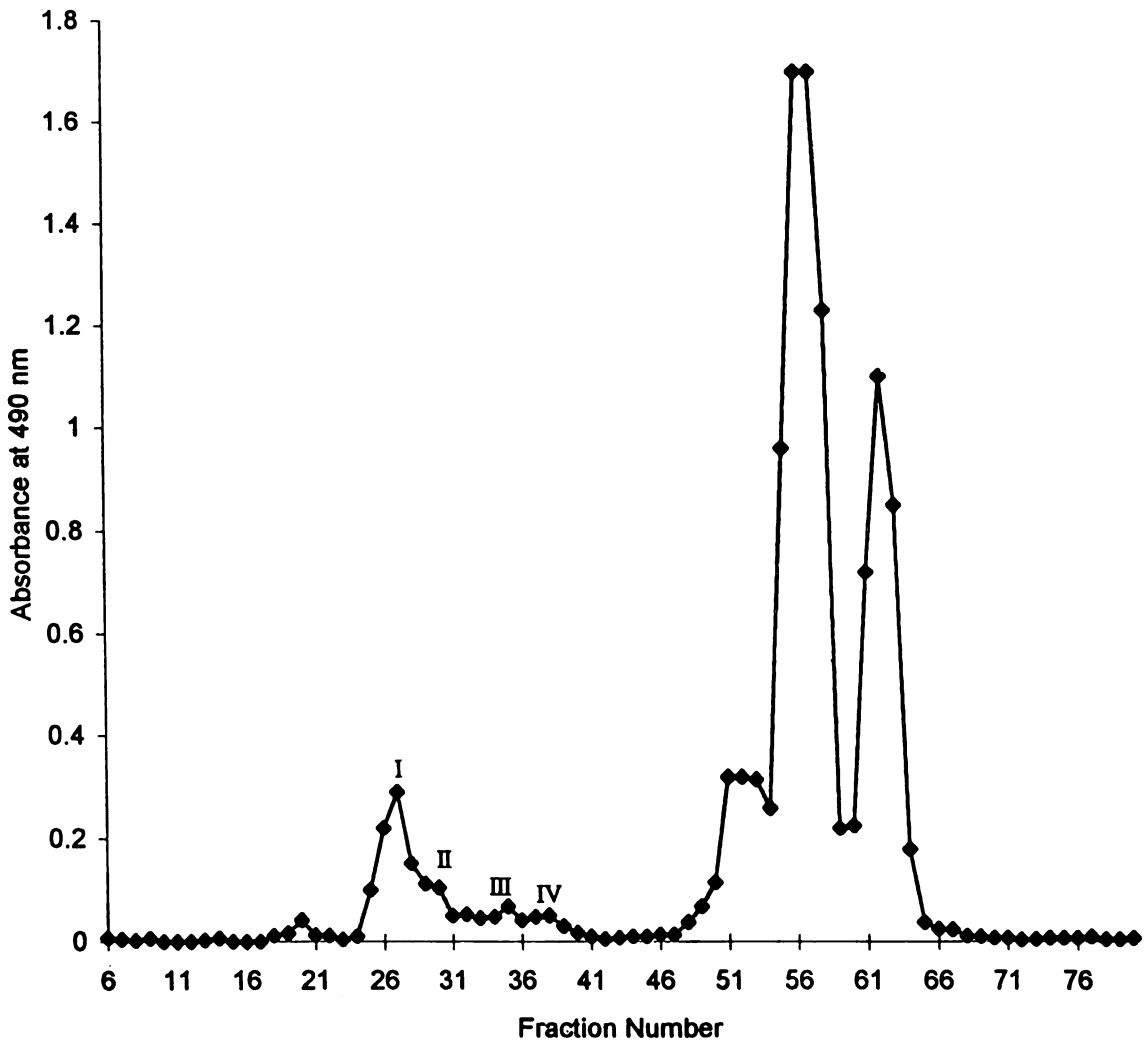

Figure 5.1: Gel filtration chromatogram on a Bio-Gel P4 column of the polar fraction of *Sarcina ventriculi* cell extracts. Note that the later eluting peaks corresponded to oligosaccharides.

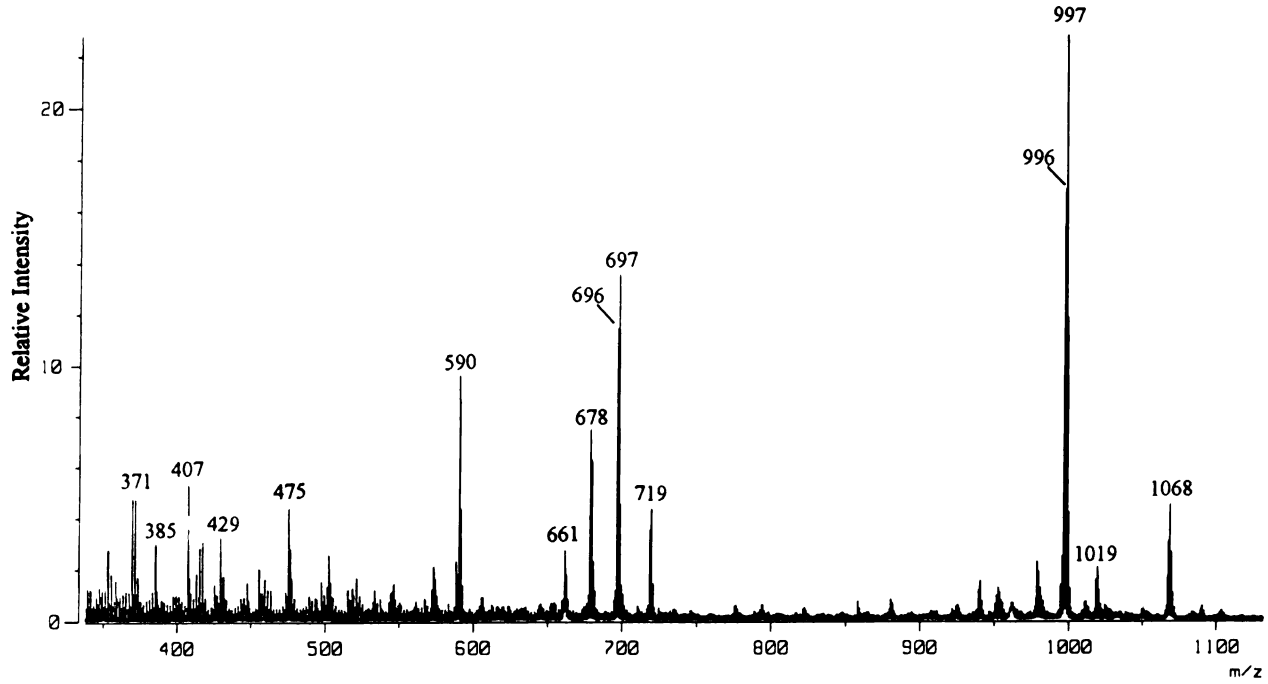

Figure 5.2: Positive ion FAB mass spectrum of the monomeric muropeptide. The complicated isotope pattern is due to the partial deuterium exchange of one amide proton because the sample was dissolved in D_2O for NMR experiments.

was observed for all of the peaks because of partial exchange of one amide proton by deuterium when the sample was dissolved in D_2O for NMR analysis. The ion at m/z 718 corresponded to the sodium adduct ion from $[M+H]^+$= 696 which appeared as a doublet at m/z 696/697 because of partial deuterium exchange. Based on carbohydrate and amino acid analyses, the ion at m/z 696 was assigned to the $[M+H]^+$ ion of the disaccharide-dipeptide :GlcNAc-MurNAc-Ala-*iso*Gln. The ion at m/z 678 was assigned to loss of water from the one at 696 although it could also be a protonated molecular ion of a 1,6-anhydromuramyl peptide [25]. However, this possibility was later excluded by 2-dimensional NMR spectroscopy. The ion at m/z 996 corresponded to the protonated ion of the muropeptide monomer GlcNAc-MurNAc-Ala-*iso*Gln-A_2pm-Ala. The ion at m/z 1067 corresponded to the monomeric muropeptide containing one more alanine residues at the C-terminal. The number of carboxylic acid groups in the various molecular species were determined by FABMS after converting them to methyl esters.

To further characterize the proposed structures, the protonated molecular ion at m/z 997 corresponding to the most intense ion in the ion cluster was analyzed by FAB-CAD-MS/MS. This is thought to be one of the most powerful mass spectrometry tool for the structural analysis of muropeptides [7, 8]. The CAD mass spectrum yielded a large number of product ions as shown in Figure 5.3. The ion at m/z 979 corresponded to the loss of water from the reducing end (Figure 5.4). The intense ions at m/z 793 and 776 corresponded to the cleavage on either side of the glycosidic oxygen and the loss of GlcNAc. Monosaccharide-related fragment ions were observed at m/z 204, corresponding to the oxonium ion of the terminal GlcNAc moiety. The ion at m/z 590 corresponded to the subsequent loss of 203 (a second GlcNAc) from m/z 793. The ion at m/z 573

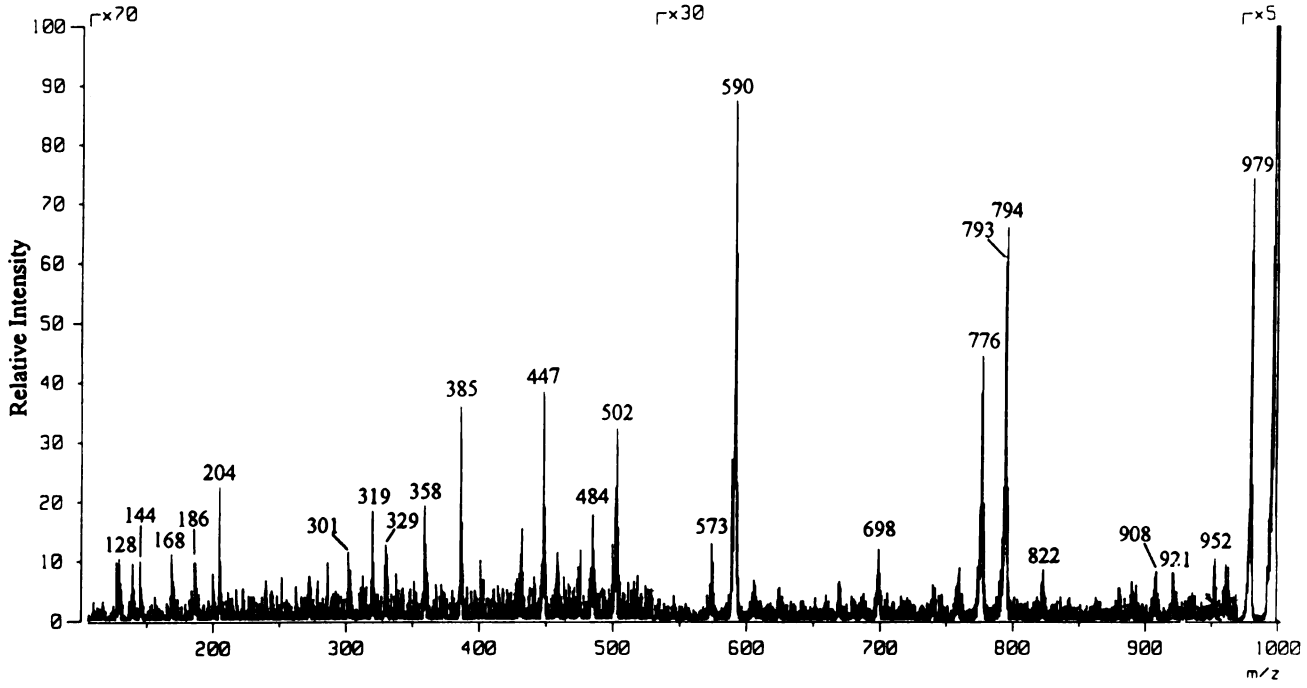

Figure 5.3: Positive ion FAB-CAD-MS/MS spectrum of GlcNAc-MurNAc-Ala-*i*Gln-A_2pm-(-Gly)-Ala, $(M+H)^+$ ion at m/z 997.

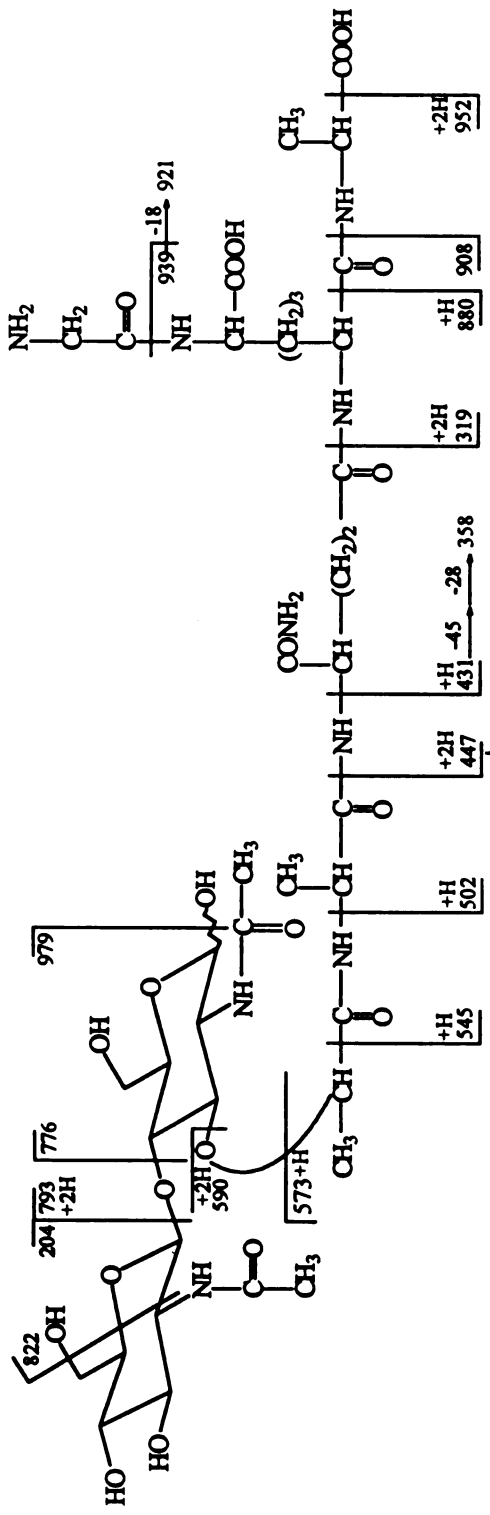

Figure 5.4: Structure and fragment ions observed in the FAB-CAD-MS/MS spectrum of $(M+H)^+$ ion at m/z 997.

represented the loss of the disaccharide moiety (GlcNAc-MurNAc) from the $[M+H]^+$ ion. The sequence of the peptide portion could be deduced from the ions associated with the cleavage along the peptide backbone. The product ion at m/z 573 further dissociated to m/z 447 and 319 by the loss of the lactyl-Ala and *i*Gln residues. The internal fragment ions at m/z 358, 301, 145, and 128 corresponding to the loss of 57, 156, and 17 daltons indicated the peptide sequence of *i*Gln-A_2pm-Gly. The glycine could be proposed to be linked to either the C-terminal alanine or the diaminopimelic acid. The fragment ion at m/z 908 indicated that the glycine was linked to the diaminopimelic acid. If the glycine residue were attached to the C-terminal alanine, the fragment ions at 922 and 895 would be observed [11].

Early eluting fraction III was analyzed by FABMS which indicated that it was a cross-linked dimer of the general structure just described. The ion at m/z 2045 corresponded to the cross-linked bis-disaccharide-penta-hexapeptide GlcNAc-MurNAc-Ala-*i*Gln-A_2pm(-Gly)-Ala → GlcNAc-MurNAc-Ala-*i*Gln-A_2pm(-Gly)-Ala-Ala (Figure 5.5). It could be deduced that the cross bridges were formed between C-terminal alanine and glycine. The ion at m/z 1974 corresponded to the bis-disaccharide-penta-pentapeptide in which the terminal alanine is lacking from the species corresponding to m/z 2045. The ions at m/z 2027 and 1956 could be attributed to loss of H_2O from the molecular ions at 2045 and 1974, respectively. There was also evidence for the presence of muropeptides containing tetrasaccharide sugars due to incomplete cleavages by muramidase. MALDI mass spectrum indicated the presence of dimers and trimers in fraction II. Table 5.1 lists the masses of the protonated molecular ions of the components detected along with their proposed structures.

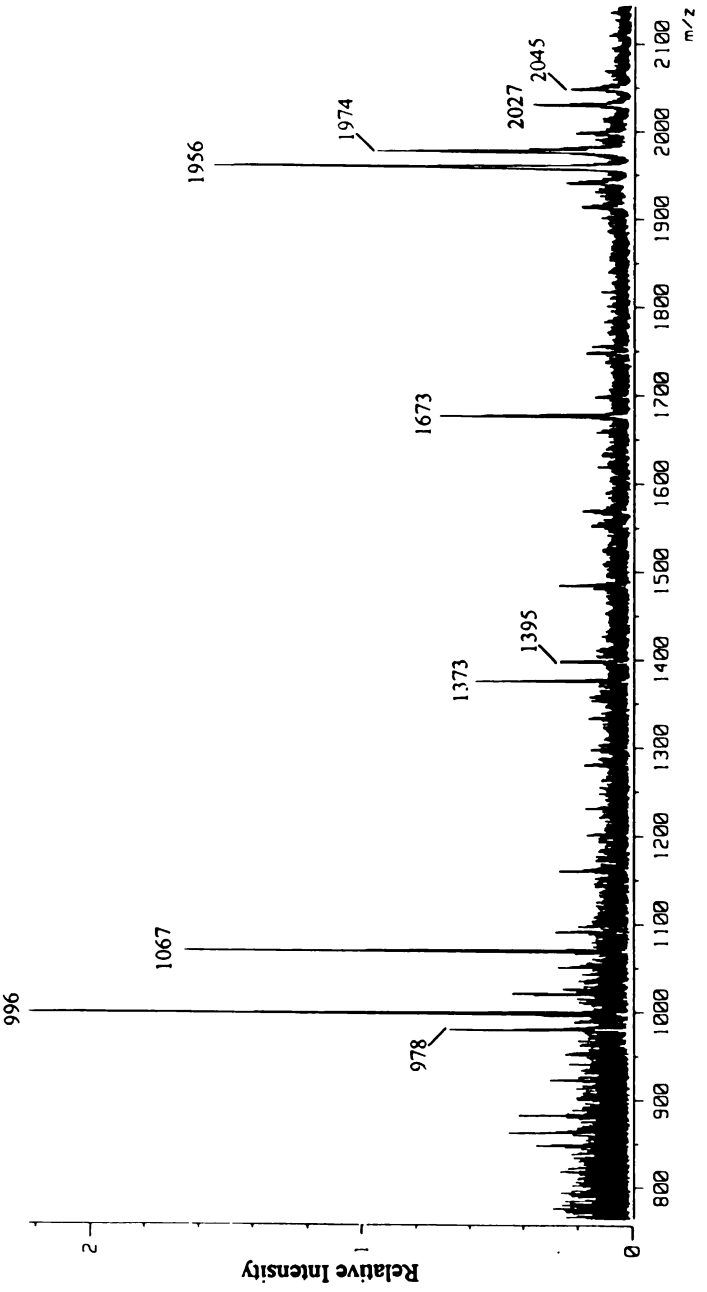

Figure 5.5: Positive ion FAB mass spectrum of the fraction III.

Table 5.1: Structures of the muropeptides from *Sarcina ventriculi*.

observed m/z	calculated m/z	Primary structure
696	695.3	GlcNAc-MurNAc-Ala-*i*Gln
996	995.4	GlcNAc-MurNAc-Ala-*i*Gln-A_2pm(Gly)-Ala
1067	1066.5	GlcNAc-MurNAc-Ala-*i*Gln-A_2pm(Gly)-Ala-Ala
1974	1972.8	GlcNAc-MurNAc-Ala-*i*Gln-A_2pm(Gly)-Ala → GlcNAc-MurNAc-Ala-*i*Gln-A_2pm(Gly)-Ala
2045	2043.9	GlcNAc-MurNAc-Ala-*i*Gln-A_2pm(Gly)-Ala-Ala → GlcNAc-MurNAc-Ala-*i*Gln-A_2pm(Gly)-Ala

In order to confirm the proposed structures, fraction IV was analyzed by 2-dimensional NMR spectroscopy. 2-D NMR spectroscopy allowed the assignments of all proton and carbon resonances unambiguously. The ^{13}C spectrum of the fraction IV is shown in Figure 5.6. The assignments of ^{1}H and ^{13}C resonances of the disaccharide moiety are presented in Table 5.2.

Table 5.2: ^{1}H and ^{13}C chemical shifts of the disaccharide residues of the muropeptide from *Sarcina ventriculi.*

^{1}H (ppm)	H-1	H-2	H-3	H-4	H-5	H-6
GlcNAc	4.46	3.66	3.34	3.47	3.32	3.69, 3.86
MurNAc (α)	5.15	3.74	3.68	3.78	3.78	3.64, 3.74
MurNAc (β)	4.56	3.64	3.51	3.76	-	-
^{13}C (ppm)	C-1	C-2	C-3	C-4	C-5	C-6
GlcNAc	99.9	55.6	75.6	73.1	69.8	60.6
MurNAc (α)	89.8	53.1	75.9	74.7	70.6	59.3
MurNAc (β)	94.6	55.2	78.8	74.9	-	-

The ^{1}H NMR spectrum showed one α- and two β-anomeric signals at 5.15, 4.57, and 4.46 ppm, respectively. The doublet at 4.46 ppm (J 8Hz) was correlated with the ^{13}C signal at 99.9 ppm in the HMQC spectrum in Figure 5.7 and was attributed to a β-anomeric carbon of GlcNAc. The ^{1}H-^{13}C correlated pair of signals at 4.57 (J 8Hz) and 94.6 ppm was assigned to the β-anomeric position of MurNAc acid. The ^{1}H-^{13}C correlated pair of signals at 5.15 and 89.8 ppm was assigned to the α-anomeric position of MurNAc. The reason for two MurNAc signals was due to the α and β forms since this residue is at the reducing end. The proton signals belonging to one continuous spin system were traced

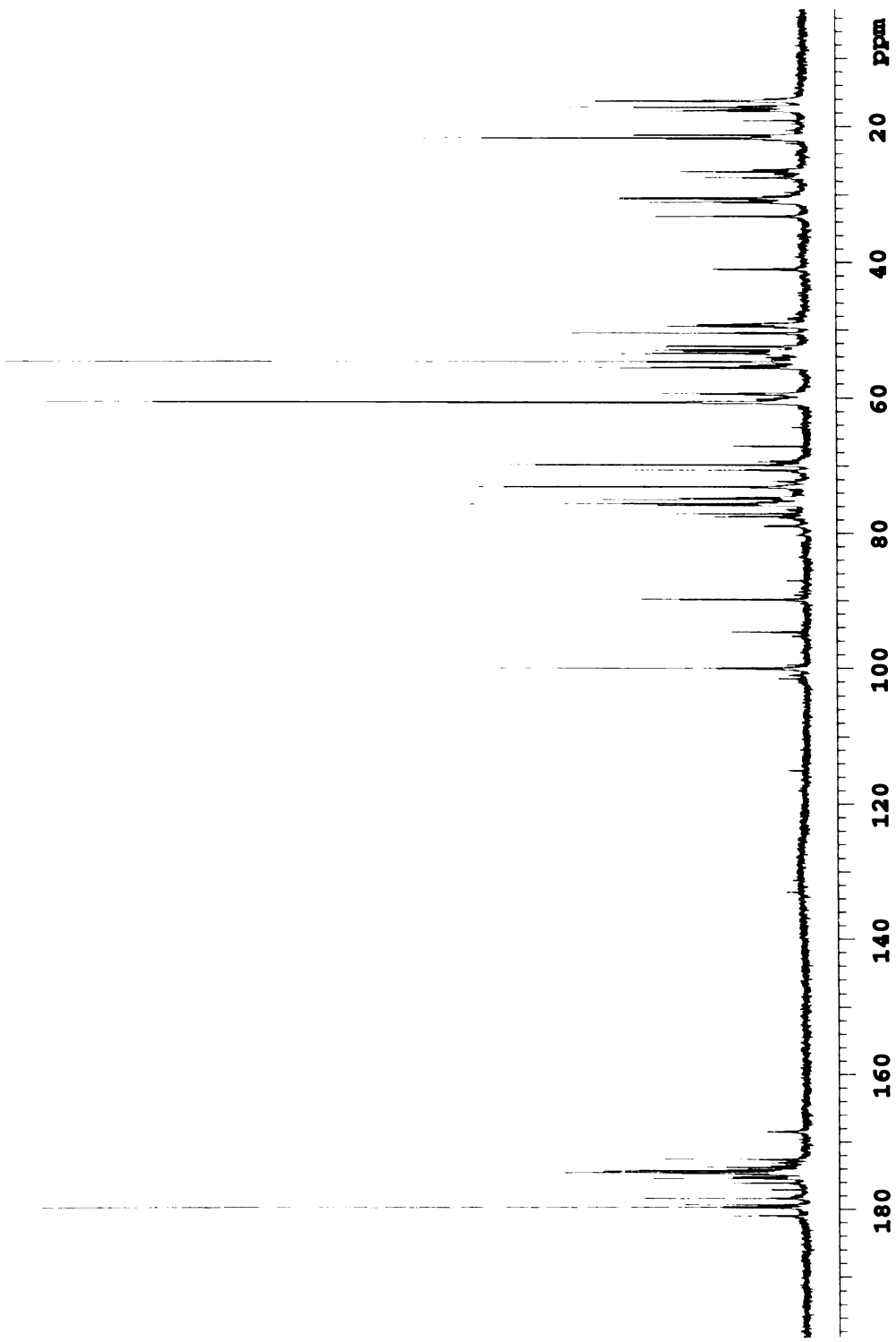

Figure 5.6: ^{13}C NMR spectrum of the monomeric muropeptide.

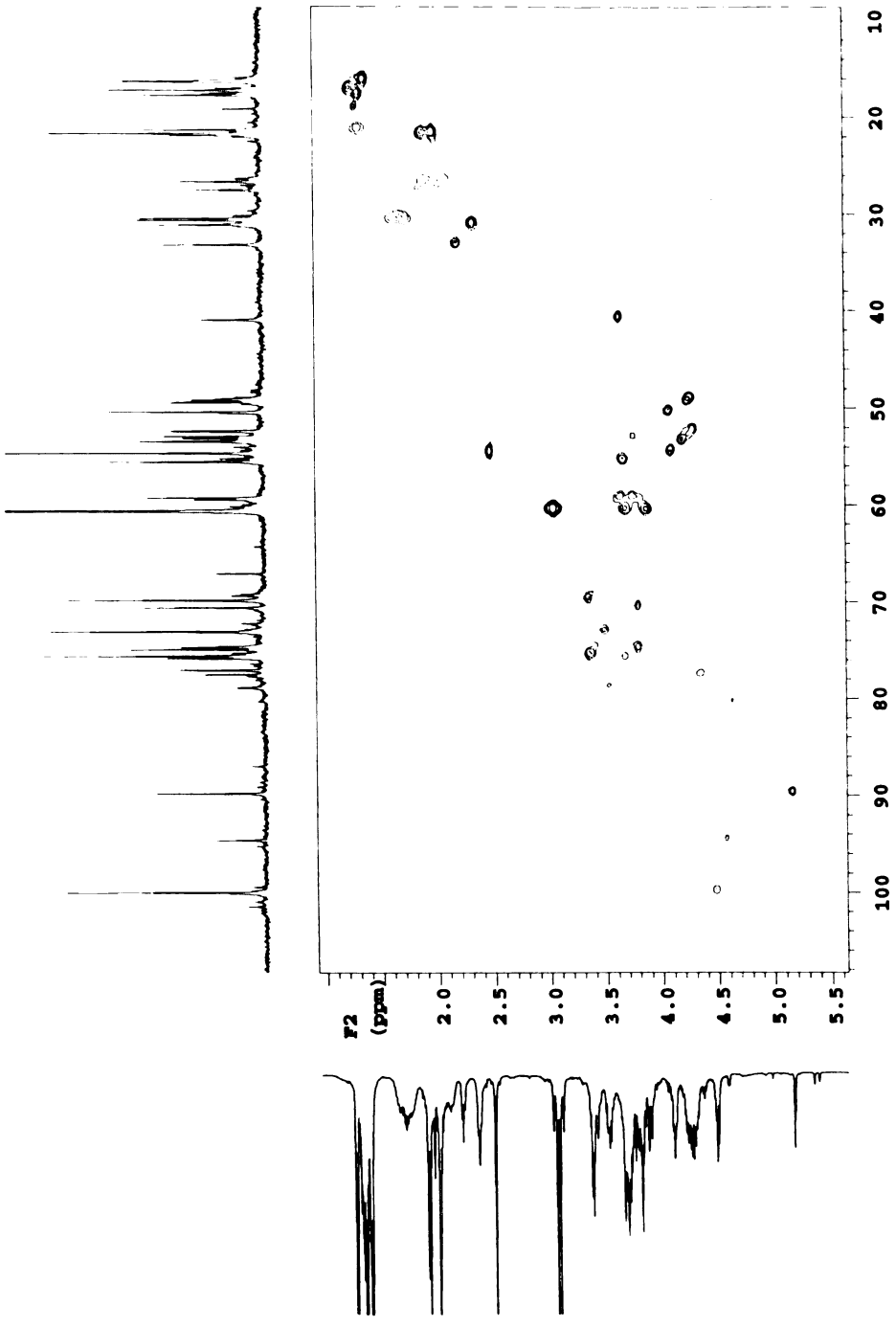

Figure 5.7: ^{1}H-^{13}C-HMQC spectrum of the monomeric muropeptide.

from the HOHAHA spectrum (Figure 5.8). The HOHAHA-traces for H-1 (4.46 ppm) of GlcNAc residue showed connectivities with three signals at 3.34, 3.47, and 3.66 ppm. The signal at 3.66 ppm was coupled to the H-1 signal in the gradient enhanced double quantum filtered J-correlated spectroscopy (ge-DQFCOSY) spectrum (Figure 5.9). This signal was also correlated with the ^{13}C signal at 55.6 ppm and was therefore assigned to H-2 of GlcNAc. The H-2 proton signal of GlcNAc was also correlated with the signal at 3.34 ppm. The latter signal at 3.34 ppm was, thus, assigned to the H-3 proton. The resonances for H-5 (3.32 ppm) was very closed to the H-3 signal and was coupled to one of the H-6 signal at 3.85 ppm. The H-6 signals appeared as two doublet of doublets at 3.86 and 3.69 ppm. The H-6 proton signals were correlated with the ^{13}C signals at 60.6 ppm. The α-anomeric proton of MurNAc showed three cross peaks at 3.68, 3.74, and 3.78 ppm in the HOHAHA spectrum. These three signals at 3.68, 3.74, and 3.78 ppm were assigned to the H-3, H-2, and H-4, respectively. The H-5 and H-6 resonances were assigned from the HMQC spectrum. The assignments were verified by a HMBC experiment showing two- and three-bond coupled cross peaks (data not shown). If MurNAc had contained a 1,6-anhydro linkage, there would have been another C-6 signal downfield of these C-6 signals. There was no indication of additional downfield C-6 signals. Thus, the ions at 678 and 978 in the FAB mass spectrum was due to the fragment ions instead of molecular ions from 1,6-anhydro muramyl compounds. The HOHAHA-trace of the β-anomeric signal of MurNAc showed four cross peaks at 3.39, 3.51(H-3), 3.64 (H-2), and 3.78 (H-4) ppm. The ge-DQFCOSY spectrum indicated that the signal at 3.39 ppm did not belong to α-MurNAc spin system. Three singlets at 1.87, 1.89, and 1.97

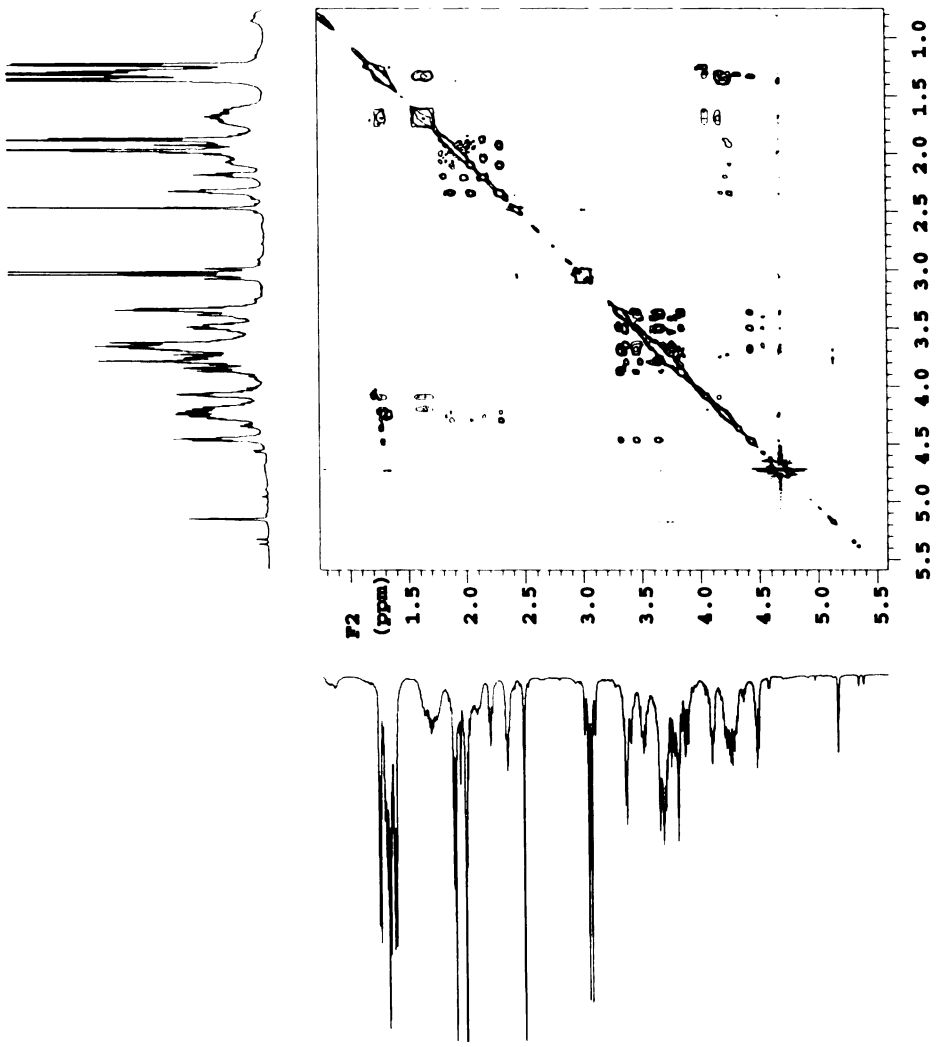

Figure 5.8: HOHAHA spectrum of the monomeric muropeptide.

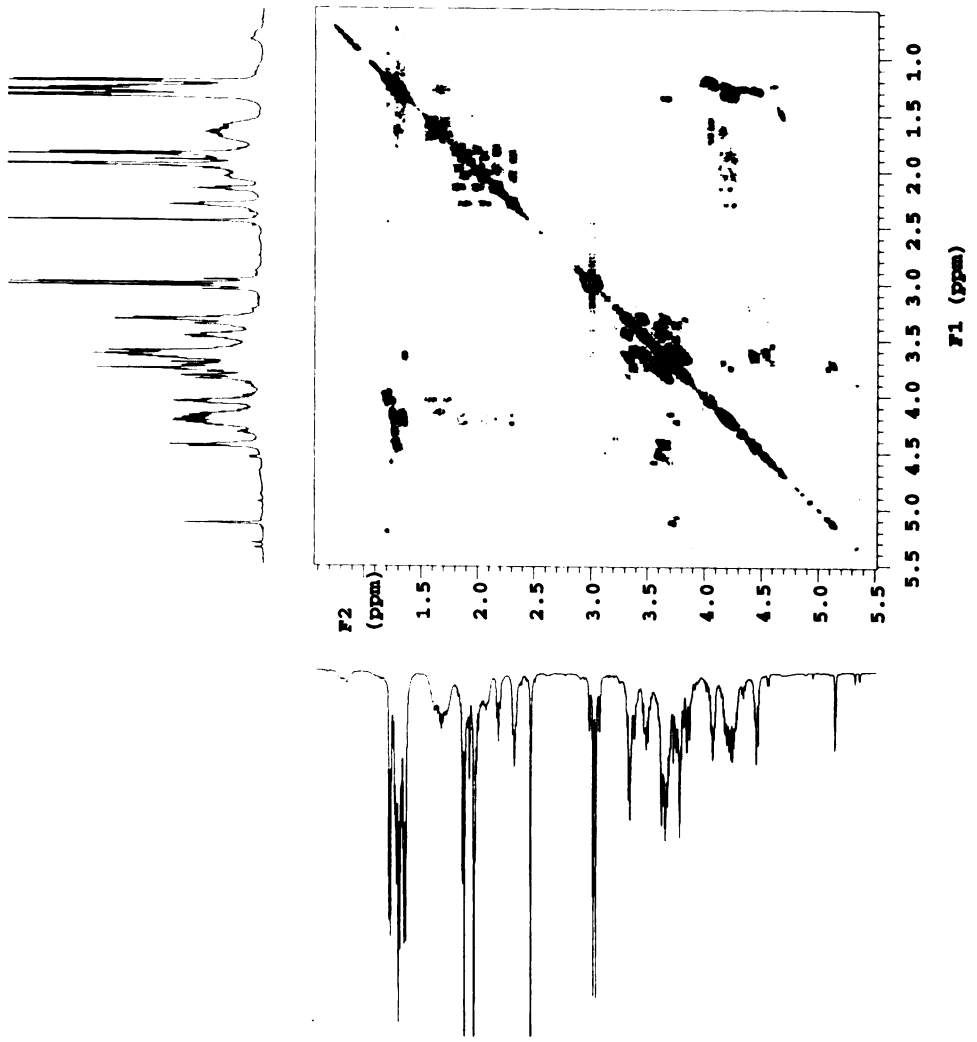

Figure 5.9: ge-DQFCOSY spectrum of the monomeric muropeptide.

ppm was assigned to the protons of *N*-acetyl groups of GlcNAc and α/β MurNAc residues, respectively. The signal at 1.31 ppm was correlated with the ^{13}C signal at 17.7 and 19.1. These methyl signals were assigned to the methyl signal of lactic group from MurNAc residue. The methyl signals of the lactic groups were coupled to the signals at 4.45 and 4.35 ppm in the HOHAHA and ge-DQFCOSY spectra. Thus, these latter signals were due to the methine signals of the lactic acid group. These methine proton signals showed cross peaks at 77.0 and 77.5 ppm in the HMQC spectrum and, as expected, were correlated with the carbonyl carbon of the lactic acid group at 175.4 ppm in the HMBC spectrum.

The assignments of ^{1}H and ^{13}C signals of the amino acid residues are presented in Table 5.3. The proton signals at 1.24 and 1.36 ppm were assigned to the H-β of alanine residue. In the HMQC spectrum, these methyl signals at 1.24 and 1.36 ppm were correlated with the ^{13}C signals at 17.2 and 16.3 ppm, respectively. These H-β of Ala were correlated with H-α at 4.06 and 4.25 ppm. The carbonyl signals at 174.5 and 179.2 ppm were assigned from the cross peaks between the H-α and carbonyl carbons in the HMBC spectrum. The signal at 179.2 ppm was assigned to the C-terminal Ala residue. The triplet signals at 2.18 and 2.33 ppm were assigned to the H-γ of the *iso*-glutamine residue. The triplet at 2.18 ppm was coupled to the signals at 1.92 and 4.23 ppm. The triplet at 2.33 ppm was correlated with the signals at 1.99 and 4.28 ppm in both HOHAHA and ge-DQFCOSY spectra. These multiplet signals at 1.92 and 1.99 ppm appeared underneath the methyl signals from *N*-acetyl groups corresponded to the H-β signals of the *i*Gln residues. The signals at 4.23 and 4.28 ppm were assigned to the H-α of the *i*Gln residue.

Table 5.3: ^{1}H and ^{13}C chemical shifts of the peptide residues of the muropeptide from *Sarcina ventriculi.*

^{1}H (ppm)	H-α	H-β	H-γ	
Gly	3.63			
Ala	4.06/4.25	1.24/1.36		
*i*Gln	4.28/4.23	1.84,2.01/1.90,2.08	2.18/2.33	
A_2pm	4.08/4.17	1.68	1.29	
^{13}C (ppm)	C-α	C-β	C-γ	Carbonyl
Gly	41.0			174.2
Ala	49.3/50.4	16.3/17.2		174.5/179.2
*i*Gln	52.4/53.0	26.6/27.5	31.1/33.2	180.8/174.4
A_2pm	53.5/54.7	30.4/30.6	21.3	172.5/178.3

More than one entry is given for some signals because of heterogeneity leading to different chemical shifts for the some nuclei in different environments. The muropeptide fraction IV contained two minor components in addition to major one.

The H-γ signals at 2.18 and 2.33 ppm showed cross peaks with the carbonyl carbons at 180.8 and 174.4 ppm in the HMBC spectrum. The signal at 180.8 was assigned to the C-terminal carboxyl group from the GlcNAc-MurNAc-Ala-*i*Gln molecule. The presence of diaminopimelic acid was further confirmed from the NMR spectra. The proton signal at 1.29 ppm was correlated with the ^{13}C signal at 21.3 ppm in the HMQC spectrum. The carbon chemical shift indicated that this signal was due to a methylene signal. This methylene signal was assigned to the H-γ of the A_2pm. The H-γ was correlated with the signals at 1.68 ppm and 4.08 and 4.17 ppm in the HOHAHA and ge-DQFCOSY spectra. The complex multiplet at 1.68 ppm which was correlated with the ^{13}C signal at 30.4 and 30.6 ppm in the HMQC spectrum corresponded to the H-β of the A_2pm. The signals at

4.08 and 4.17 ppm was assigned to the H-α. Two sets of the H-α and H-β signals appeared with different chemical shifts due to the different chemical environments of the two terminals of the diaminopimelic acid residue.

The peptide unit of peptidoglycan usually consists of four amino acids, with the general sequence Ala-Glu-X-Ala, where X is usually lysine or diaminopimelic acid. The glutamyl linkage is always in the γ position and the α-carboxyl of the glutamic acid may either remain unsubstituted, be amidated (as in *Staphylococcus aureus*) or aminoacylated (as in *Micrococcus luteus*) [26]. The peptidoglycan monomer of *Sarcina ventriculi* described earlier [15] and verified here belongs to the group A3γ according to Kandler classification [27]. This type of cross-linkage is also observed in *Propionibacteria*, some *Arthobacter*, *Clostridia* and *Streptomyces* [27]. The very short interpeptide bridge observed in *Sarcina ventriculi* should result in a more tightly cross-linked structure. However, the general structural conservation of peptidoglycan in *Sarcina ventriculi* is still remarkable and indicates that the adaptation process to very extreme environments occurs largely at the level of plasma membrane chemistry [17, 28, 29].

The 3-dimensional structure of peptidoglycans is still not known. The 3-dimensional structure of peptidoglycan from *Sarcina ventriculi* is especially important to us because of ongoing efforts to define the chemistry of the cell wall of this organism in extreme in detail in order to understand its organization and the structural modifications it undergoes during bacterial adaptation. The NMR spectroscopy assignments will make the calculation of the 3-dimensional structure a real possibility.

REFERENCES

1. W. Weidel and H. Pelzer, *Adv. Enzymol.*, 1964, **26**,193-232.

2. K.H Schleifer and O. Kandler, *Microbiol. Rev.*, 1972, **36**, 407-477.

3. T.J. Dougherty, *J. Bacteriol.*, 1985, **163**, 69-74.

4. B. Glauner, *Anal. Biochem.*, 1988, **172**, 451-464.

5. G. Allmanier, M.C. Rodriguez, and E. Pittenauer, *Rapid Commun. Mass Spectrom.*, 1992, **6**, 284-288.

6. E. Pittenauer, G. Allmaier, and E.R. Schmid, 1993, in *Bacterial growth and lysis: metabolism and structure of the bacterial sacculus,* pp 39-46 (M.A. de Pedro, J.-V. Höltje, and W. Löffelhardt, eds.), Plenum Press, New York.

7. J.C. Quintela, E. Pittenauer, G. Allmaier, V. Aran, and M.A. de Pedro, *J. Bacteriol.*, 1995, **177**, 4947-4962.

8. S.A. Martin, M.L. Karnovsky, J.M. Krueger, J.R. Pappenheimer, and K. Biemann, *J. Biol. Chem.*, 1984, **259**, 12652-12658.

9. S.A. Martin, R.S. Rosenthal, and K. Biemann, *J. Biol. Chem.*, 1987, 262, 7514-7522.

10. W.J. Folkening, W. Nogami, S.A. Martin, and R.S. Rosenthal, *J. Bacteriol.*, 1987, **169**, 4223-4227.

11. S.A. Martin, 1988, in *Antibiotic Inhibition of Bacterial Cell Surface Assembly and Function*, pp 129-145 (P. Actor, L. Daneo-Moore, M.L. Higgins, M.R.J. Salton, G.D. Shockman, eds.), American Society for Microbiology, Washington.

12. J.F. Garcia-Bustos, B.T. Chait, and A. Tomasz, *J. Biol. Chem.*, 1987, **262**, 15400-15405.

13. M. Caparrós, E. Pittenauer, E.R. Schmid, M.A. de Pedro, and G. Allmaier, *FEBS Lett.*, 1993, **316**, 181-185.

14. J.-M. Ghuysen, *Bacteriol. Rev.*, 1968, **32**, 425-464.

15. O. Kandler, D. Claus, and A. Moore, *Arch. Mikrobiol.*, 1972, **82**, 140-146.

16. S.E. Lowe, H.S. Pankratz, and J.G. Zeikus, *J. Bacteriol.*, 1989, **171**, 3775-3781.

17. S. Jung, S.E. Lowe, R.I. Hollingsworth, and J.G. Zeikus, *J. Biol. Chem.*, 1993, **268**, 2828-2835.

18. J. Lee and R.I. Hollingsworth, *Tetrahedron,* 1996, **52**, 3873-3878.

19. U. Vijaranakul, M.J. Nadakavukaren, B.L.M. de Jonge, B.J. Wilkinson, and R.K. Jayaswal, *J. Bacteriol.,* 1995, **177**, 5116-5121.

20. M. Dubois, K.A. Gilles, J.K. Hamilton, P.A. Rebers, and F. Smith, *Anal. Chem.*, 1956, **28**, 350-356.

21. M. Takayama, *J. Mass Spectrom. Soc. Jpn.*, 1994, **42**, 11-23.

22. K.R. Jennings and R.S. Mason, 1983, in *Tandem Mass Spectrometry Utilizing Linked Scanning of Double Focusing Instruments* (F.W. McLafferty, ed.), Wiley, New York.

23. A. Bax and S. Subramanian, *J. Magn. Reson.*, 1986, **67**, 565-569.

24. A. Bax and D.G. Davis, *J. Magn. Reson.*, 1985, 65, 355-360.

25. B. Glauner, J.-V. Höltje, and U. Schwarz, *J. Biol. Chem.*, 1988, 263, 10088-10095.

26. N. Sharon, 1975, in *Complex Carbohydrates: Their Chemistry, Biosynthesis, and Functions,* pp 258-281, Addison-Weseley Publishing, Massachusetts.

27. K. H. Schleifer and O. Kandler, *Bacteriol. Rev.*, 1972, **36**, 407-477.

28. S. Jung and R.I. Hollingsworth, *J. Theor. Biol.*, 1995, **172**, 121-126.

29. S. Jung and R.I. Hollingsworth, *J. Lipid. Res.*, 1994, **35**, 1932-1945.

CHAPTER VI

A CONFORMATIONAL STUDY OF MONOGLUCOSYLDIGLYCERIDE BY NMR NUCLEAR OVERHAUSER AND EXCHANGE SPECTROSCOPY (NOESY) AND MOLECULAR MECHANICS CALCULATIONS

ABSTRACT

Our current knowledge of the conformation of glycolipids in both crystal and solution is very limited. The orientation and the dynamics of headgroup of only a few glycolipids have been studied. These studies were performed using ^{2}H-NMR spectroscopy. An understanding of the conformational preferences of lipid molecules is critical to understanding their roles in biological membranes. Also, the conformation of biosynthetic precursor will provide insight into understand the regioselectivity in biosynthesis. To this end, the three-dimensional structure of monoglucosyldiacylglycerol (MGDG) in solution was determined by a combination of NMR spectroscopy and molecular mechanics calculations. The distance constraints obtained by NOE experiments were incorporated into molecular mechanics calculations to obtain minimum-energy conformers. The angles describing the conformation of the glycosidc bond (ϕ and φ) were 47° and 169°, respectively, implying the glucose ring is extended away from the bilayer plane assuming a lamellar packing arrangement. To gain insight into the relative flexibility of the different parts of molecule, a molecular dynamics simulation was also performed. The rotamer populations for the two C-C bonds of the glycerol moiety of MGDG were obtained from vicinal spin-spin coupling constants using a Karplus treatment. There is a preferred conformation in the C(2)-C(3) bond which allow the parallel alignment of the hydrocarbon chains whereas the C(1)-C(2) bond is flexible, as is evident from nearly populated rotamers around this bond. We can postulate that the sufficient proximity and appropriate orientation of sugar residues in well-packed systems

such as biological membranes determine the linkage position of glycosidic bond in glycolipids containing disaccharides and even higher homologues.

INTRODUCTION

Glyceroglycolipids, in which a sugar residue is attached via an α or β linkage to 1,2-di-*O*-acyl-*sn*-glycerol, are major membrane lipids in a wide variety of plant tissues [1], bacteria [2] and mycoplasma membranes [3]. They have been reported to resemble phosphatidylethanolamines with respect to hydration capacity, phase transition temperature and the ability to form nonlamellar mesophases [4]. However, their roles in the biological membranes is not well understood. The knowledge of the orientation of the carbohydrate residues relative to the membrane surface and dynamical behavior of the head group are essential for an understanding of their functional roles in biological membranes. The observed physical properties of glycerolglycolipid membranes have been interpreted in terms of strong direct intermolecular hydrogen bonds between the hydroxyl groups of sugar moieties, head-group flexibility and molecular shape [5]. The conformational details of lipid molecules are also important in developing a reasonable model for the supramolecular structure of the membrane. X-ray single crystal studies have provided the most detailed and accurate information on molecular conformation and packing. It has, however, proved difficult to grow well-ordered crystals of amphiphilic lipid molecules suitable for X-ray analysis. Thus, the molecular conformation of lipid

molecules dispersed in water have been studied by X-ray diffraction, neutron diffraction, and NMR spectroscopy such as ^{31}P and ^{2}H broad-line analyses [6,7].

Sarcina ventriculi is a Gram-positive eubacterium that rapidly adapts to a large variety of extreme conditions such as pH, temperature and the presence organic solvents. We have demonstrated that this organism is capable of maintaining membrane stability and function by cross-linking the tails of membrane lipids from opposite sides of the bilayer, forming transmembrane, bifunctional fatty acid species and by altering the lipid composition in response to changes in its environment [8,9]. It is clear that any environmental perturbation of bilayer arrangement and motional dynamics of membrane lipids will trigger adaptative mechanisms to counteract these changes. Such a covalently cross-linked bilayer in the plasma membrane of *S. ventriculi* is thought to be responsible for maintaining membrane fluidity and stability under extreme environmental stresses and to serve as a barrier against the diffusion of hydrogen ions or metabolic acids into the cell. In view of the key role played by the membranes in the adaptation of *S. ventriculi* under environmental stresses, several studies have been carried out to characterize the membrane lipids. The major lipids of the cell membrane of *S. ventriculi* grown at pH 7 and 37°C are diacylglycerol (DAG), phosphatidylglycerol (PG), lysophosphatidylglycerol (lyso-PG), monoglucosyldiacylglycerol (MGDG) and trace of transmembrane lipids. One prominent characteristic of the lipids of this bacterium grown at pH 3 is the presence of novel glycolipids including alkylsophoroside and acylsophoroside [9]. The occurrences of alkylsophoroside and acylsophoroside have not been described in other bacteria. Such an ability to synthesize these novel glycolipids represents another adaptative mechanism

enabling *S. ventriculi* to maintain membrane fluidity and function at low pH. Although the biosynthesis of the sophorosides has not been established, it may occur by a route analogous to that of the glyceroglycolipid. It has been suggested that the biosynthesis of galactolipids in plants occurs by a stepwise addition of galactose residues to diacylglycerol from UDP-galactose (UDP-gal). In this case, UDP-gal is the galactosyl donor for the galactosylation of endogenous diacylglycerol [10]. Van Besouw and Wintermans observed that digalactosyldiacylglycerol (DGalDG) formation could indeed occur even in the absence of UDP-gal and proposed a different mechanism to synthesize DGalDG and higher homologues by interlipid galactosyl transfer by a galactolipid:galactolipid galactosyltransferase. The galactosyl transfer proceeds by direct exchange of galactosyl groups between molecules of galactolipids. It can be hypothesized that MGDG would be a biosynthetic precursor of the sophorosides as in the case of DGalDG. This can only be possible if the carbohydrate group in MGDG has the correct orientation to allow the connection of the 2-hydroxyl group of one molecule to the C1 position of the other. For this reason, it is important to know the solution conformation of the head group and glycerol moiety of MGDG.

The present study focuses on the average solution conformation of MGDG by the powerful combination of ^{1}H nuclear Overhauser enhancement (NOE) NMR spectroscopy measurements, molecular mechanics and molecular dynamics calculations. The NOE experiments provide the information on spatial proximity of protons because the volume of the cross-peaks (actually the rate of build-up of the cross-peak intensity) is a function of the internuclear distance to the inverse sixth power at very short mixing time away

from the spin diffusion limit. The internuclear distances obtained by the NOE experiments were incorporated into the molecular mechanics calculations.

MATERIALS AND METHODS

Nomenclature

Sundaralingam's atom numbering and notation of torsion angles were used [12]. The polar head group is attached to atom C(1) of the glycerol and is designated the α-chain. Note that this is opposite to the stereospecific numbering (*sn*) convention where this atom is *sn*-C3. The fatty acyl chain linked to carbon atoms C(2) and C(3) are designated the β- and γ-chains, respectively. The structure with the atomic labelling of MGDG in given in **1**. The relative orientation of the molecule is described by the torsion angles ϕ, φ, θ_1, θ_2, θ_3, and θ_4 ,respectively, defined as:

ϕ = H(1′)–C(1′)–O(11)–C(1) φ = C(1′)–O(11)–C(1)–C(2)

θ_1 = O(11)–C(1)–C(2)–C(3) θ_2 = O(11)–C(1)–C(2)–O(21)

θ_3 = C(1)–C(2)–C(3)–O(31) θ_4 = O(21)-C(2)-C(3)-O(31)

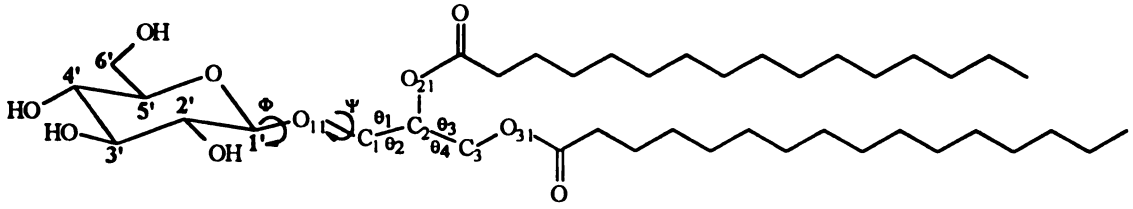

1

Isolation and Purification of Lipids

Sarcina ventriculi was cultured and harvested as previously described [8]. Cells were stirred at 40°C with a mixture of chloroform/methanol/water (15:3:3, by vol.) for 2 h. Cell suspensions were filtered. The filtrates were transferred into separatory funnel and the organic phase was removed. The residue (cell debris) was extracted again with chloroform/methanol (5:1, by vol.) and then with chloroform/methanol/water (15:3:3, by vol.). The organic phases containing the lipids were pooled and evaporated to dryness. Membrane lipids were purified by TLC on a silica gel plate developed with a mobile phase system consisting of chloroform/methanol/ammonia/water (3.3:1.0:0.1:0.05 by vol.). The plate was dried to remove all trace of solvents, then sprayed with orcinol to locate lipid bands. Lipid bands were scraped from the plate and extracted with three aliquots of chloroform/methanol (1:1, by vol.). The extracts were filtered and evaporated to dryness.

NMR Spectroscopy

NMR spectroscopy was carried out on a Varian VXR500 NMR spectrometer operating at 500MHz for protons. NMR spectra were obtained in CD_3OD and at 30°C. The residual methanol line at 3.30 ppm was used as a reference. Homonuclear multiquantum coherence (HMQC) spectra were acquired for a total of 256 data sets with 256 transients at 1024 data points. Phase sensitive NOESY spectra were acquired with mixing times of 100, 200, 300, and 400 ms. The 1024 and 256 complex points were collected in the t_2 and t_1 domains, respectively. For each t1 value, 64 scans were collected

with a relaxation delay of 2s between transients. The data were processed using a Gaussian weighting function in both dimensions. Volume integrations of the cross-peaks were performed using the standard VARIAN software. Cross-peak volumes were used in the calculation of interproton distances using reference distance of H(1′)-H(5′) of 2.5 Å.

Molecular Mechanics and Molecular Dynamics

Molecular mechanics calculations were performed on a Silicon Graphics 4D310 computer using the DREIDING force fields [13] implemented in the BIOGRAF (Molecular simulations Inc., Waltham, MA 02154) program. The default parameters given in this program for the carbohydrate rings were used without modification since they have been found to be consistent with physical measurements [14]. For molecular dynamic (MD) simulations, the lowest conformer found in the NOE constrained conformation was extended as a monolayer with a 5×5 array and with a similar molecular arrangement and cell dimension as observed in phosphatydylethanolamine [15]. MD simulation with dielectric constant of 80 were carried out using isothermal dynamics (TVN) for 80 ps. A nonbonded cutoff distance of 9.0 Å was used. Charges were calculated using the method of Gastiger and Marsili [16]. The time for heating and equilibrium was 0.1 ps. Trajectory frames were saved every 0.4 ps. The history of fluctuations of some dihedral angles were obtained by looking at the center molecule surrounded by other hexagonally arranged molecules in the cluster.

RESULTS AND DISCUSSION

The ^{1}H and ^{13}C chemical shifts have assigned by using a combination of 1D and 2D NMR spectroscopy (Table 6.1). The proton and HMQC spectra are shown in Figure 6.1 and 6.2, respectively. The MGDG purified from *S. ventriculi* was heterogeneous due to different fatty acyl chains. The three-dimensional structures can be established by NMR nuclear Overhauser effect spectroscopy and molecular mechanics-based calculations. For rigid molecules undergoing isotropic rotational reorientation, and neglecting complexities due to strong coupling and cross-correlation effects, the cross-peak intensity between proton pairs in NOESY spectra for a given mixing time, τ_m, is function of the distance between the protons (r_{ij}), the overall rotational correlation time of the molecule (τ_c), and the ^{1}H-NMR resonance frequency (ω) [17]. In order to determine distances from cross-peak intensities, τ_c must be known. At very short mixing times, the absolute volumes of the cross-peaks can be used as a measure of the rate of NOE buildup and are directly proportional to the inverse sixth power of the distance separating a pair of protons. For longer mixing times, when $\omega\tau_c \gg 1$, indirect relaxation contributions to the observed NOE can be significant making the distance dependence of the NOE much more complicated. When the cross-peak intensity build-up is in the linear regime, the cross-peak intensity (NOE_{ref}) between a proton pair having a known, fixed distance (r_{ref}) can be used [18]. Thus, an unknown distance, r_{ij}, can be calculated from equation (1).

$$r_{ij} = r_{ref}[NOE_{ref}/NOE_{ij}]^{1/6} \quad (1)$$

where r_{ij} and NOE_{ij} corresponded to the internuclear distance and cross-peak intensity between the spins *i* and *j* whose distance is being determined. Because of the existence of intramolecular motion occurring on the NMR time scale equal to, or shorter than, that of the overall molecular tumbling, the 'NOE constraints' do not have a simple geometry interpretation which limits their utility in building 3D structures [19]. This is generally only a problem for large systems with highly flexible regions and high degrees of independent internal motion.

The average conformation of glycolipids in solution has been shown to be independent of the solvent used and of the state of aggregation suggesting that it is mainly determined by intramolecular forces. Replacing the water of hydration by CD_3OD for NOESY experiments, therefore, has little or no effect on the conformation [15]. Although the intensity of the cross-peaks increase with the mixing time, a longer mixing time departs from the linear regime of the NOE build-up, spin-diffusions occur and equation (1) is no longer valid. Four different mixing times were tested and a mixing time of 300 ms was used to calculate volumes of NOE cross-peaks which ensured that we were within the initial rate approximation as well as good signal-to-noise. The NOESY spectrum at 300 ms mixing time contained cross-peaks corresponding to interactions between anomeric proton, H1′ and H1 of the glycerol moiety as well as H2′, H3′ and H5′ (Figure 6.3). The H2 of the glycerol moiety also showed cross-peaks with H1 and H3 protons. Equation (1) was used to calculate the distances between spins *i* and *j* by comparing NOE volumes with the H(1′)-H(5′) distance of 2.50 Å (standard for the

glucosyl ring) as a reference. The interproton distance constraints obtained from NOESY experiments are listed in Table 6.2.

The NOE-defined conformation often does not correspond to a single conformation but rather to a statistically averaged conformation. In the present study, the determination of the solution conformation is complicated by the degree of freedom defined by the torsional angles ϕ and φ about the glycosidic linkage. The molecule was first oriented into a conformation that lies close to the one obtained by the much less accurate ^{2}H-NMR method [7]. The internal energy of this structure was then minimized using the conjugate gradient method. This was followed by constrained energy minimization using internuclear distance derived from NOE measurements. The restrained minimum distances with force constant of 100 are compared with NOE-derived target distances in Table 6.2. The overall conformation obtained by this procedure (k=100) is shown in Figure 6.4. The associated force constant, k=100 for these constraints is chosen to be relatively low to so as not to lock the molecule in an incorrect conformation if the NOE constraints contained errors because of motional averaging. For relatively rigid systems with few internal degrees of freedom, constrained minimizations should converge quickly. In systems which are flexible with several local minima with closely spaced energies this is often not the case. Clore and coworkers have shown that for oligonucleotides the convergence properties of constrained energy minimization are dependent on the starting structure [20]. Thus, for generating structures from NMR data in very flexible systems the starting structure used as input should be close to the final optimum structure [21]. To test the convergence properties of this method, several

Table 6.1: ^{1}H and ^{13}C chemical shift assignments of monoglucosyldiacylglycerol

glycerol backbone	^{1}H (ppm)	^{13}C (ppm)
1	3.73(dd, J=11.0, 5.5), 3.98 (dd, J=11.0, 5.7)	68.8
2	5.26 (multiplet)	71.8
3	4.20 (dd, J=12.1, 6.77) 4.44 (dd, J=12.1, 2.96)	64.0
glucose residue	^{1}H (ppm)	^{13}C (ppm)
1	4.264, 4.279	104.7
2	3.17	75.0
3	3.34	77.9
4	3.28	71.5
5	3.27	78.1
6	3.85, 3.87	62.7

Table 6.2: Comparison of NOE-derived target distances verse restrained minimum distances measured from the energy minimized conformer.

proton pairs	target distance (Å)	restr min distance (Å) ($k=100$ kcalmol^{-1}Å^{-2})
H1′-H5′	2.50	2.50
H1′-H3′	2.67	2.68
H1′-H1a	2.48	2.48
H1′-H1b	2.72	2.71
H2-H1a	3.14	3.11
H2-H1b	2.94	2.83
H2-H3a	3.25	3.14
H2-H3b	2.68	2.63

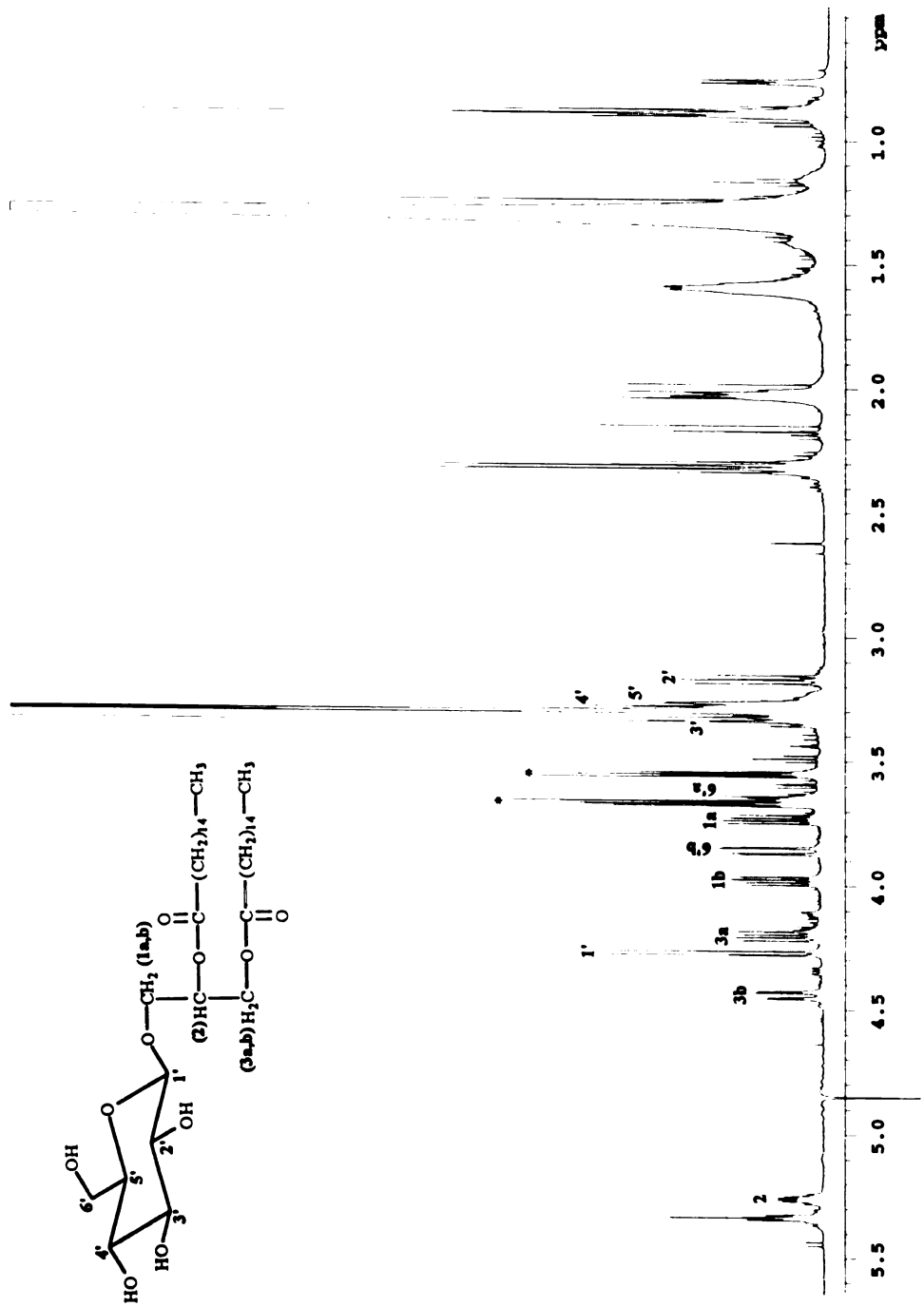

Figure 6.1: ^{1}H NMR spectrum of monoglucosyldiacylglycerol. Contaminant peaks are designated by an asterisk.

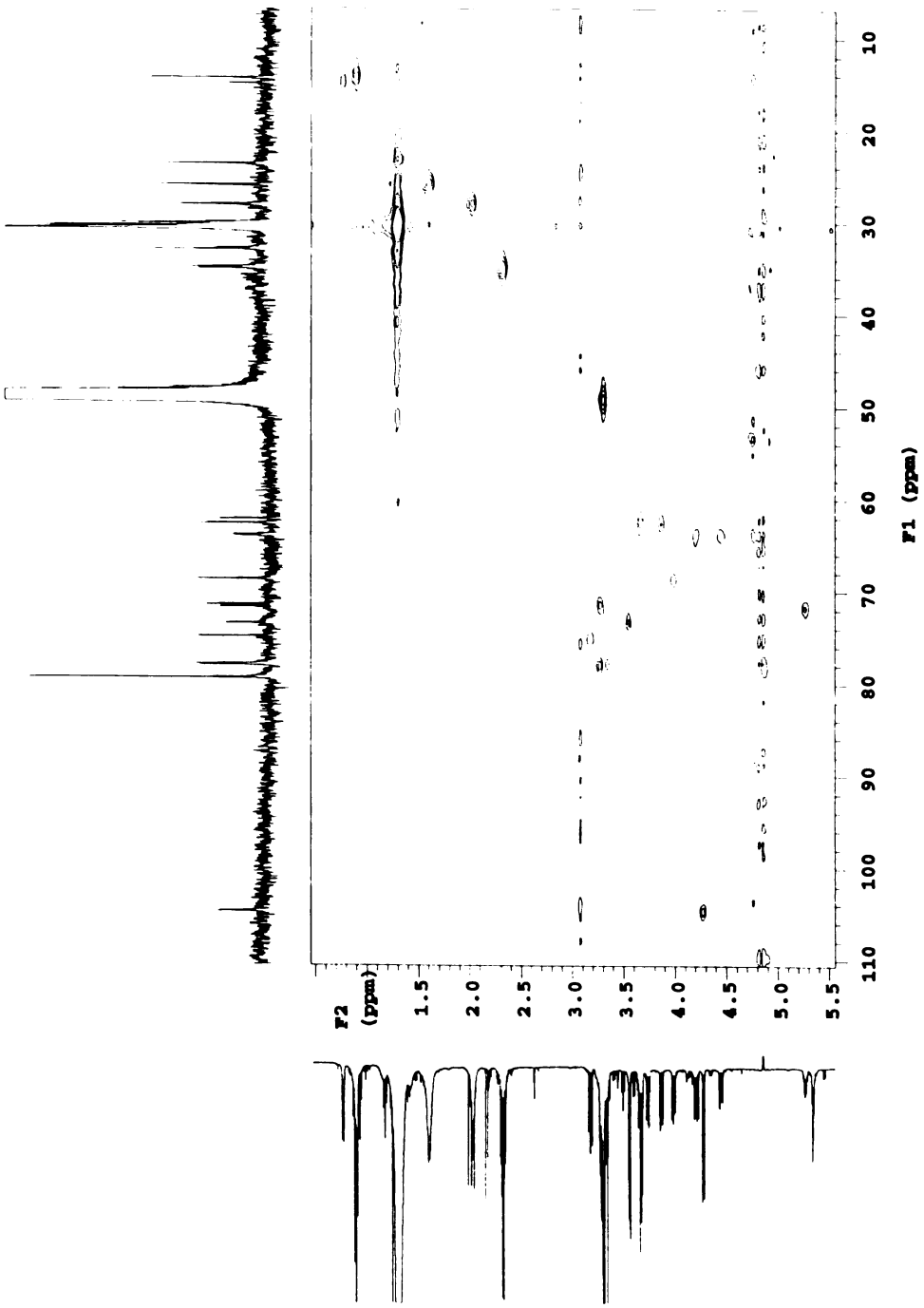

Figure 6.2: ^{1}H-^{13}C HMQC spectrum of MGDG.

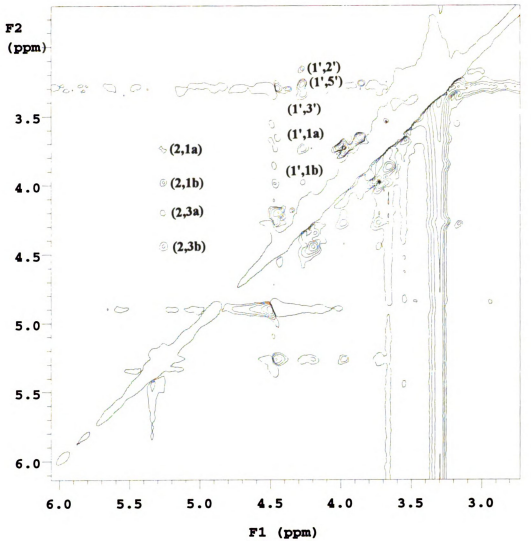

Figure 6.3: Partial NOESY spectrum of MGDG at 300 ms mixing time showing the various key interactions.

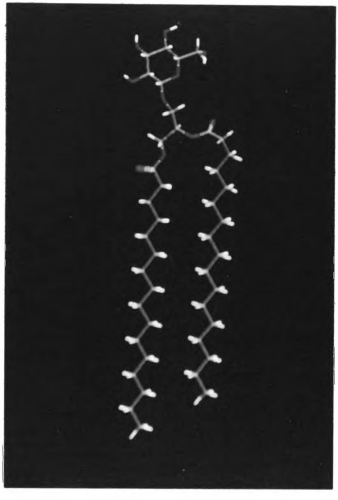

Figure 6.4: Conformation of MGDG molecule obtained by constrained energy minimization.

different starting structures were subjected to constrained energy minimizations. These gave the same general conformation but indicated some variability in angles φ and θ_2. This is an indication that there is more than one value that these angles can have. It also indicates some mobility about bonds.

The dihedral angles of MGDG energy-minimized conformer are given in Table 6.3.

Table 6.3: Dihedral angles for the energy-minimized conformer by NOE constraints.

	ϕ	φ	θ_1	θ_2	θ_3	θ_4
k=10,000	43	174	90	-158	-173	70
k=100	47	169	89	-156	-169	71

Recent investigations have explored the conformation, orientation and motional properties of 1,2-di-*O*-tetradecyl-3-*O*-(β-D-glucopyranosyl)-sn-glycerol (DTGL) by deuterium NMR spectroscopy [6,7]. The results indicated that there was some motion on the time scale of 10^5 s^{-1} about the C1′(glucose)-O11-C1(glycerol) glycosidic bond but that its amplitude was very restricted. This is consistent with our analysis. The conformation about the glycosidic bond of the glycolipid was such that the sugar ring was fully extended away from the bilayer surface into the aqueous phase. In the present study the angle φ, which reflects the conformation about the C(1′)-O(11) bond was 169°. The C(1′)-O(11) bond was almost antiperiplanar (trans) to the C(1)-C(2) bond, and as a result, the glucose ring was again extended away from the bilayer plane. The conformation about the C(1′)-O(11) bond, as given by the angle ϕ was 47°. This value

was in good agreement with φ values of ca. 50° for simple β-glycopyranoside in single crystals. The torsion angle, θ_1 and θ_3 in this study was 89° and -169°, respectively.

Another method in the refinement of structures using NMR data is constrained molecular dynamics. Unlike constrained energy minimization, however, constrained molecular dynamics has a greater capacity for overcoming energy barriers between local minima due to the kinetic energy available to the system in the calculations. To obtain information on the relative flexibility of the different parts of the molecule, the molecular dynamic simulations was started with a structure which had been minimized with NOE-derived distance constraints. Starting from the lowest energy conformation, a 80-ps molecular dynamics (MD) trajectory was computed at 300K. The fluctuation of dihedral angles, θ_1 and θ_3 for the trajectory is displayed in Figure 6.5. The overall conformation of MGDG molecule was essentially rigid on the 80 ps time scale. The trajectory indicated that the dihedral angle θ_3 is fairly rigid whereas the angle θ_1 is flexible. The another source of flexibility occurred at the glycosidic linkage. These results were consistent with the constrained minimization analysis.

The conformational structure with respect to θ_1 and θ_3 is the most important factor in deciding the overall lipid structure since these two angles control the relative orientation of the β and γ chains in glycerolipids. Information on these angles can also be obtained by looking at the vicinal coupling constants (the 5-spin system consisting of protons on C1, C2 and C3). It has been suggested that phospholipids in aqueous dispersions and dissolved in organic solvents have a great deal of molecular and segmental motion at room temperature and consequently, motionally averaged

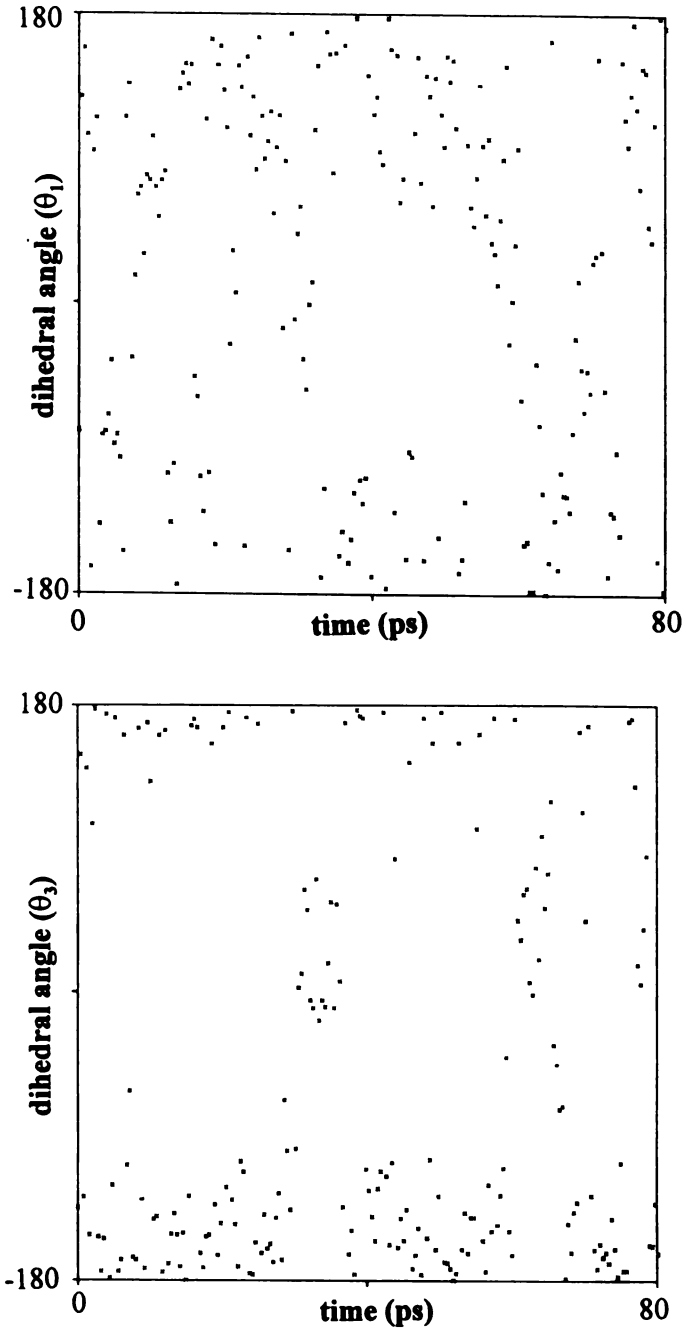

Figure 6.5: History of fluctuations of the dihedral angles, θ_1 and θ_3 from MD trajectory.

conformations are observed [15]. The observed NMR pattern of the 5 proton spins in the glycerol fragment can be explained in terms of chain flipping and conformational equilibrium for the three staggered structures [23]. From the vicinal coupling constants, rotamer populations can be calculated from a Karplus-type treatment [24]. The observed vicinal coupling constants can be expressed as the population-weighted average of the component coupling constants for the three staggered conformations (Figure 6.6). The observed vicinal coupling constants of H(2)-H(3a) and H(2)-H(3b) were J_{ax} 6.8 Hz and J_{bx} 3.0 Hz, respectively. By use of the component coupling constants ($J_{AX}^{(I)}$ 5.8, $J_{BX}^{(I)}$ 11.7, $J_{AX}^{(II)}$ 11.5, $J_{BX}^{(II)}$ 2.7, $J_{AX}^{(III)}$ 0.6, and $J_{BX}^{(III)}$ 2.7 Hz) the observed averaged vicinal coupling constants are given by equations (1) and (2), where

$$J_{AX} = P_{(I)}J_{AX}^{(I)} + P_{(II)}J_{AX}^{(II)} + P_{(III)}J_{AX}^{(III)} \quad (2)$$

$$J_{BX} = P_{(I)}J_{BX}^{(I)} + P_{(II)}J_{BX}^{(II)} + P_{(III)}J_{BX}^{(III)} \quad (3)$$

$$P_{(I)} + P_{(II)} + P_{(III)} = 1 \quad (4)$$

These equations can be solved to give estimates of the fractional populations. In such an analysis it is not possible to distinguish between rotamers (I) and (II) if H_A and H_B cannot be assigned unambiguously. The two sets of fractional populations were obtained: $P_{(I)}$=0.02, $P_{(II)}$=0.56, $P_{(III)}$=0.42 ($J_{AX}>J_{BX}$) and $P_{(I)}$=0.46, $P_{(II)}$=0.001, $P_{(III)}$=0.54 ($J_{AX}<J_{BX}$). However, the set of values with $J_{AX}<J_{BX}$ can be ruled out in which the rotamer with θ_4 = antiplanar becomes significant. A large proportion of that rotamer cannot be present because a torsion angle θ_4 = 180° would not allow for the well-known parallel alignment of the two hydrocarbon chains optimizing hydrophobic interactions both intra- and intermolecularly. The conformation derived from NOE constraints showed the rotamer

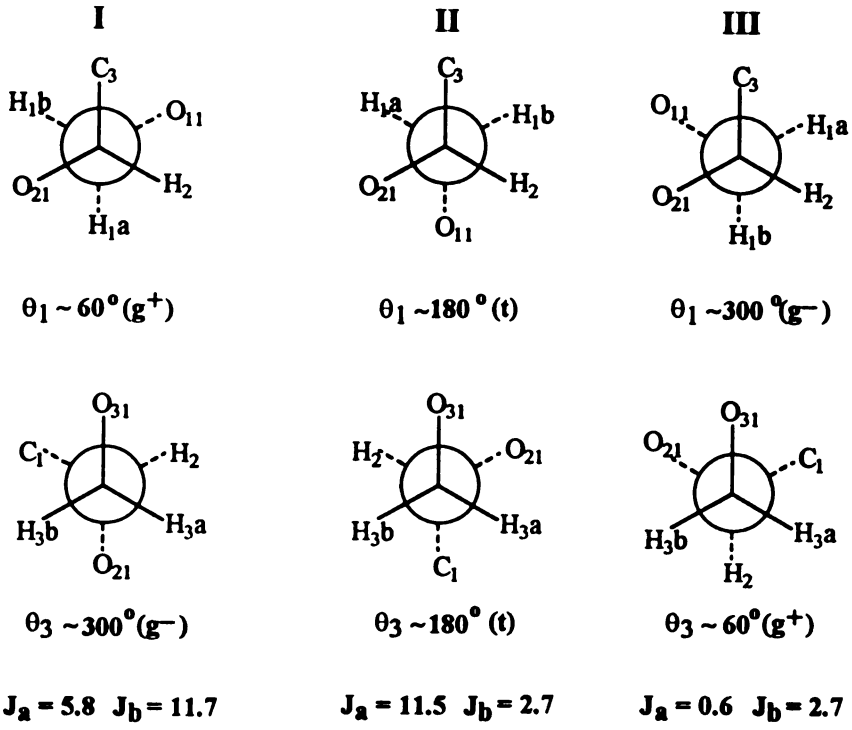

Figure 6.6: Newman projections around the bonds θ_1 and θ_3 and values of component coupling constants. Note that the dihedral angles for θ_1 (O11–C1–C2–C3) and θ_3 (C1-C2-C3-O31).

with θ_3 = -154°. The C(1)-C(2) moiety gives $P_{(I)}$=0.35, $P_{(II)}$=0.31, $P_{(III)}$=0.34 ($(J_{AX}>J_{BX})$ and $P_{(I)}$=0.35, $P_{(II)}$=0.28, $P_{(III)}$=0.37 ($J_{AX}<J_{BX}$) [25]. The fractional populations of the three staggered conformations are summarized in Table 6.4.

Table 6.4: Rotamer populations of the glycerol moiety of MGDG by using vicinal coupling constants

bond	torsion angle	staggered conformations	fractional population
R_1COCH_2-CHOCR_2	$\theta_3(\theta_4)$	gauche(-gauche)	0.02
		antiplanar(gauche)	0.56
		-gauche(antiplanar)	0.42
R_2COCH_2-CHOGlc	$\theta_1(\theta_2)$	-gauche(gauche)	0.35(0.35)
		antiplanar(-gauche)	0.31(0.28)
		gauche(antiplanar)	0.34(0.37)

Evaluating the coupling constants in terms of fractional populations showed that three possible staggered rotamers about the C(1)-C(2) bond were equally populated. It has been shown that both in solid state as well as in the solvated monomeric and aggregated state there is no preferred conformation about the C(1)-C(2) glycerol bond [26]. If the segmental motion of glycerol moiety has no constraints and the interconversion between the different conformations is rapid on the NMR time scale, the molecule must have no preferred conformation about the C-C bond. However, it has been suggested that the glycerol backbone has a fixed conformation and moves about the director as a rigid unit [27]. The conformation based upon interproton distances gave dihedral angles H(1a)-C(1)-C(2)-H(2) of -152° and H(1b)-C(1)-C(2)-H(2) of 90°. These dihedral angles seem to be inconsistent with the calculated fractional populations using the vicinal

coupling constants and support the first model.

The interaction between headgroups may contribute to the organization of the membrane and lead to the closely packed configuration. Strong interaction between neighboring headgroups can be assumed. The monolayer of these MGDG molecules is illustrated in Figure 6.7. The closest hydroxyl group to the anomeric protons are at the 2- or 6-position. In the closely packed arrangement of membrane lipids, the proximity of functional groups should be responsible for the observed linkage between two glucose residues. A model which describes the regulation of the linkage position of glycolipids containing two sugars can be related to the fact that the linkages in DGalDG and DGDG are mainly at the 2- and 6-positions [28]. To effect this transfer reaction, the glycosidic linkage of MGDG would be cleaved by a glucosidase and the carbocation attacked by the C2 or C6 hydroxyl group from the nearest MGDG unit. In the case where the nucleophile is a free acid or alcohol then an acyl or alkyl glycoside would be formed as demonstrated in Figure 6.8.

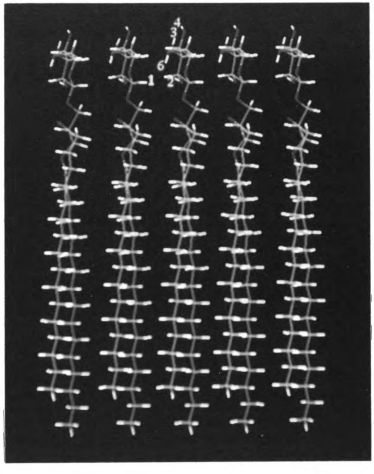

Figure 6.7: Molecular arrangement of MGDG monolayer showing the proximity of OH groups of the glucose residue between molecules.

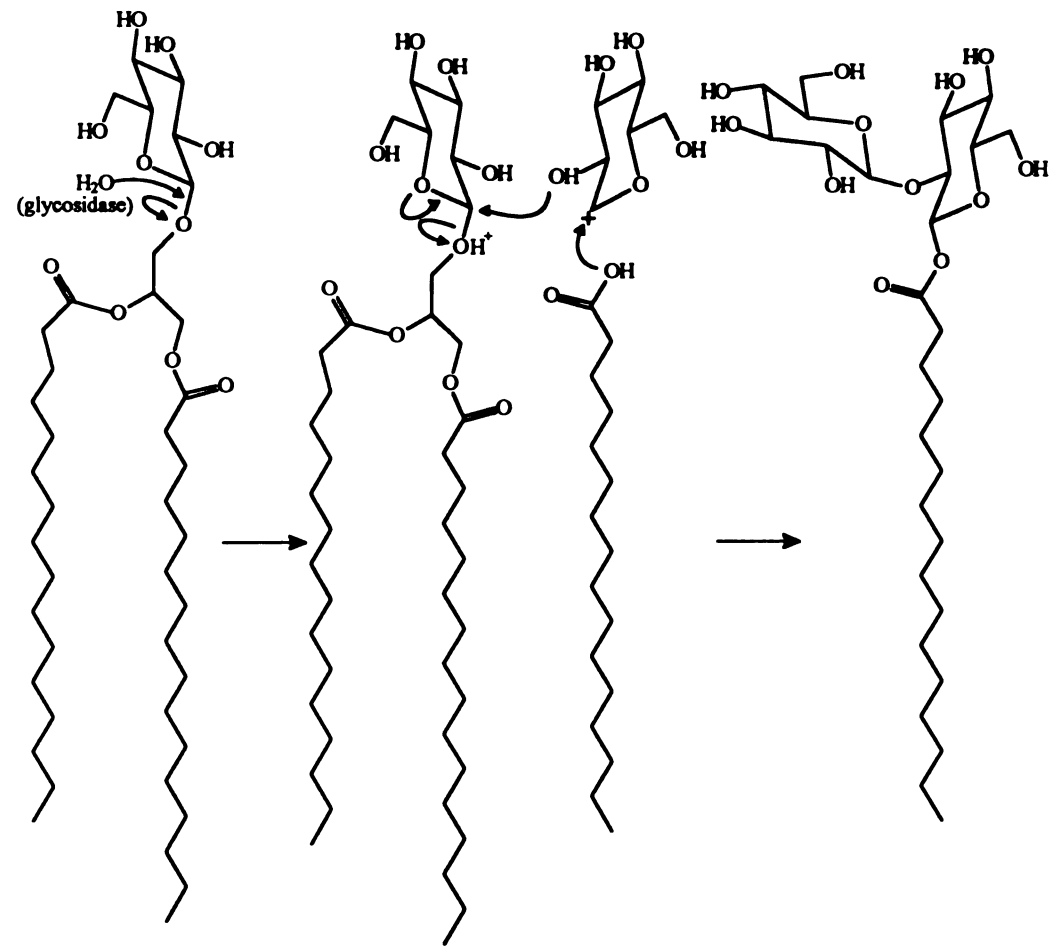

Figure 6.8: Proposed model for the biosynthesis of alkyl and acyl sophorosides in *S. ventriculi*.

REFERENCES

1. P.J. Quinn and W.P. Williams, *Prog. Biophys. Mol. Biol.*, 1978, **34**, 109-179.

2. J.M. Boggus, *Can. J. Biochem.*, 1980, **58**, 755-770.

3. B. de Kruijff, R.A. Demel, and L.L.M. van Deenen, *Biochim. Biophys. Acta*, 1979, **553**, 331-347.

4. D.A. Mannock, R.N.A.H. Lewis, A. Sen, and R.N. McElhaney, *Biochemistry*, 1988, **27**, 6852-6859.
5. H. Goldfine and N.C. Johnson, *Biochemistry*, 1987, **26**, 2814-2922

6. H.C. Jarrell, J.B. Giziewicz, and I.C.P. Smith, *Biochemistry*, 1986, **25**, 3950-3957.

7. H.C. Jarrell, P.Å. Jovall, J.B. Giziewicz, L.A. Turner, and I.C.P. Smith, *Biochemistry*, 1987, **26**, 1805-1811.

8. S. Jung, S.E. Lowe, R.I. Hollingsworth, and J.G. Zeikus, *J. Biol. Chem.*, 1993, **269**, 2828-2835.

9. J. Lee and R.I. Hollingsworth, *Tetrahedron*, 1996, **52**, 3873-3878.

10. J. Joyard and R. Douce,. *Biochim. Biophys. Acta,* 1976, **424**, 125-131.

11. A. Van. Besouw and J.F.G.M. Wintermans, *Biochim. Biophys. Acta*, 1978, **529**, 44-53.

12. M. Sundaralingam, *Ann. N.Y. Acad. Sci. U.S.A.,* 1972, **195**, 324-355.

13. S.L. Mayo, B.D. Olafson, and W.A. Goddard, *J. Phys. Chem.*, 1990, **94**, 8897-8909.

14. Y. Wang and R.I. Hollingsworth, *Biochemistry*, 1996, **35**, 5647-5654.

15. H. Hauser, I. Pascher, R.H. Pearson, and S. Sundell, *Biochim. Biophys. Acta,* 1981, **650**, 21-51.

16. J. Gastiger and M. Marsili, *Tetrahedron*, 1980, **36**, 3219-3228.

17. D. Neuhaus and M.P. Williamson, 1989, *The nuclear Overhauser effect in structural and conformational analysis*, VCH Publishers, Inc., New York.

18. G. Widmalm, R.A. Byrd, and W. Egan, *Carbohydr. Res.*, 1992, **229**, 195-211.

19. L. Poppe, *J. Am. Chem. Soc.*, 1993, **115**, 8421-8426.

20. G.M. Clore, A.M. Gronenborn, A.T. Brünger, and M. Karplus, *J. Mol. Biol.*, 1985, **186**, 435-455.

21. S.W. Fesik, G. Bolis, H.L. Sham, and E.T. Olejniczak, *Biochemistry*, 1987, **26**, 1851-1859.

22. G.A. Geffrey, R.K. McMullan, and S. Takagi, *Acta Crystallogr., Sec. B:Struct. Crystallogr. Cryst. Chem.* 1977, **B33**, 728-737.

23. H. Hauser, W. Guyer, I. Pascher, P. Skrabal, and S. Sundell, *Biochemistry*, 1980, **19**, 366-373.

24. M. Karplus, *J. Chem. Phys.*, 1957, **30**, 11-15.

25. N.J.M. Birdsall, J.Feeney, A.G. Lee, Y. K. Levine, and J.C. Metcalfe, *J. Chem. Soc. Perkin II*, 1972, 1441-1445.

26. R.H. Pearson and I. Pascher, *Nature*, 1979, **281**, 499-501.

27. Strenk, P.W. Westerman, and J.W. *Biophys. J.*, 1985, **48**, 765-770.

28. N. Shaw, *Bacteriol. Rev.*, 1970, **34**, 365-377.

CHAPTER VII

CONFORMATIONAL AND SUPRAMOLECULAR STRUCTURE OF β-1-*O*-HEXADECYL-β-1,2-DIGLUCOSYL GLYCOSIDE

ABSTRACT

β-1-*O*-β-1,2-diglucosyl glycoside (β-1-*O*-hexadecylsophoroside) has been isolated and characterized from membrane lipids of *Sarcina ventriculi* grown at pH 3. Systematic studies on this amphiphilic molecule are especially interesting since they can give insight into the interplay of conformational and packing behavior with possible biological roles in the biological membrane of this bacterium at low pH. For this purpose, β-1-*O*-hexadecylsophoroside was synthesized. The three-dimensional structures of synthetic β-1-*O*-hexadecylsophoroside in solution has been established by NMR nuclear Overhauser effect spectroscopy and molecular mechanics-based calculations. The packing behavior of this molecule has been studied by X-ray diffraction, polarizing microscopy and differential scanning calorimetry. The gel to liquid crystalline transition temperature was 57°C implying the strong interaction between head groups. The lamellar distance of 49 Å was obtained at fully hydrated state by X-ray diffraction study. These physical properties are very similar to monoglucosyldiacylglycerol containing two hexadecanoyl chains. It may be indicative of similar functional roles of both classes of lipids in the biological membranes.

INTRODUCTION

Biological membranes have adaptive mechanisms in order to ensure an optimal degree of bilayer stability and membrane fluidity. Adaptive mechanism can be

modification of the chain length distribution and the degree of unsaturation of fatty acid or synthesis of cyclohexane-containing fatty acids and hopanes. Changes occur also in the lipid composition which can be extensively modulated by environmental and nutritional factors to regulate membrane fluidity, charge, and their interactions with membrane proteins. However, the relation between lipid composition and membrane function in biological membranes is poorly understood.

Sarcina ventriculi is a Gram-positive eubacterium that rapidly adapts to a large variety of extreme conditions such as pH, temperature, and the presence organic solvents. This anaerobic bacterium develops energetically inexpensive adaptive mechanisms. We have demonstrated that this organism is capable of maintaining membrane stability and function by cross-linking the tails of membrane lipids from opposite sides of the bilayer, forming transmembrane lipids and by altering the lipid composition in response to changes in environments [1]. This covalently bound bilayer plasma membrane is thought to be responsible for maintaining membrane fluidity and stability under extreme environmental stress. It also might act as a barrier against the diffusion of hydrogen ions or metabolic acids into the cell. In view of the key role played by the membrane in the adaptation of *S. ventriculi* to environmental stress, studies have been carried out to characterize the membrane lipids. The prominent characteristic of the lipids of this bacterium grown at pH 3 are the predominant increase of novel glycolipids including β-1-*O*-alkyl- and β-1-*O*-acyl-sophoroside with concomitant decrease of monoglucosyl diacylglycerol [2]. Amphiphilic molecules involving sugar moieties and alkyl chains are widespread in plants and bacteria. In glycolipids, the mono- and disaccharides are

combined with long-chain fatty acids, hydroxy acids, polyols, and ceramides through glycosidic, ester, and amide linkages. The occurrence of these sophorosides has not been described in other bacteria. This ability to synthesize these novel glycolipids represents another adaptive mechanism enabling *S. ventriculi* to maintain membrane fluidity and function at low pH. Low pH would disturb membrane packing by protonating phosphate groups, reducing their charge, and hence reducing the extent of their interaction with divalent cations. The study showed that synthetic diglycosyl dipalmitylglycerols in aqueous solution could form liposomes and function as a barrier against water soluble small molecules such as glucose, UmP and H^+ when assayed below their Tc, whereas monoglucosyl dipalmitoylglycerols showed no appreciable trapping activity [3]. The three lauryl disaccharide detergents, lauryl maltoside, lauryl lactoside, and lauryl cellobioside had strikingly different properties, implicating the conformation of the sugar moiety as the critical factor in influencing the ability of the detergent to form micelles. These new glycolipids would significantly increase the effective size of the polar head group and also the possibility for hydrogen bonding. For a better understanding of the adaptive mechanism it is of great to study the properties of these glycolipids. In order to relate structural features of this glycolipid to their physical and biological properties, a detailed description of their conformational preference and packing behavior are required. The three-dimensional structure of glycolipids in the solid-state can be experimentally determined by X-ray crystal structure analysis. However, only a few X-ray structures of glycolipids have been published due to difficulties in growing single-crystals. Also, direct structural studies on the liquid crystal phase will always be difficult and ambiguous due to the limited degree of molecular order. The present study describes the three-

dimensional structure, and packing behavior of β-1-*O*-hexadecylsophoroside by the powerful combination of NMR spectroscopy, molecular mechanics calculations, thermal analysis, polarizing microscopy, and X-ray diffraction. The three-dimensional structure of the molecule in solution was determined by ^{1}H nuclear Overhauser enhancement (NOE) measurements [4] and molecular mechanics calculations.

MATERIALS AND METHODS

NMR Spectroscopy

NMR spectroscopy was carried out on a Varian VXR500 NMR spectrometer operating at 500 MHz for protons. For phase sensitive NOESY experiments, 256 data sets were also collected with 32 acquisition transients each with a relaxation delay of 2s between transients. Mixing times of 100, 200, 300 and 400 ms were used. The data were processed using a Gaussian weighting function in both dimensions. Volume integrations of the crosspeaks were performed using the standard VARIAN software. Cross-peak volumes were used in the calculation of interproton distances using reference distance of interresidue, H(1′)-H(5′). A mixing time of 300 ms was used to calculate volumes of NOE cross-peaks which ensured that we were within the initial rate approximation as well as ensuring good signal-to-noise ratios.

Molecular Mechanics Calculations

The conformation of the carbohydrate part of the glycolipid is defined by the torsional angles representing the orientations of the rings. Theses are defined as ϕ = H1-C1-O2′-C2′ and ψ = C1-O2′-C2′-H2′ of the glycosidic bond. The torsion angle θ = H1′-C1′-O_x-C_x. corresponded to the linkage of the glycosidic bond to the alkyl chain. Molecular mechanics calculations were performed on a Silicon Graphics 4D310 computer using the DREIDING force fields [5] implemented in the BIOGRAF (Molecular simulations Inc., Waltham, MA 02154) program. The default parameters given in this program for the carbohydrate rings were used without modification since they have been validated earlier [6]. The MM calculations were performed in vacuo. Calculated NOE distance constraints were included as harmonic restraints with different force constants (100 and 10 kcal mol^{-1} $Å^{-2}$).

Polarized-Light Microscopy

The sample dissolved in methanol and water was deposited on a clean microscope slide and covered with a glass cover slip. The sample was observed with a Zeiss Microscope (LSM210), equipped with polarization optics.

Differential Scanning Calorimetry

Calorimetric studies were carried out with a MC-2 Microcal differential scanning calorimeter. Hexadecylsophoroside was dispersed in water and injected into the cell. A scan rate was 60°C /h and several cycles were repeated.

X-ray Diffraction

Homogeneous dispersions of the sample were prepared by repeated centrifugation through a narrow glass capillary. The sample was then sealed and heated to 60°C for 3 h to ensure fully hydration. X-ray diffraction pattern was recorded using Rigaku Rataflex rotating anode operating at tube voltage 45 kV and 100 mA.

RESULTS AND DISCUSSION

The synthesis and assignments of proton and carbon signals of NMR spectra of β-1-*O*-hexadecylsophoroside were described in Chapter III. The ^{1}H NMR spectra and their assignments are given in Figure 7.1 and Table 7.1, respectively.

Table 7.1: ^{1}H chemical shifts of the disaccharide residue of β-1-*O*-hexadecyl-β-1,2-diglucosyl glycoside.

^{1}H (ppm)	H-1	H-2	H-3	H-4	H-5	H-6
Glu-1	4.39	3.42	3.54	3.32	3.25	3.65/3.84
Glu-1′	4.59	3.22	3.36	3.26	3.25	3.67/3.81

The 2-D ^{1}H nuclear Overhauser effect (NOE) experiment is a powerful method to determine spatial proximity of protons. At very short mixing times, the volumes of the cross peaks are directly proportional to the inverse sixth power of the distance separating a pair of protons [7]. If the cross-peak intensity build-up is in the linear regime, an unknown distance, r_{ij}, can be calculated by comparing the cross-peak intensity , NOE_{ref}

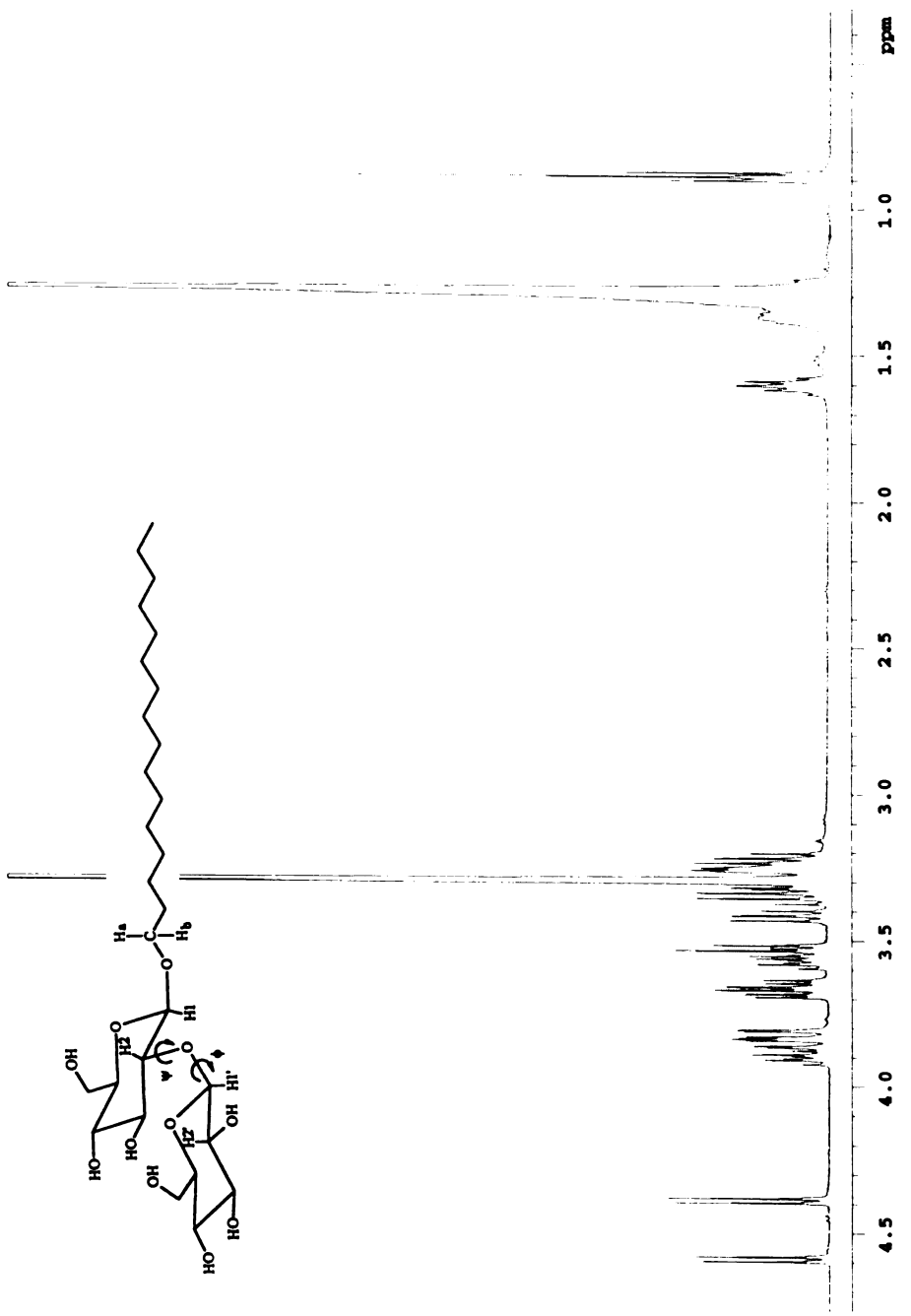

Figure 7.1: ^{1}H NMR spectrum and the structure of β-1-*O*-hexadecylsophoroside.

between a proton pair having a known, fixed distance, r_{ref} and NOE_{ij} between the spins *i* and *j* whose distance is being determined as shown in equation (1).

$$r_{ij} = r_{ref}[NOE_{ref}/NOE_{ij}]^{1/6} \quad (1)$$

The NOE volumes were measured by NOESY experiments. The inter-residue interproton distance, H(1′)-H(5′) of 2.51 Å was used as a reference. Equation (1) was used to calculate the distances between spins *i* and *j* by comparing NOE volumes. Four different mixing times were tested and the mixing time of 300 ms was chosen to calculate volumes of NOE cross-peaks which ensured that we were in within the initial rate approximation as well as an adequate signal-to-noise ratio (Figure 7.2). The distance of H1′-Ha was estimated by subtracting the volume of H1-H3 cross-peak since two cross-peaks of H1-H3 and H1′-Ha were overlapped. The interproton distance constraints obtained from NOESY experiments are listed in Table 7.2.

Table 7.2: Comparison of NOE-derived target distances verse restrained minimum distances obtained with force constant of 10 kcal mol^{-1} Å^{-2}.

	H1′–H3′	H1′–H2	H1′–H5′	H1-H_a	H1-H_b
target distance (Å)	2.66	2.32	2.47	2.64	3.50
restr min distance	2.66	2.31	2.50	2.54	3.26

In this present study, the determination of the solution conformation is complicated by the fact that the number of degree of freedom defined by the torsional angles about the glycosidic linkage. Clore and coworkers have shown that for oligonucleotides the convergence properties of constrained energy minimization are dependent on the starting

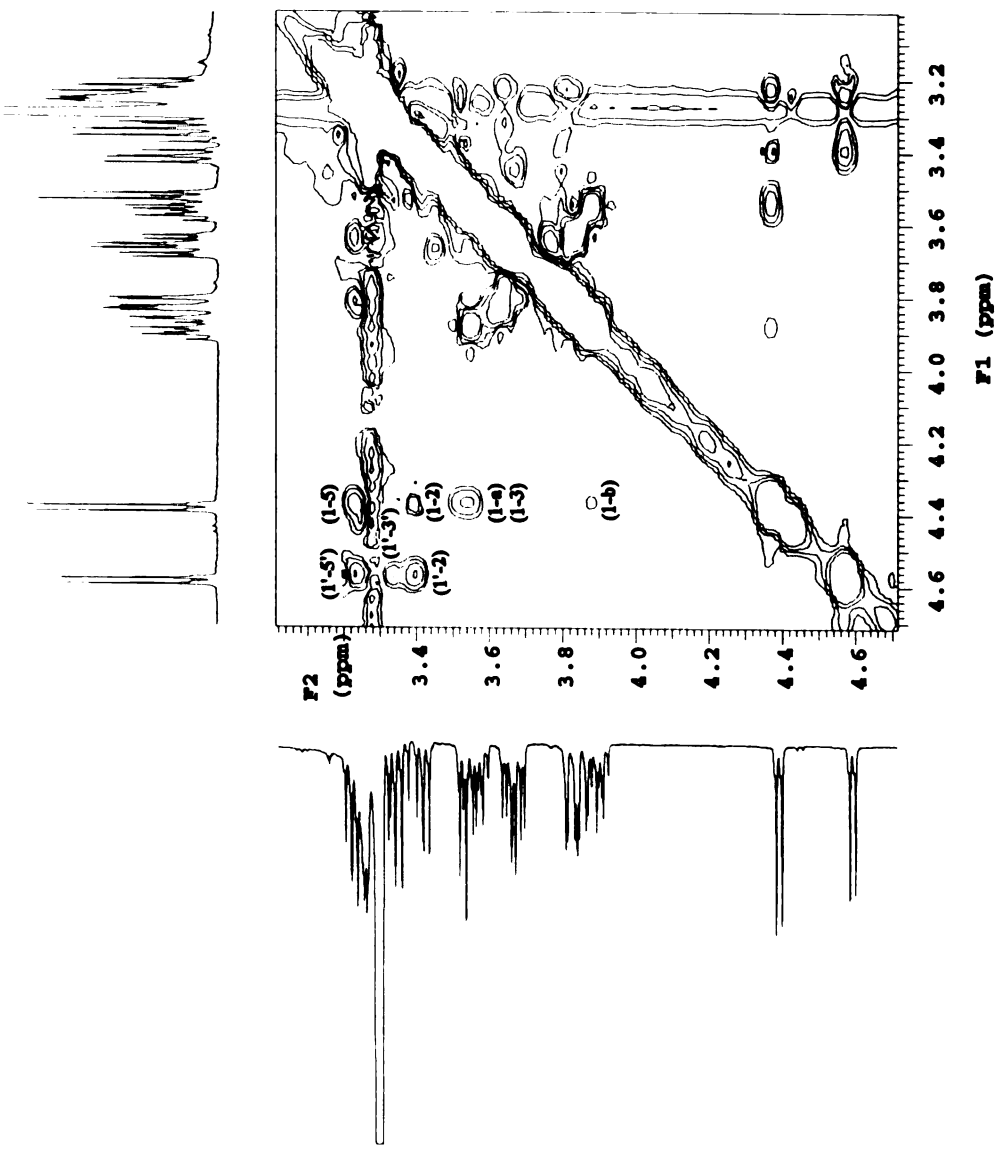

Figure 7.2: Partial NOESY spectrum of β-1-*O*-hexadecylsophoroside at 300 ms mixing time.

structure [8]. Constrained energy minimization does not have good convergent properties due to its inability to overcome local energy minima and is therefore an unsatisfactory method for generating structures from NMR data unless the starting structure used as input is close to the final optimum structure [9]. Therefore the internal energy of the molecule was minimized to get global minima with the torsional angles (ϕ,ψ = 48°, -8°) for β-sophorose proposed by MM3 calculations. This was followed by constrained energy minimization using internuclear distances derived from NOE measurements. The overall conformation obtained by this procedure is shown in Figure 7.3. It is reasonable that the lipid head group is extended away from the bilayer surface into the aqueous phase. The associated force constants for these constraints are chosen to be relatively low (10 kcal mol^{-1} $Å^{-2}$) to reflect the possibility of motional averaging with consequent large errors in NOE constraints. This new geometry after inclusion of NOE constraints is similar to that with distances constraints imposed by NOE measurement with the exception of the internuclear distances of H1′-H_a and H1′-H_b. It indicated that the NOE constraints do not significantly perturb the conformation. The values obtained in this study showed the torsion angles ϕ = 18 ° and ψ = 24 °. The observed NOEs may be interpreted as the result of a single information or as the result of a statistically averaged conformation. More recent studies have addressed that the orientation of two glycosidically linked monosaccharide residues may undergo torsional oscillations about the global minimum. In the majority of linkage types, these fluctuations are restricted to narrow torsional oscillations within a single, deep potential well, and the "average" conformation is closely approximated by the global energy minimum configuration [10]. The torsion

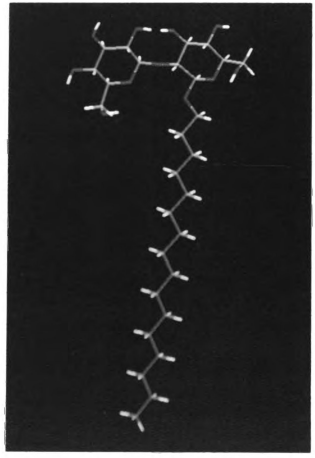

Figure 7.3: Conformation of β-1-*O*-hexadecylsophoroside obtained by constrained energy minimization using NOE-derived distance constraints.

angles obtained in this study were consistent with the deepest energy well of the MM3 energy surface calculated for β-sophorose by Dowd et al. For β-sophorose the two lowest energy minima based on the MM3 force-field were obtained, at ϕ/ψ = 48°/-8° and ϕ,ψ = 34°/-43° (denoted A and A′, respectively). The other local minimum-energy conformation were found, at ϕ/ψ = 35°/169° and ϕ/ψ = 180°/9° (denoted B and C, respectively) [11]. It was suggested by York [12] that the several internuclear distances could be related to the torsional angles ϕ and ψ using the HSEA method. It indicated that glycosidic bonds in conformation A, B, and C would exhibit strong H(1)-H(2′), H(1)-H(1′), and H(2)-H(2′) NOEs, respectively. The internuclear distances of 2.32 Å was obtained for the H1′-H2 in this study. This distance corresponded closely to that for conformation A. In contrast, no H(1)-H(1′) or H(1)-H(2′) cross-peaks were observed in the NOESY spectrum. Thus, these observations are not in agreement with conformers B or C. [12]. However, since only one NOE was measurable across glycosidic linkages, the possibility of large torsional oscillations cannot be ruled out. At 300 K, thermal motions are present, and it is therefore important to consider the implications of motional averaging within the molecule, particularly about glycosidic torsional angles.

The mesophase that lipids spontaneously adopt upon hydration depends upon intrinsic factors such as the size of the polar headgroup, the hydrophobic volume occupied by the hydrocarbon chains, and their lengths or extrinsic factors such as hydration, temperature, pH, ionic strength, divalent cations and the presence of other lipids or proteins. Recent investigations have been suggested that amphiphilic carbohydrates form thermotropic and lyotropic liquid crystals if the molecules have an

appropriate shape [13]. Smectic A_d phases are well established for amphiphilic carbohydrates with one aliphatic chain [14]. The gel consisting of a mixture of alkyl and acyl sophoroside showed very similar texture classified as smectic A_d phase (data not shown) [15]. The texture of β-1-*O*-hexadecylsophoroside by polarizing microscopy is shown in Figure 5.4. Unlike other carbohydrate amphiphiles, the gel was formed at relatively low concentration due to the low solubility in water. In the gel the intermolecular strong hydrogen bonds probably link the molecules together.

The β-anomer has proved more difficult to obtain as crystals suitable for X-ray analysis than the α-anomer. No crystal structures of alkyl β-glucopyranosides have been determined due to the difficulty of obtaining crystals large enough for single crystal X-ray structure analysis. The crystals of β-1-*O*-hexadecylsophoroside in methanol have been shown to have a substructure consisting of very fine fiber. When amphiphilic molecules are dispersed in water they form phases with some kind of periodic order, usually multilamellar arrangements, which can be studied by diffraction techniques [16]. It appeared that the mesophases of carbohydrate amphiphiles were bilayer regardless of weather the sugar moiety was cyclic or acyclic. X-ray diffraction pattern of aqueous dispersions of β-1-*O*-hexadecylsophoroside is shown in Figure 7.5. The X-ray diffraction pattern showed intense peak at 38 Å and 49 Å. In the smectic A_d phase of the alkyl glycosides the d-spacing is 1.3 to 1.6 times the extended length of a molecule corresponding to interdigitated biomolecular layers [17]. The extended length of the single molecule estimated from the molecular model in energy-minimized conformation was about 26 Å. The peak at 50 Å is about 2-times the length of the fully extended

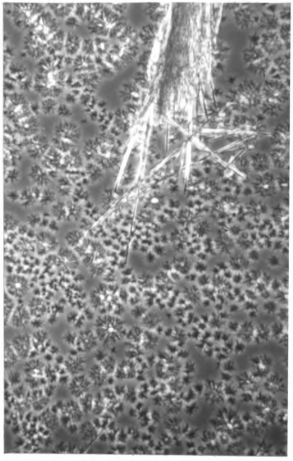

Figure 7.4: Texture of the smectic phase (tentatively assigned) of β-1-*O*-hexadecylsophoroside.

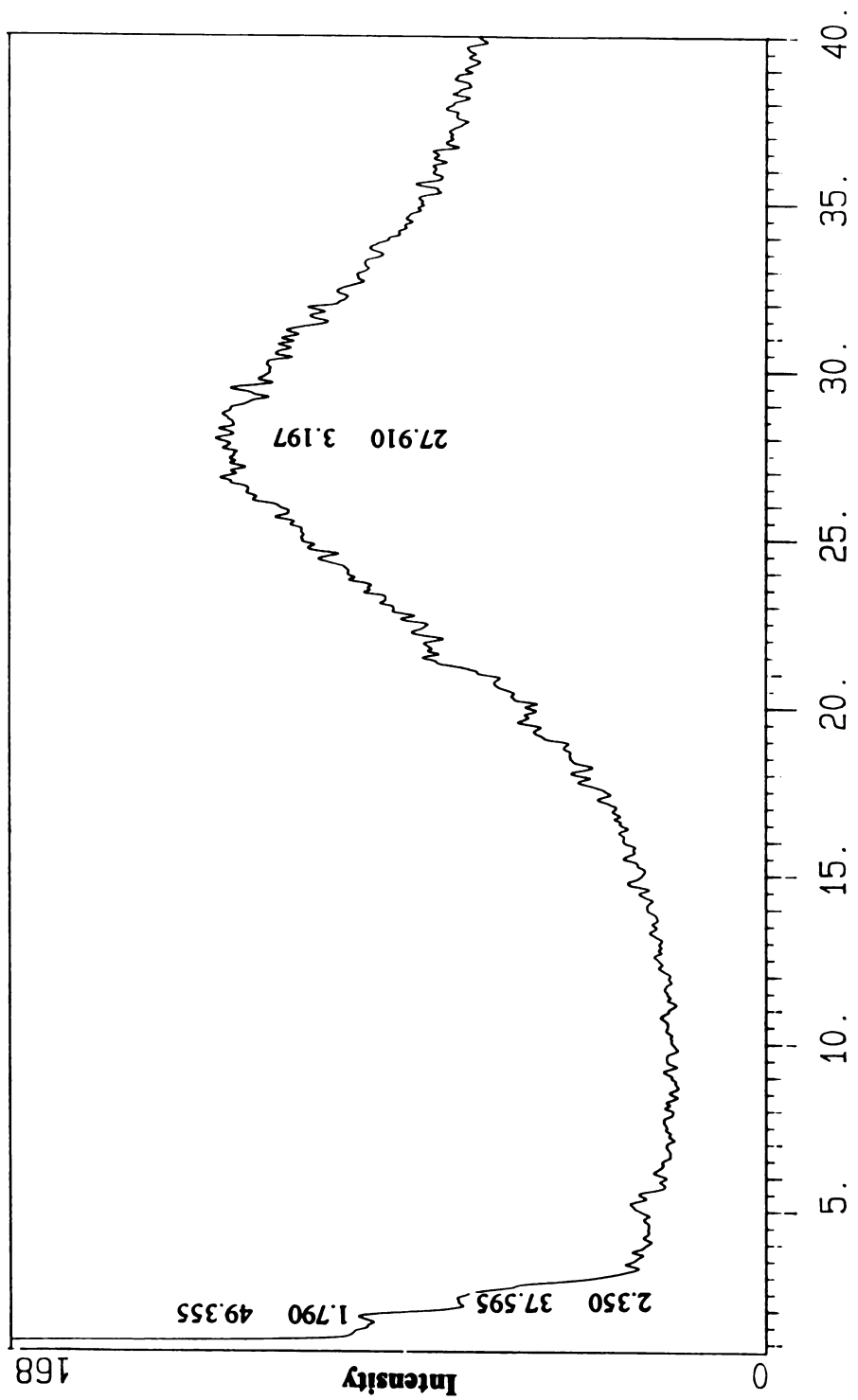

Figure 7.5: X-ray diffraction pattern of hydrated β-1-*O*-hexadecylsophoroside.

molecules. The lamellar repeat spacing varies with hydration as well as with temperature. However, the lamella repeat distance, 50 Å observed in X-ray diffraction includes water layer thickness. The bilayer thickness can be calculated from the lamella repeat spacing (observed *d*-spacing) and the concentration of the lipid at saturated hydration. The thickness of water layer of hydrated digalactosyl diglyceride can be large as ~ 13 Å at maximum water uptakes. Thus the lipid bilayer thickness would be smaller than the observed layer spacing of 50 Å. Thus the lamella repeat distance of 50 Å is an evidence for a structure with interdigitated hydrocarbon chains. The layer spacing of 38 Å was not consistent with the second order diffraction of lamella or hexagonal phase. Thus it might be *d*-spacing of different molecular packing. The diffraction lines do not permit an equivocal distinction between the lamellar and hexagonal types of structure due to the absence of higher order of reflections. A relatively sharp peak in the wide angle region at about 3.2 Å was also observed instead of the anticipated sharp 4.2 Å diffraction typical of hexagonally close-packed hydrocarbon chains of a gel structure. It also different from the diffusive X-ray diffraction line at 4.6 Å of phospholipid acyl chains packed in the disordered lamellar liquid-crystalline phase [18]. It has been shown that X-ray diffraction pattern in the wide-angle range is hydration-dependent and is broaden with increasing hydration [19]. The relatively broad reflection compared to the diffraction of hydrocarbon chains in hexagonally close packed lattice indicates that the two-dimensional packing lattice of acyl chains has low symmetry in fully hydrated bilayer but still in the gel state. The small lateral separation of the alkyl chains in the present study might be an indication that hydrocarbon chains are very closely packed with a partial interdigitation to accommodate the relatively large headgroups. The intermolecular interaction by

hydrogen bondings also form a very compact, rigid head group network at the bilayer surface. The packing behavior of lipids depends on space requirement, intermolecular interaction and hydration of the head group. If the area occupied by the head group is larger than the sum of the cross-sections of the two hydrocarbon chains, the chains must tilt in order to establish close-packing contact without leaving voids. The energy-minimized conformation showed tilting of hydrocarbon chains when the polar group was arranged to maximize contacting with bilayer surface. The lowest energy packing arrangement tends to maximize the van der Waals interaction in the bilayer interior. For the glycolipid studied the large lateral chain-chain interactions are possible only with interdigitated alkyl chains. The ability of bilayer lipids to form interdigitated states has been recently come into focus as a means to significantly alter membrane bilayer properties [19]. Interdigitated bilayers, as a consequence of unusual packing arrangement of the molecules, provide for the possible formation of discrete domains within the plane of the bilayer. Interdigitation may influence the activity of integral membrane proteins by modulating the bilayer thickness.

The thermal behavior of the total lipids extracted from *S. ventriculi* grown at pH 3 gave a broad endothermic transition (onset temperature ~12°C, peak temperature ~30°C). There were two small endothermic transition between about 50 and 60°C with peaks at about 52 and 56°C [20]. The thermal behavior of the synthetic hexadecylsophoroside is shown in Figure 7.6. Detection of the gel-to-liquid crystal phase transition by differential scanning calorimetry (DSC) strongly suggests the presence of aligned alkyl chains in the

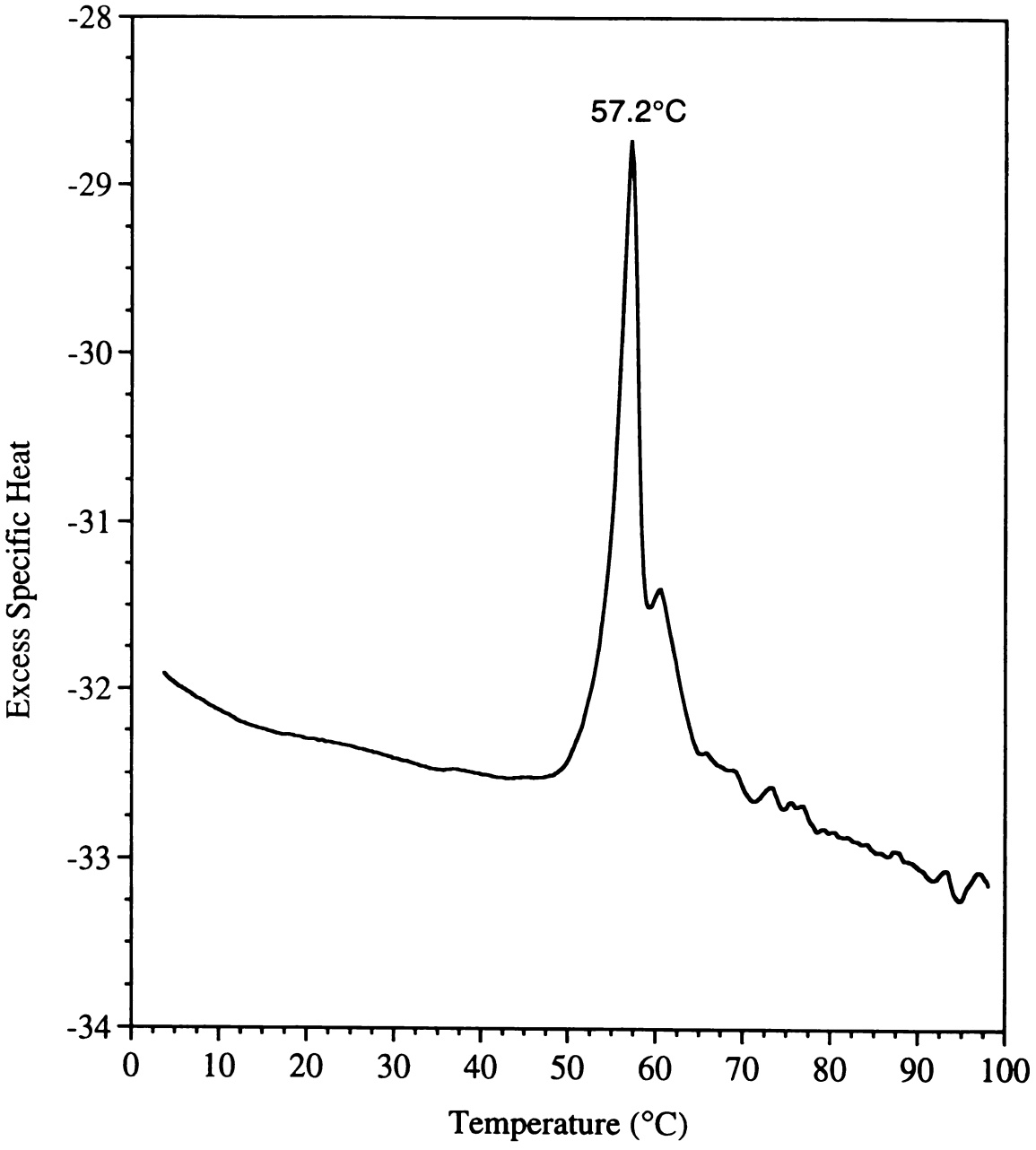

Figure 7.6: Differential scanning thermogram of β-1-*O*-hexadecylsophoroside.

aggregate. Heating fully hydrated lipid from 0°C gave a major endothermic transition with an onset temperature of 49°C with a peak at 57.2°C followed by a small endothermic transition at 62.5°C. The main transition at 57.2°C can be safely identified with the gel to liquid-crystal phase transition. It is unknown at this present which structural change is associated with a less energetic endothermic transition at 62.5°C. On the basis of a comparison of the heating curves of total lipid extract and the hexadecylsophoroside, the high temperature transitions observed with the total lipid extract may be contributed from the hexadecylsophoroside. The interaction between neighboring headgroups which probably involve intermolecular hydrogen bonds might be responsible for the observed high transition temperature. The thermal behavior of this lipid would be different at the real physiological condition (pH 3) since the transition temperature is sensitive to variations in pH in those where the ionization of the polar head groups is affected. However in sugar containing lipids where the direct effects of pH and ionic strength are probably negligible [21].

REFERENCES

1. S. Jung, S.E. Lowe, R.I. Hollingsworth, and J.G. Zeikus, *J. Biol. Chem.*, 1993, **269**, 2828-2835.

2. J. Lee and R.I. Hollingsworth, *Tetrahedron*, 1996, **52**, 3873-3878.

3. K. Iwamoto, J. Sunamoto, K. Inoue, T. Endo and S. Nojima, *Biochim. Biophys. Acta*, 1982, **691**, 44-51.

4. E.T. Olejniczak, R.T. Gampe, Jr., and S. W. Fesik, *J. Magn. Reson.*, 1986, **67**, 28-41.

5. S.L. Mayo, B.D. Olafson, and W.A. Goddard, *J. Phys. Chem.*, 1990, **94**, 8897-8909.

6. Y. Wang and R.I. Hollingsworth, *Biochemistry*, 1996, **35**, 5647-5654.

7. G. Widmalm, R.A. Byrd, and W. Egan, *Carbohydr. Res.*, 1992, **229**, 195-211.

8. G.M. Clore, A.M. Gronenborn, A.T. Brünger, and M. Karplus, *J. Mol. Biol.*, 1985, **186**, 435-455.

9. T. Peters, B. Meyer, R. Tuike-Prill, R. Somorjai, and J.-R. Brisson, *Carbohydr. Res.* 1993, **238**, 49-73.

10. S.W. Homans, A. Pastore, R.A. Dwek, T.W. Rademacher, *Biochemistry*, 1987, **26**, 6649-6655.

11. M.K. Dowd, A.D. French, and P.J. Reilly, *Carbohydr. Res.*, 1992, **233**, 15-34.

12. W.S. York, *Carbohydr. Res.*, 1995, **278**, 205-225.

13. G.A. Jeffrey, *Mol. Cryst. Liq. Cryst.*, 1990, **185**, 209-213.

14. J.W. Goodby, *Mol. Cryst. Liq. Cryst.*, 1984, **110**, 205-219.

15. G.G. Shipley, J.P. Green, and B.W. Nichols, *Biochim. Biophys. Acta*, 1973, **311**, 531-544.

16. S.W. Homans, C.J. Edge, M.A.J. Ferguson, R.A. Dwek, and T.W. Rademacher, *Biochemistry*, 1989, **28**, 2881-2887.

17. H. Hauser, I. Pascher, R.H. Pearson, and S. Sundell, *Biochim. Biophys. Acta.*, 1981, **650**, 21-51.

18. V. Luzzati, 1968, in *Biological Membranes* (D. Chapman, ed.), pp 71-124, Academic Press, New York.

19. J.L. Slater and C.-h. Huang, 1992, in *The Structure of Biological Membranes,* pp. 175-210 (P. Yeagle ed.), CRC Press, Boca Raton.

20. L.R. Bérubé, 1995, *Studies on the Dynamics of Lipid Alkyl Chains in Biological Membranes Subjected to Environmental Stress.* Doctoral Dissertation, Michigan State University, Department of Biochemistry.

21. D.A. Mannock, R.N.A.H. Lewis, A. Sen, and R.N. McElhaney, *Biochemistry*, 1988, **27**, 6852-6859.

CHAPTER VIII

SUMMARY AND PERSPECTIVES

How much have I learned about a single cell organism, *Sarcina ventriculi* in the aspect of membrane chemistry over the years? The answer to this question is that I have just climbed a small hill to see a limited horizon. However, I hope this small step is essential for a long journey towards understanding the beauty of nature in the future.

Understanding how bacteria survive under extreme environmental conditions at the molecular level is probably primary to understand life-relating phenomena and to outline the evolution of life ultimately. Adaptation is a very complex process in which it is necessary to satisfy the very well balanced and manifold functional roles of individual cell components. To understand microscopic membrane adaptations to extreme environmental conditions, the membrane has to be characterized at several levels. One has to follow subtle changes including the actual structures of the individual membrane lipids, their conformations, how they are packed in a supramolecular sense and how mobile they are (their dynamics). However, these tasks are complicated and challenging for several reasons. The difficulty encountered first is that membranes are very complex and heterogeneous. They contain thousands of molecular species. Thus, the complete separation and characterization of these species is almost impossible. Another complication is that all biological structures are very dynamic implying the biological state is a time-dependent phenomenon. When environmental perturbations such as a change in pH or temperature or the addition of organic solvents applied to living organisms, the membrane chemistry is immediately altered to maintain their motional dynamics and stability in the face of these environmental changes that might offset.

Sarcina ventriculi grown at low pH was used as a case study to explore membrane structural reorganizations which allow some organisms to be tolerant or adaptable to

environmental extremes. The impact of pH on membrane structure and function has not been explored as intensively as temperature change. The prominent lipids from *S. ventriculi* cells grown at pH 7 were DAG, MGDG, lyso-PG and PG. When the cells were grown at pH 3 this organism was found to be capable of a variety of unusual and dramatic adaptative processes. Among the many fascinating modifications that occur is the formation of tail-to-tail coupled lipids by chemical linking of hydrocarbon chains from opposite ends of the membrane bilayer to form transmembrane bifunctional fatty acid species that span the bilayer. This work provides a rationale for the existence and function of very long bifunctional fatty acids and ethers [1,2] found in the membrane lipids of this bacterium. These changes are important for maintaining the optimum dynamic range of molecular motion and energy transfer [3]. The formation of head-to-head coupled lipids has also been observed. It could be explained by the formation of the acetal linkage from the addition of hydroxyl groups to enol ether function of a plasmalogen with assistance of either a proton or a metal ion. The adaptative processes occur dynamically and instantaneously and render this organism tolerant to organic solvents, extreme pH, moderately high temperatures and a wide spectrum of antibiotics at concentrations as high as 200 μg / mL.

The novel glycolipids of *Sarcina ventriculi* cells grown at pH 3 were isolated and characterized by 2-D NMR spectroscopy and mass spectrometry. The structure of one of these glycolipids was identified as β-1-*O*-acyl-β-1,2-diglucosyl glycoside containing predominantly 16:0, 18:1 and 18:0 acyl chains [4]. Another glycolipid was β-1-*O*-hexadecyl-β-1,2-diglucosyl glycoside. Their levels are regulated by environmental

conditions such as pH and temperature. Even though a few 1-*O*-acyl-D-glucoses have been found in nature this represents the first report of this class of molecules in bacteria. This unusual family of glycosides represents the major proportion of the chloroform-methanol extractable lipids formed by this organism at low pH. These findings suggest that these glycolipids might have some function in regulating the properties of the cell membranes at low pH. These disaccharide-containing alkyl and acyl glycosides especially those with unusual linkages and anomerically pure are also interesting for the preparation of liquid crystalline materials. *Sarcina ventriculi* and related organisms may prove to be a very valuable source of them in the future.

After the discovery of these novel glycolipids, our attention shifted to finding the higher homologues of these glycolipids. This lead to the discovery of a new class of membrane components in this organism. The structure of a family of unusual glucans from *Sarcina ventriculi* has been characterized by NMR spectroscopy, methylation analysis, and mass spectrometry. One was a trisaccharide containing a β-1,3 and a β-1,4-linkage. The other was a hexasaccharide that is simply a β-1,4-linked dimer of the trisaccharide unit. Beta-1,2-linked glucans are regular glucose oligomers that have been found thus far only in Gram-negative bacteria. They are thought to function in maintaining the osmolality of the periplasm, thus protecting the organism from osmotic stress [5-7]. This is the first report of β-glucan biosynthesis in a Gram-positive organism. This would expand the link that had already been established between adaptability of bacteria and β-glucan biosynthesis.

It is known that peptidoglycan structure might be sensitive to environmental

conditions [8]. Whether the peptidoglycan has any unusual structural feature in cells grown under these conditions is unknown. Therefore, the isolation and characterization of peptidoglycan of *Sarcina ventriculi* from cells grown at pH 3 was carried out by a combination of mass spectrometry and NMR spectroscopy in an effort to determine whether there are any unusual modifications. The basic muropeptide subunit consisted of a *N*-acetylglucosamine-β-1,4-*N*-acetylmuramic acid disaccharide substituted with an oligopeptide with the sequence Ala-*iso*Gln-A_2pm(-Gly)-Ala. The dimeric muropeptide was also characterized. It was a cross-linked bis-disaccharide-penta-hexapeptide with the structure GlcNAc-MurNAc-Ala-*iso*Gln-A_2pm(-Gly)-Ala → GlcNAc-MurNAc-Ala-*iso*Gln-A_2pm(-Gly)-Ala-Ala. This is completely consistent with a structure proposed based on enzymatic degradation and chemical modifications but with no use of spectroscopic information [9]. The cell wall in this organism is very tightly cross-linked and is much more rigid than in most other Gram-positive bacteria. There is, however, a large degree of conservation in the general structure indicating that the plasma membrane does play a more important role in adaptation. The NMR spectroscopy assignments will be a prerequisite step in determining the 3-dimensional structure of peptidoglycan in order to understand its organization and the structural modifications it undergoes during bacterial adaptation in the future.

An understanding of the conformational preferences of the membrane lipids is critical to an understanding of the biological function and interactions of the lipids with each other and with other membrane constituents such as proteins. Only a few glycolipids have been studied for the orientation and the dynamics of headgroup by ^{2}H-NMR

spectroscopy. The conformation of monoglucosyldiacylglycerol (MGDG) in solution was studied by a combination of NMR spectroscopy and molecular mechanics calculation. This study was very exiting, challenging and necessary to test our hypothesis that sufficient proximity and appropriate orientation of sugar residues in highly ordered aggregate such as biological membranes may determine the glycosidic linkages between subunits in glycolipids containing disaccharides and even higher homologues. The premise here is that MGDG is the biosynthetic precursor of alkyl and acyl sophorosides. From a quantitative analysis of NOE cross-peaks, proton-proton distances were calculated. These distance constraints were incorporated into molecular mechanics calculation. In the present study the angle φ and ϕ were 169° and 47°, respectively, implying the glucose ring is normal to the bilayer plane assuming a lamellar packing arrangement. In addition, to gain insight into the relative flexibility of the different parts of the molecule, a molecular dynamics simulation was also performed. The rotamer populations for the two C-C bonds of the glycerol moiety of MGDG were obtained from vicinal spin-spin coupling constants using a Karplus treatment [10]. It indicated that there is a preferred conformation in the C(2)-C(3) bond whereas the C(1)-C(2) bond is flexible, as is evident from nearly populated rotamers around this bond.

The conformation, order, phase behavior and other properties of β-1-*O*-hexadecylsophoroside are especially interesting since it is synthesized in the ordered environment of a biological membrane. Studies on such systems can give insight into the interplay of conformational and packing behavior with the observed structural diversity of membrane lipids. Which groups are in close proximity to each other and might

combine to form need lipid species, for instance. Its three-dimensional structure in solution was established by NMR nuclear Overhauser effect spectroscopy and molecular mechanics calculations. The packing behavior of this molecule was studied by X-ray diffraction, polarizing microscopy and differential scanning calorimetry. The gel to liquid crystalline transition temperature was 57°C implying strong interaction between head groups. The lamellar distance of 49 Å was obtained with the lipids in their fully hydrated state by X-ray diffraction studies. These physical properties are very similar to MGDG containing two hexadecanoyl chains. The lamellar gel to liquid crystalline phase transition temperature of the latter glycolipid was 61°C. The X-ray diffraction spacing obtained from aqueous dispersions for lamellar gel was 51.6 Å [11]. The similar physical properties of alkyl sophoroside and MGDG may be indicative of similar functional roles of lipids in the biological membranes at two different pHs. However, if our assumption that MGDG is the biosynthetic precursor for β-1-*O*-hexadecylsophoroside in *S. ventriculi* at pH 3 is true, the formation of this novel glycolipid at low pH would have other profound functional roles in addition to provide similar physical properties.

Although the present studies have revealed very important features relating membrane composition to environmental state, several questions must be explored in future research. Efforts were undertaken to separate pure transmembrane lipid molecules. These included column chromatography such as C18, silica gel and silicic acid and gel filtration chromatography. NMR spectroscopy and GC analysis indicated the presence of reasonably pure and highly cross-liked transmembrane lipids. However, it was not possible to detect their molecular ions by mass spectrometry using ionization methods

such as FAB, MALDI and ESI techniques to determine their molecular weights even for samples containing a large proportion of long chain fatty acids (more than 80 per cent). This may imply that they were larger oligomeric or polygomeric structures and that is not possible to detect them by mass spectrometry. If this were so, it is understandable why a high proportion of lipids with single fatty alkyl or acyl chains also have to be synthesized to produce same fluidity.

It has been shown that *S. ventriculi* produce cellulose or a closely related compound as intercellular cementing material which remains tightly associated with the cell wall [12]. The Gram-negative *Acetobacter xylinum* have been reported to produce a variety of water-soluble β-linked glucose polymers such as β-1,2-glucan chains and substituted β-1,4-glucan chains in addition to crystalline cellulose [13]. It is now evident that polymerization of bacterial cellulose is a membrane-associated event. However, no relationship has been established to suggest that the β-glucans observed in this study can be intermediate for cellulose in this bacterium. In *in vitro* membrane-derived oligosaccharides biosynthesis, exogenously added primers such as octyl β-glucoside is required [14,15]. Thus, the occurrences of the alkyl and acyl sophorosides might be related to the biosynthesis of the glucans.

Previous studies have shown very similar changes in fatty acid profiles at high temperature as observed in cells grown at low pH [3]. However, further studies are necessary to determine whether similar adaptative changes in lipid head-groups, such as the formations of alkyl or acyl sophorosides occur. Such studies should contribute greatly

to our understanding of the principles underlying biosynthesis of these glycolipids and may provide insight into their functional roles in biological membranes.

As demonstrated in this study *S. ventriculi* has a very sophisticated and fascinating adaptative mechanisms to extreme environments. This adaptative mechanism is very effective and dynamic without requiring new protein or lipid synthesis. The proposed model for the overall adaptation of *S. ventriculi* at pH 3 is summarized in Figure 8.1. It is possible to see the origins of any one lipid structure by enlogating the structures of the others. The various lipids are often simply combinations or sub-structures of the others. These fragments are recombined, mixed and separated in a continuous fashion in response to environmental pressures such that the physical properties are maintained. The consequences of this is that the complexity (heterogeneity) of the membrane escalates dramatically as it goes from condition to condition. The determination of the heterogeneity, lipid conformation and supramolecular structure of biomembranes therefore represents one of the obligate challenges for the analytical chemistry of living systems.

This study provides evidence on how nature selects the less energetic and easiest way to arrive at a stable and functional molecular organization such that similar or the same results from radically different perturbations in a general and consistent manner. It is hoped that the present study will be helpful in providing not only new views on adaptative mechanism to extreme environments in microorganisms but also analytical techniques to follow the changes in structural modification during the adaptation.

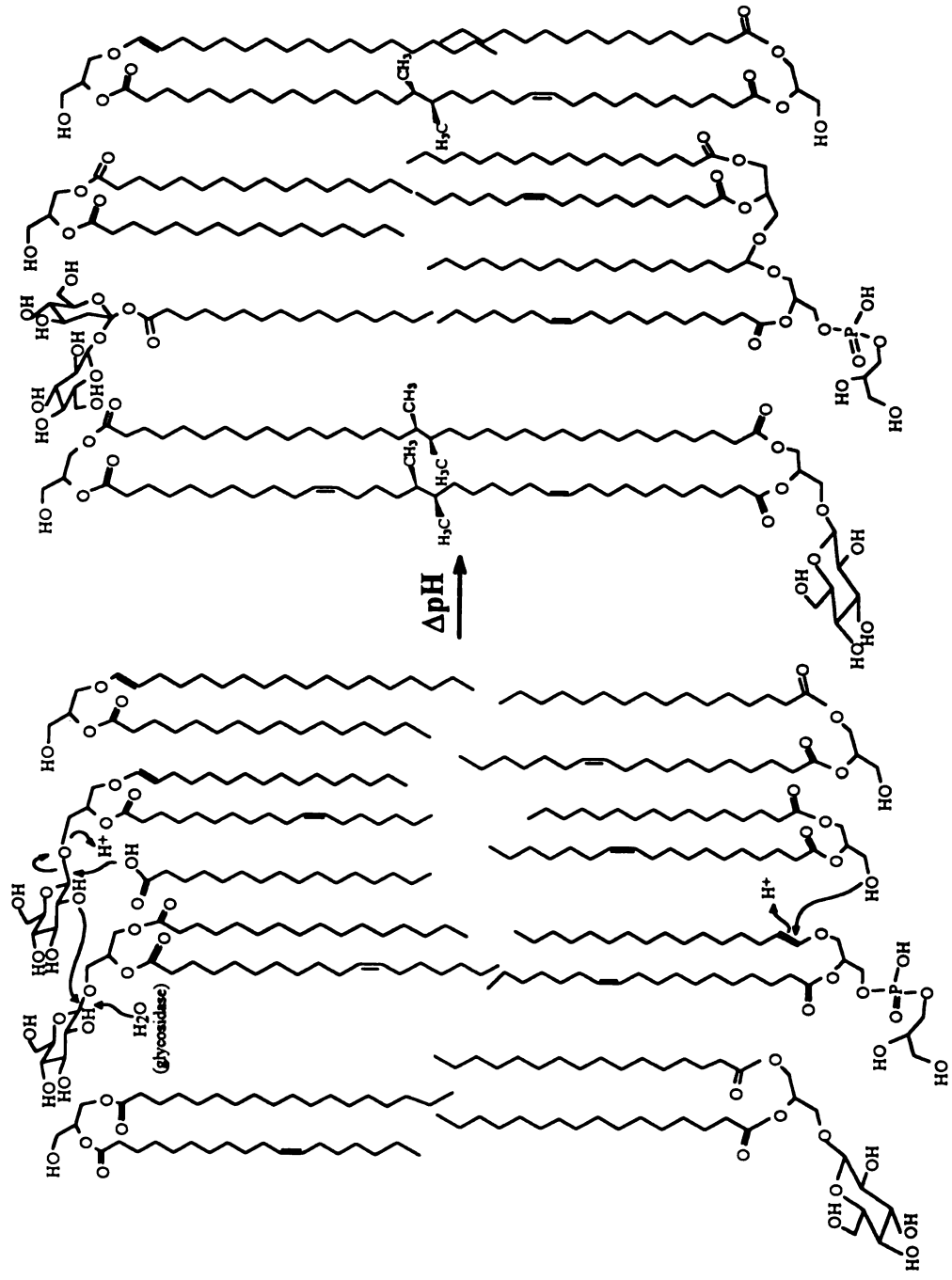

Figure 8.1: Representation of the adaptation mechanism of *Sarcina ventriculi* at pH 3.

REFERENCES

1. S. Jung, S.E. Lowe, R.I. Hollingsworth, and J.G. Zeikus, *J. Biol. Chem.*, 1993, **268**, 2828-2835.

2. G.D. Sprott, M. Meloche, and J.C. Richards, *J. Bacteriol.*, 1991, **173**, 3907-3915.

3. L. Bérubé, 1995, *Studies on the Dynamics of Lipid Alkyl Chains in Biological Membranes Subjected to Environmental Stress*, Doctoral Dissertation, Michigan State University, Department of Biochemistry.

4. J. Lee and R.I. Hollingsworth, *Tetrahedron*, 1996, **52**, 3873-3878.

5. E.P. Kennedy and M.K. Rumley, *J. Bacteriol.*, 1988, **170**, 2457-2461.

6. J. Quandt, A. Hillemann, K. Niehaus, W. Arnold, and A. Puhler, *Mol. Plant-Microb. Interact.*, 1992, **5**, 420-427.

7. O. Geiger, F.D. Russo, T.J. Silhavy, and E.P. Kennedy, *J. Bacteriol.*, 1992, **174**, 1410-1413.

8. U. Vijaranakul, M.J. Nadakavukaren, B.L.M. de Jonge, B.J. Wilkinson, and R.K. Jayaswal, *J. Bacteriol.*, 1995, 177, 5116-5121.

9. O. Kandler, D. Claus, and A. Moore, *Arch. Mikrobiol.*, 1972, **82**, 140-146.

10. M. Karplus, *J. Chem. Phys.*, 1957, **30**, 11-15.

11. D.A. Mannock, R.N.A.H. Lewis, A. Sen, and R.N. McElhaney, *Biochemistry*, 1988, 27, 6852-6859.

12. E. Canale-Parola, *Bacteriol. Rev.*, 1970, **34**, 82-97.

13. H. Sandermann and R.F.H. Dekker, *FEBS Lett.*, 1979, **107**, 237-240.

14. E.P. Kennedy, 1987, in *Escherichia coli and Salmonellar typhimurim,* pp 672-679. (F.C. Neidhart, J.L. Ingraham, K.B. Low, B. Magasanik, M. Schaechter, and H.E. Umbarger, eds.) American Society for Microbiology, Washington, D.C.

15. A.C. Weissborn and E.P. Kennedy, *J. Biol. Chem.*, 1984, **25**, 12644-12651.